

AD-A219 033

DTIC FILE COPY

AGARD-AG-307

1

AGARD-AG-307

# AGARD

ADVISORY GROUP FOR AEROSPACE RESEARCH & DEVELOPMENT

7 RUE ANCELLE 92200 NEUILLY SUR SEINE FRANCE

AGARDograph No. 307

## Measurement Uncertainty Within the Uniform Engine Test Programme

DTIC

ELECTE

MAR 07 1990

S D

ck

DISTRIBUTION STATEMENT A  
Approved for public release  
Distribution Unlimited

NORTH ATLANTIC TREATY ORGANIZATION



DISTRIBUTION AND AVAILABILITY  
ON BACK COVER

90 03 06 008

BEST  
AVAILABLE COPY

NORTH ATLANTIC TREATY ORGANIZATION  
ADVISORY GROUP FOR AEROSPACE RESEARCH AND DEVELOPMENT  
(ORGANISATION DU TRAITE DE L'ATLANTIQUE NORD)

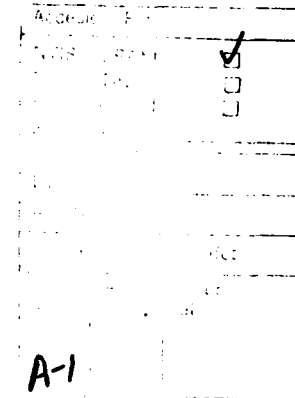
AGARDograph No.307

**MEASUREMENT UNCERTAINTY WITHIN THE  
UNIFORM ENGINE TEST PROGRAMME**

**Report of the Sub-Group on Uncertainty Assessment**

Edited by

J.P.K. Vleghert  
National Aerospace Laboratory  
Anthony Fokkerweg 2  
PO Box 90502  
1006 BM Amsterdam  
Netherlands



This AGARDograph was prepared at the request of the Propulsion  
and Energetics Panel of AGARD.

## THE MISSION OF AGARD

According to its Charter, the mission of AGARD is to bring together the leading personalities of the NATO nations in the fields of science and technology relating to aerospace for the following purposes:

- Recommending effective ways for the member nations to use their research and development capabilities for the common benefit of the NATO community;
- Providing scientific and technical advice and assistance to the Military Committee in the field of aerospace research and development (with particular regard to its military application);
- Continuously stimulating advances in the aerospace sciences relevant to strengthening the common defence posture;
- Improving the co-operation among member nations in aerospace research and development;
- Exchange of scientific and technical information;
- Providing assistance to member nations for the purpose of increasing their scientific and technical potential;
- Rendering scientific and technical assistance, as requested, to other NATO bodies and to member nations in connection with research and development problems in the aerospace field.

The highest authority within AGARD is the National Delegates Board consisting of officially appointed senior representatives from each member nation. The mission of AGARD is carried out through the Panels which are composed of experts appointed by the National Delegates, the Consultant and Exchange Programme and the Aerospace Applications Studies Programme. The results of AGARD work are reported to the member nations and the NATO Authorities through the AGARD series of publications of which this is one.

Participation in AGARD activities is by invitation only and is normally limited to citizens of the NATO nations.

The content of this publication has been reproduced  
directly from material supplied by AGARD or the authors.

Published May 1989

Copyright © AGARD 1989  
All Rights Reserved

ISBN 92-835-0508-5



Printed by Specialised Printing Services Limited  
40 Chigwell Lane, Loughton, Essex IG10 3TZ

## RECENT PUBLICATIONS OF THE PROPULSION AND ENERGETICS PANEL

### Conference Proceedings

Testing and Measurement Techniques in Heat Transfer and Combustion  
AGARD Conference Proceedings No.281, 55th A Meeting, May 1980

Centrifugal Compressors, Flow Phenomena and Performance  
AGARD Conference Proceedings No.282, 56th B Meeting, May 1980

Turbine Engine Testing  
AGARD Conference Proceedings No.293, 56th Meeting, Sep/October 1980

Helicopter Propulsion Systems  
AGARD Conference Proceedings No.302, 57th Meeting, May 1981

Ramjets and Ramrockets for Military Applications  
AGARD Conference Proceedings No.307, 58th Meeting, October 1981

Problems in Bearings and Lubrication  
AGARD Conference Proceedings No.323, 59th Meeting, May/June 1982

Engine Handling  
AGARD Conference Proceedings No.324, 60th Meeting, October 1982

Viscous Effects in Turbomachines  
AGARD Conference Proceedings No.351, 61st A Meeting, June 1983

Auxiliary Power Systems  
AGARD Conference Proceedings 352, 61st B Meeting, May 1983

Combustion Problems in Turbine Engines  
AGARD Conference Proceedings 353, 62nd Meeting, October 1983

Hazard Studies for Solid Propellant Rocket Motors  
AGARD Conference Proceedings 367, 63rd A Meeting, May/June 1984

Engine Cyclic Durability by Analysis and Testing  
AGARD Conference Proceedings No.368, 63rd B Meeting, May/June 1984

Gears and Power Transmission Systems for Helicopters and Turboprops  
AGARD Conference Proceedings No.369, 64th Meeting October 1984

Heat Transfer and Cooling in Gas Turbines  
AGARD Conference Proceedings No.390, 65th Meeting, May 1985

Smokeless Propellants  
AGARD Conference Proceedings No.391, 66th A Meeting, September 1985

Interior Ballistics of Guns  
AGARD Conference Proceedings No.392, 66th B Meeting, September 1985

Advanced Instrumentation for Aero Engine Components  
AGARD Conference Proceedings No.399, 67th Meeting, May 1986

Engine Response to Distorted Inflow Conditions  
AGARD Conference Proceedings No.400, 68th A Meeting, September 1986

Transonic and Supersonic Phenomena in Turbomachines  
AGARD Conference Proceedings No.401, 68th B Meeting, September 1986

Advanced Technology for Aero Engine Components  
AGARD Conference Proceedings No.421, 69th Meeting, September 1987

Combustion and Fuels in Gas Turbine Engine  
AGARD Conference Proceedings No.422, 70th Meeting, October 1987

Engine Condition Monitoring – Technology and Experience  
AGARD Conference Proceedings No.448, 71st Meeting, May/June 1988

### **Working Group Reports**

#### **Aircraft Fire Safety**

AGARD Advisory Report 132, Vol.1 and Vol.2, Results of WG 11 (September and November 1979)

#### **Turbulent Transport Phenomena (in English and French)**

AGARD Advisory Report 150, Results of WG 09 (February 1980)

#### **Through Flow Calculations in Axial Turbomachines**

AGARD Advisory Report 175, Results of WG 12 (October 1981)

#### **Alternative Jet Engine Fuels**

AGARD Advisory Report 181, Vol.1 and Vol.2, Results of WG 13 (July 1982)

#### **Suitable Averaging Techniques in Non-Uniform Internal Flows**

AGARD Advisory Report 182 (in English and French), Results of WG 14 (June/August 1983)

#### **Producibility and Cost Studies of Aviation Kerosines**

AGARD Advisory Report 227, Results of WG 16 (June 1985)

#### **Performance of Rocket Motors with Metallized Propellants**

AGARD Advisory Report 230, Results of WG 17 (September 1986)

### **Lecture Series**

#### **Non-Destructive Inspection Methods for Propulsion Systems and Components**

AGARD LS 103 (April 1979)

#### **The Application of Design to Cost and Life Cycle Cost to Aircraft Engines**

AGARD LS 107 (May 1980)

#### **Microcomputer Applications in Power and Propulsion Systems**

AGARD LS 113 (April 1981)

#### **Aircraft Fire Safety**

AGARD LS 123 (June 1982)

#### **Operation and Performance Measurement of Engines in Sea Level Test Facilities**

AGARD LS 132 (April 1984)

#### **Ramjet and Ramrocket Propulsion Systems for Missiles**

AGARD LS 136 (September 1984)

#### **3-D Computation Techniques Applied to Internal Flows in Propulsion Systems**

AGARD LS 140 (June 1985)

#### **Engine Airframe Integration for Rotorcraft**

AGARD LS 148 (June 1986)

#### **Design Methods Used in Solid Rocket Motors**

AGARD LS 150 (April 1987)

AGARD LS 150 (Revised) (April 1988)

### **Other Publications**

#### **Airbreathing Engine Test Facility Register**

AGARD AG 269 (July 1981)

#### **Rocket Altitude Test Facility Register**

AGARD AG 297 (March 1987)

#### **Manual for Aeroelasticity in Turbomachines**

AGARD AG 298/1 (March 1987)

AGARD AG 298/2 (June 1988)

#### **Application of Modified Loss and Deviation Correlations to Transonic Axial Compressors**

AGARD Report 745 (November 1987)

## FOREWORD

Performance of the propulsion system must be known to a high degree of accuracy throughout the entire flight envelope to achieve the level of operational capability demanded from today's high-performance aircraft. The starting point for a synthesis of propulsion system behaviour is the performance of the basic engine, and this is normally obtained from measurements made during full scale tests on the ground in test beds and altitude simulation facilities. In the latter, the environmental conditions of pressure and temperature met in flight can be accurately reproduced.

During the late 1970s joint engine development and licensed production programs among companies from different countries were becoming common. Further, engines which were developed in one country often were used in airframes developed in another. Both situations require engine performance information which can be interpreted internationally and provide a valid basis for performance comparisons. However, experience showed that there was poor understanding of the meaning of engine performance characteristics as derived from test facility measurements in the different countries.

Because of the critical nature of engine test measurements and their influence on aircraft performance predictions, as well as the need for a sound understanding of test-related factors, which may influence such measurements, an inter-facility comparison was proposed by the Propulsion and Energetics Panel (PEP) of AGARD. The basic idea was that a nominated engine would be tested in several facilities, both ground level and altitude, the results then compared, and explanations sought for any observed differences.

AGARD offered a unique structure to execute such a program and precedent for AGARD sponsorship existed in the earlier testing of uniform aerodynamic models in wind tunnels under the auspices of the Fluid Dynamics Panel. A formal proposal was presented to the Propulsion and Energetics Panel (PEP) of AGARD in April 1979 by the US Delegation. Although the scope of the effort was of a magnitude and timespan uncharacteristic for an AGARD undertaking, the PEP agreed to sponsorship and Working Group 15 was chartered to conduct the project which became known as the Uniform Engine Test Program (UETP). Dr James G. Mitchell, then Chief Scientist at the U.S. Arnold Engineering Development Center, was appointed as Chairman of this major new effort and members of the engine test community throughout AGARD were selected to serve on Working Group 15 along with PEP representatives.

Two specially prepared and instrumented turbine engines were tested in ground test beds and altitude facilities in five countries (eight test facilities) in a closely controlled test program. The participating agencies bore the entire cost of testing and the costs of all subsequent data analyses. These testing agencies in order of testing were: National Aeronautics and Space Administration Lewis Research Center (NASA, U.S.), Air Force Arnold Engineering Development Center (AEDC, U.S.), National Research Council of Canada (NRCC, Canada), Centre d'Essais des Propulseurs (CEPr, France), Turkish Air Force Overhaul Base (TUAF, Turkey), Royal Aircraft Establishment at Farnborough (RAE(P), U.K.), and Naval Air Propulsion Center (NAPC, U.S.).

The UETP began with the primary objective of providing an international test facility calibration program to permit inter-facility comparisons of engine performance. It became apparent early on that facility measurement uncertainty estimates would be an important consideration in the UETP from the standpoint that the interpretation of the interfacility comparisons would depend on a consistent, well founded treatment of the different measurement processes used by each facility. Also, interpretation of the observed data differences could provide valuable insight into the validity of each facility's estimated measurement uncertainties and result in the improvement of measurement uncertainty estimation methodology. Such an opportunity to observe a wide variety of testing influences and the means to provide a directly-comparable, quantitative evaluation of the quality of the different test methods and measurement equipment in use at the various facilities had never before been presented. As a result, a new appreciation of the sensitivities of some of the testing engine variables and their interactions could be gained. It is likely that the use of this information to improve testing techniques, testing hardware, and data acquisition/handling could become the most important contribution of the UETP.

To address test facility measurement uncertainties, a Sub-group of the main Working Group was formed with Mr J.P.K. Vleghert appointed as the Chairman. In addition, members of the test facilities conversant with the measurement uncertainty estimation process were also selected to serve on this Sub-Group. The Sub-group met for the first time at AGARD Headquarters in Paris, France, from 29 April – 3 May 1985 to discuss the Elemental Error Audit put together earlier by the North American facilities and to identify the type of information further required and the reporting requirements for each of the test participants. Subsequent meetings of the Sub Group were held at RAE(P) in November 1987, and February 1988, and at NRCC in June 1988.

The reader interested in the UETP interfacility engine performance comparisons for both altitude and ground level test facilities including the interpretation and analyses of the performance differences is referred to AGARD AR 248 'The Uniform Engine Test Programme', by P.F. Ashwood (Reference 12). Much of the background information and facility description was taken from this report and is repeated herein for completeness. Nevertheless, it is advisable for the reader to have this report and the 'Handbook Uncertainty in Gas Turbine Measurements', by R.B. Abernethy and J.W. Thompson (Reference 2) available when studying this AGARDograph.

## THEME

The AGARDograph is an outcome of the Propulsion and Energetics Panel Working Group 15 on 'Uniform Engine Testing Programme' (AGARD AR 248). During the performance of this Group it appeared that the results of some test runs were somewhat scattered without an obvious explanation. The Group, therefore, formed a sub-Group with the task of carefully assessing the uncertainties of the measured data in order to find out whether the scattering was within the expected uncertainty or whether an explanation must be found. Since the results of the efforts of the sub-Group have some importance beyond the Working Group 15 tests, it was decided to report them in the form of an AGARDograph. In Chapter 5 the different uncertainties are estimated. The discussion on the uncertainties appears in Chapter 6, and in the following Chapter 7, ten conclusions are drawn from the efforts.

This AGARDograph was prepared at the request of the Propulsion and Energetics Panel of AGARD.

\* \* \*

Cette AGARDographie a pour origine les travaux du Groupe de travail 15 du Panel AGARD de Propulsion et d'Energétique sur "Le Programme d'Essai Uniforme des Moteurs" (AGARD AR 248). Au cours des activités de ce groupe une dispersion non-négligeable a été observée dans les résultats de certaines séries d'essais et ceci sans explication évident. Le Groupe a donc décidé de créer un sous-groupe qui aurait pour mission de faire une évaluation détaillée du degré d'incertitude sur les données obtenues par la mesure, afin de déterminer si la dispersion constatée se conformait au degré d'incertitude attendu, ou s'il fallait en trouver une explication. Etant donné que l'importance des résultats obtenus par le sous-groupe dépassait le cadre des essais conduits par le groupe de travail No. 15, il a été décidé de les publier sous forme d'AGARDographie. Une évaluation des différentes incertitudes est faite au chapitre 5 de cette publication. Le chapitre 6 contient le texte des discussions qui ont eu lieu sur les incertitudes et les conclusions sont indiquées au chapitre 7.

Cette AGARDographie a été réalisée à la demande du Panel AGARD de Propulsion et d'Energétique.

## CONTENTS

	Page
<b>RECENT PUBLICATIONS OF PEP</b>	iii
<b>FOREWORD</b>	v
<b>ABSTRACT</b>	vi
<b>LIST OF FIGURES</b>	x
<b>LIST OF TABLES</b>	x
<b>EXECUTIVE SUMMARY</b>	1
<b>1 INTRODUCTION</b>	2
<b>2 TEST PROGRAMME</b>	3
2.1 Test Article	3
2.2 Test Instrumentation	4
2.3 Test Conditions	5
2.3.1 Altitude Testing	5
2.3.2 Ground Level Testing	5
2.4 Data Scan Changes during Testing	6
2.5 Measurement Uncertainty	6
<b>3 UNCERTAINTY METHODOLOGY</b>	6
3.1 Introduction	6
3.2 Error Types	7
3.2.1 Precision (or Random) Error	7
3.2.2 Bias (or Fixed) Error	7
3.2.3 Combined Error	7
3.3 Error Evaluation	7
3.3.1 Data Sequence	7
3.3.2 Error Propagation	8
3.4 Error Sources	8
3.4.1 Elemental Error Sources	8
a) Calibration Hierarchy	9
b) Data Acquisition	10
c) Data Reduction	10
d) Other Effects	10
3.4.2 Basic Measurement Error	11
3.4.3 Influence Coefficients	11
3.4.4 Curve Shift Effect	11
3.5 Estimated Uncertainty	11
3.6 Test Data Assessment	11
<b>4 INSTRUMENTATION, DATA ACQUISITION AND CALIBRATION</b>	11
4.1 Instrumentation	11
4.2 Data Acquisition and Calibration	12
<b>5 UNCERTAINTY ESTIMATES</b>	12
5.1 Introduction	12
5.2 Errors in Basic Measurements	12
5.2.1 Scale Force	13
5.2.2 Fuel Flow	13
5.2.3 Compressor Inlet Pressure	13
5.2.4 Compressor Inlet Temperature	13
5.2.5 Rotor Speed	13
5.2.6 Area Measurement	13
5.3 Errors in Calculated Engine Performance Parameters	14
<b>6 DISCUSSIONS</b>	14
6.1 Validation within the Facility	14
6.2 Error Variation over Transducer Range	14
6.3 Use of Multiple Measurements	15
6.4 Test Data Analysis	15

	Page
<b>6.5 The Relationship between Standard Error of Estimate (SEE) and Estimated Precision Index(s)</b>	<b>16</b>
<b>6.6 Engine Power Handling</b>	<b>16</b>
<b>6.7 The Relationship between Measured Inter-facility Spreads and Estimated Uncertainties</b>	<b>16</b>
<b>7 CONCLUSIONS</b>	<b>18</b>
<b>REFERENCES</b>	<b>19</b>
<b>APPENDICES</b>	<b>40</b>
<b>I Membership of Sub-group on Uncertainty Assessment</b>	<b>40</b>
<b>II NAPC Measurement Uncertainty</b>	<b>41</b>
<b>III Nomenclature</b>	<b>42</b>
<b>IV Glossary of Terminology</b>	<b>43</b>
<b>V Description of Ground Level Test Beds and Altitude Test Cells</b>	<b>46</b>

## LIST OF FIGURES

	Page
Fig. 2.1	UETP Engine Referee Instrumentation
Fig. 2.2	Power Setting Sequence
Fig. 3.1	Graphical Propagation of Bias Error
Fig. 4.1	Sampling Systems
Fig. 5.1	Elemental Error Audit for the Basic Measurement of Scale Force
Fig. 5.2	Elemental Error Audit for the Basic Measurement of Fuel Flow
Fig. 5.3	Elemental Error Audit for the Basic Measurement of Intake Total Pressure
Fig. 5.4	Elemental Errors for Basic Measurements
Fig. 5.5	Estimated Errors for Performance Parameters
Fig. 6.1	Schematic of Data Flow
Fig. 6.2	Error Variation over Measuring Range
Fig. 6.3	Random Error Limit of Curve Fit at RAE(P) for each Test Condition
Fig. 6.4	DMP split over two days
Fig. 6.5	Comparison of Predicted Precision with Measured RSD
Fig. 6.6	Differences in Gross Thrust between First and Second Data Scans
Fig. 6.7	Spreads in Net Thrust, Airflow and SFC Altitude Facilities

## LIST OF TABLES

Table 2-1	UETP Test Chronology	3
Table 2-2	UETP Test Conditions	5
Table 2-3	Number of Data Points used for Analysis	6
Table 3-1A	Force Measurement Error Source Diagram	20
Table 3-1B	Force Measurement System	21
Table 3-2 A/B	Fuel Flow Measurement Error Source Diagram/System	22
Table 3-3 A/B	Pressure Measurement Error Source Diagram/System	23
Table 3-4 A/B	Temperature Measurement Error Source Diagram/System	24
Table 3-5 A/B	Rotor Speed Measurement Error Source Diagram/System	25
Table 3-6 A/B	Area Measurement Error Source Diagram/System	26
Table 5-1	Error Propagation at Test Condition 6 and 9	27
Table 5-2	NASA Calculated Performance Parameter Uncertainty Estimates	28
Table 5-3	AEDC Calculated Performance Parameter Uncertainty Estimates	29
Table 5-4	CEPR Calculated Performance Parameter Uncertainty Estimates	30
Table 5-5	RAE(P) Calculated Performance Parameter Uncertainty Estimates	31
Table 5-6	NRCC Calculated Performance Parameter Uncertainty Estimates	32
Table 5-7	TUAF Calculated Performance Parameter Uncertainty Estimates	32
Table 6-1	Estimated Uncertainty Interval Calculation	33

## EXECUTIVE SUMMARY

The UETP is one of the most extensive experimental and analytical programs ever sponsored by AGARD. The program was proposed by the Propulsion and Energetics Panel and approved by AGARD in 1980. The objectives of the program were:

"To provide a basis for upgrading the standards of turbine engine testing within AGARD countries by comparing test procedures, instrumentation techniques and data reduction methods, thereby increasing confidence in performance data obtained from engine test facilities.

To compare the performance of an engine measured in ground level test facilities and in altitude facilities at the same non-dimensional conditions and establish the reasons for any observed differences."

The UETP involved testing of two turbojet engines in five countries (US, Canada, France, Turkey and UK) using four altitude test facilities and four ground-level test beds. The testing program began in 1981 and extended over a period of approximately seven years, with the supporting data analysis program progressing concurrently on a cooperative multi-national basis. The programme has a historic importance in that for the first time it has made possible direct comparison of engine performance as measured in a closely controlled test program over a range of altitudes and flight speeds, in different facilities, and using different methods of data acquisition and processing.

The test facilities which participated in the test program are noted in the order of testing and with comments on the type of test program.

National Aeronautics and Space Administration (NASA)	2 engines at altitude
Arnold Engineering Development Center (AEDC)	2 engines at altitude
National Research Council of Canada (NRCC)	2 engines at ground level
Centre d'Esaïs des Propulseurs (CEPr)	2 engines at ground level
Turkish Air Force Overhaul Base (TUSAf)	1 engine at altitude
Royal Aircraft Establishment Farnborough (RAE(F))	1 engine at ground level
Naval Air Propulsion Center (NAPC)	1 engine at altitude
	1 engine at ground level
	(open air facility)

NOTE: NASA and NRCC performed repeat testing prior to testing at NAPC.

The test vehicle selected for the program was the Pratt & Whitney J57-P-19W twin-spool turbojet. This engine was chosen because of its rugged, mature configuration with minimum mechanical variable geometry features which could introduce small performance variations from test to test. It was also of a size which made it acceptable for test in the facilities under consideration. The fact that, by modern standards, it is of modest aero-thermodynamic design was of no consequence. Two engines were loaned to the program by the U.S. Air Force. Due to higher priority test workload at the participating facilities, it was not possible to test both engines in all facilities as was the original intention.

At the commencement of the program a General Test Plan was prepared which defined the location and extent of the engine instrumentation, the test conditions, the test procedure and the equations to be used for calculating the engine performance parameters. Test results were only interchanged between facilities after each completed their test program so that each facility went into its testing 'blind' and with no basis for comparison. As the program progressed, interfacility comparisons became possible and extensive investigations were undertaken to discover the cause of the observed differences.

The General Test Plan called for a pre-test evaluation and declaration of measurement uncertainty and this eventually developed into a subsidiary investigation, which is reported here. The subject of error analysis is highly specialized and required rigorous treatment; this is exemplified by the error audit procedure developed by the North American test facilities and applied by each of the participating facilities. This was a valuable outcome of the UETP and resulted in better identification of error sources with consequent improvement in overall standards. In particular, the error analysis program demonstrated the importance of setting up procedures for checking all measurement systems and applying them continuously at all stages of the test program.

The measurement systems (including sensors, scanning devices, power supplies, transducers, cabling, data acquisition and processing equipment) used for the UETP differed widely among the various test facilities. Two common measuring system characteristics, however, were the use of electronic scanning and conditioning equipment and computerized acquisition and processing. The exception was the TUSAf measurement systems which included a large number of mechanical gages and manually recorded data. Although a common methodology was used to make the measurement uncertainty estimates, there is some flexibility in the definition of the elements of the measurement process and the allocation of the bias and precision errors for those elements. As a consequence, there was a much wider variation in the elemental bias and precision errors between facilities than for the estimated total measurement uncertainty for the engine performance parameters. The range of the estimated measurement uncertainties for some of the basic measurements and engine performance parameters at approximately the mid-thrust level of the engine power range tested are noted below. The ground level facility results correspond to standard day test conditions; the altitude facility results correspond to an engine inlet temperature of 288°K and a low altitude ( $P_2 = 82.7\text{ kPa}$ ) and high altitude ( $P_2 = 20.7\text{ kPa}$ ) test condition.

Range of Estimated Uncertainties

BASIC MEASUREMENTS	Ground Level Facilities		Altitude Facilities	
	P2 = 101.3 kPa	P2 = 82.7 kPa	P2 = 20.7 kPa	P2 = 20.7 kPa
Scale Force	FS $\pm$ 0.4 to 0.5%	$\pm$ 0.3 to 0.7%	$\pm$ 0.6 to 3.0%	
Fuel Flow	WF $\pm$ 0.4 to 0.6%	$\pm$ 0.2 to 1.17	$\pm$ 0.5 to 1.6%	
Engine Inlet Pressure	P2 $\pm$ 0.2 to 0.3%	$\pm$ 0.1 to 0.5%	$\pm$ 0.1 to 1.2%	
Engine Inlet Temperature T2	T2 $\pm$ 0.3 to 0.8%	$\pm$ 0.3 to 0.6%	$\pm$ 0.3 to 0.4%	

ENGINE PERFORMANCE PARAMETERS				
Net Thrust	FNRD $\pm$ 0.5 to 0.6%	$\pm$ 0.4 to 1.2%	$\pm$ 1.6 to 3.2%	
Specific Fuel Consumption	SFCRD $\pm$ 0.9 to 1.2%	$\pm$ 0.6 to 1.7%	$\pm$ 2.1 to 3.5%	
Airflow	WAIRD $\pm$ 0.3 to 0.7%	$\pm$ 0.4 to 0.8%	$\pm$ 0.8 to 2.6%	

Key contributions of the UETP measurement uncertainty assessment to the AGARD participating countries are:

- Major advances in the assessment and communication of data quality were made by the AGARD turbine test community during the course of this program. A single methodology for estimating the bias limits, precision indices, and overall uncertainties of the measured and calculated engine performance parameters was adopted for the UETP. Implementation at each facility followed local practice.
- The UETP provided a quantitative evaluation of the quality of the different measurement methods and equipment in use at the various facilities. In no case were all of the best features concentrated at a single facility. Thus, a systematic basis is now available for each facility to identify and implement future improvements in test capability.
- Engine speeds had the lowest uncertainty of the performance parameters. However, due to sensitivity (curve shift) effects, comparisons of performance on the basis of engine speed do not necessarily give the lowest overall uncertainty. Engine specific fuel consumption had the largest predicted uncertainty of the performance parameters. The other key performance measurements, thrust, fuel flow and airflow, lay between these extremes. Two measurement systems were specially notable for demonstrated low measurement uncertainty within their category, i.e. the positive displacement fuel flow meters at RAE(P) and the sonic airflow meter at AEDC.
- Well-established national test centers have been provided an incentive to improve their turbine engine test measurement techniques by adopting better methodology, procedures and equipment.

Finally, the extent to which the UETP has been of value and will lead to improvements in future measurement techniques will depend upon actions taken by each participating facility. However, there is no doubt that the growth in knowledge of better ways of assessing and understanding test facility measurement uncertainties will be reflected in an improved and more standardized test operation for all the participating countries.

I INTRODUCTION

The UETP is one of the most extensive experimental and analytical programs ever sponsored by AGARD. The program was proposed by the Propulsion and Energetics Panel and approved by AGARD in 1980. The objectives of the program were:

To provide a basis for upgrading the standards of turbine engine testing within AGARD countries by comparing test procedures, instrumentation techniques and data reduction methods, thereby increasing confidence in performance data obtained from engine test facilities.

To compare the performance of an engine measured in ground level test facilities at<sup>1</sup> in altitude facilities at the same non-dimensional conditions and establish the reasons for any observed differences.<sup>2</sup>

The UETP involved testing of two turbojet engines in five countries (US, Canada, France, Turkey and UK) using four altitude test facilities and four ground-level test beds. The testing program began in 1981 and extended over a period of approximately seven years, with the supporting data analysis program progressing concurrently on a cooperative multi-national basis. The program has an historic importance in that for the first time it has made possible test program over a range of altitudes and flight speeds, in different facilities, and using different methods of data acquisition and processing.

The test facilities which participated in the test program are noted in the order of testing and with comments on the type of test program.

National Aeronautics and Space Administration (NASA)	2 engines at altitude
Arnold Engineering Development Center (AEDC)	2 engines at altitude
National Research Council of Canada (NRCC)	2 engines at ground level
Centre d'Essais des Propulseurs (CEPr)	2 engines at ground level
Turkish Air Force Overhaul Base (TUAf)	1 engine at altitude
Royal Aircraft Establishment Farnborough (RAF(P))	1 engine at ground level
Naval Air Propulsion Center (NAPC)	1 engine at altitude (open air facility)
	1 engine at ground level

NOTE: NASA and NRCC performed repeat testing prior to testing at NAPC.

At the commencement of the program a General Test Plan (GTP, Ref.1) was prepared which defined the location and extent of the referee instrumentation, the test conditions, the test procedure, and the equations to be used for calculating the engine performance parameters. Test results were only interchanged between facilities after each completed their test program so that each facility went into its testing 'blind' and with no basis for comparison. As the program progressed, interfacility comparisons became possible and extensive investigations were undertaken to discover the cause of the observed differences.

To quantify interfacility differences attributable to measurement systems and to provide a common basis for comparisons of the quality of different measurement systems, the

GTP called for an evaluation and declaration of measurement uncertainty based on the methodology developed by Dr. R.B. Aherne and J.W. Thompson (Ref.2). The initial measurement uncertainty estimates differed widely between the different test facilities, therefore it was proposed to go into further detail in the estimation procedure. To this end the North American facilities put together an Error Audit (Ref.3) which all participants were requested to follow to clarify the differences in the uncertainty results. A Sub-Group on Uncertainty Assessment was formed (see Appendix I - J.P.K. Vleghert, Chairman) which met for the first time in Paris from 29 April - 3 May 1985. This meeting, which was very helpful in clarifying the procedures used by the different facilities, is reported in Ref.4. Subsequent meetings of the Sub-Group were held at RAE(P) in November 1987 and February 1988 and at NRCC in July 1988.

The present report includes a review of the UETP measurement uncertainty methodology as it was finally implemented and the measurement systems used at each facility for engine performance determination. Samples of the detailed information provided by each facility are shown and a detailed comparison of the measurement uncertainties and a discussion of some of the major differences are presented. The elemental error values are mainly a question of classification, and this differed in detail between the participants. The information presented is a compilation of the reports on data uncertainty from the different facilities, given as Refs.5-11. Comparison of the facility measurement uncertainty estimates with test data results is contained in the main report of the Working Group (Ref.12).

## 2 TEST PROGRAMME

Two engines were made available for the programme and it was intended that both would be tested in each of the participating facilities thus providing a back-up in the event of failure of one engine. However, restrictions on facility availability resulted in only one engine being tested in the altitude facilities at CEPr and KAE(P) and one on the ground level bed in Turkey and at NAPC.

Due to a higher priority workload it did not prove possible to undertake testing at NAPC until after the other UETP tests had been completed and the major part of this Report compiled. For this reason the NAPC uncertainty results are reported separately in Appendix II, and are not discussed in this report. The chronological order of testing and the types of test are shown in Table 2-1:

TABLE 2-1 - UETP TEST CHRONOLOGY

FACILITY	ALTITUDE		GROUND LEVEL		
	ENGINE	607594	615037	607594	615037
NASA (FE)	US	T	T	NT	NT
AEDC	US	T	T	NT	NT
NRCC (FE)	Can	NT	NT	T	T
CEPr	Fr	T*	NT	T	T
RAE (P)	UK	T	NT	NT	NT
TUAF	TU	NT	NT	NT	T
RAE (P)	UK	T	NT	NT	NT
NASA (SE)	US	T	T	NT	NT
NRCC (SE)	Can	NT	NT	T	T
NAPC	US	NT	NT	NT	T

T = Tested      NT = Not Tested      T\* = Test Aborted

FE = First Entry (first test series)    SE = Second Entry (second test series)

### 2.1 Test Article

Two J57-19W non-afterburning turbojet engines, were furnished by the US Air Force for the UETP, with serial numbers F607594 and F615037. The basic J57 engine is a two spool axial flow machine with a nine-stage low pressure compressor, seven stage high pressure compressor, canular combustor, single stage high pressure turbine, two stage low pressure turbine and fixed convergent nozzle with a tail cone extending through the nozzle exit plane. The only variable geometry features are the intercompressor on/off bleed which discharges air overboard during starting and low power operation and the aerodynamically coupled spools. This limited variable geometry ensured better repeatability of performance than would be the case with mechanically controlled variable incidence vanes and/or exit nozzle. The engine was of a size which made it acceptable for tests in the facilities under consideration. The fact that, by modern standards, it is of modest aero-thermodynamic design was of no consequence.

The trilcone on the standard J57 engine extends through the nozzle exit plane and it was felt that this arrangement would make it difficult to determine with sufficient accuracy the nozzle flow and thrust coefficients, parameters considered to be of prime importance in establishing engine performance.

Accordingly the standard nozzle was replaced by a cylindrical tailpipe and a convergent nozzle, fabricated by rolling sheet metal, to provide a more uniform nozzle profile as well as providing a more suitable platform for the pressure and temperature instrumentation needed to establish the nozzle inlet conditions.

## 2.2 Test Instrumentation

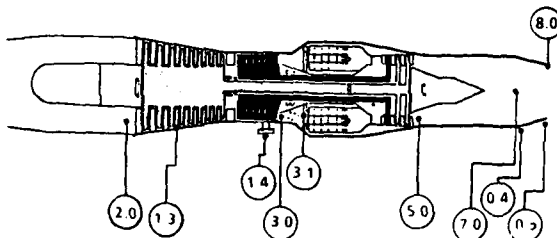
The instrumentation package was divided into two categories: facility peculiar, or primary instrumentation, and engine peculiar or referee instrumentation (fig. 2.1). The primary instrumentation was that used to measure those parameters required to calculate inlet total airflow, net thrust and specific fuel consumption (SFC) and pressures and temperatures to monitor test cell environment and engine oil condition. The referee instrumentation was used to set test conditions, monitor engine health, and record engine performance retention. It consisted of pressure and temperature probes at the engine inlet, combustor inlet (high compressor discharge), turbine discharge, exhaust nozzle inlet, and exhaust nozzle trailing edge. Referee instrumentation also included speed sensors, turbine type fuel flow meters and associated thermocouples, and vibration pickups.

Special attention was directed to the measurement of the total pressure and temperature at the compressor inlet (Station 2) and the static pressure at the nozzle outlet (Station 0.5) as these parameters have a critical influence on engine performance.

A special engine inlet bullet-nose was manufactured and used in conjunction with an instrumentation spool piece which contained an array of total pressure rakes, temperature rakes and boundary layer probes. These provided 20 mainstream total pressure measurements, 10 mainstream total temperature measurements with 16 and 10 probes measuring the total pressures in the boundary layers adjacent to the outer and inner walls respectively of the inlet annulus. Details of the location of the rakes and probes are given in Figure 4 on Page 92 of Reference 1.

PAME was measured using probes attached to the outside of the nozzle at Station 0.5. Details of the probes and their location are given in Ref. 1. Instrumentation was provided at the high pressure compressor discharge. This instrumentation provided data for some of the component performance calculations.

The locations for the majority of the instruments are shown schematically in Figure 2-1. The numbering system used to identify internal engine stations is in general agreement with SAE ARP 755A recommendations and is not the one traditionally assigned to this engine.



ENGINE INSTRUMENTATION STATION LOCATIONS

STATION NUMBER	DESCRIPTION	NUMBER OF MEASUREMENTS				
		PRESSURES			TEMPERATURES	
		TOTAL	STATIC	DYNAMIC	TOTAL	SKIN
2.0	ENGINE OR LPC INLET	46	8	2	10	2
1.3	LPC BLEED ANNULUS	0	1	0	0	0
1.4	LPC BLEED PORT	2	0	0	4	0
3.0	COMBUSTOR INLET (HPC DISCHARGE)	6	0	0	6	0
3.1	COMBUSTOR DIFFUSER EXIT	0	2	0	0	0
5.0	LPT EXIT	1	0	0	5	0
7.0	EXHAUST NOZZLE INLET	36	4	0	36	4
8.0	EXHAUST NOZZLE EXIT (INTERNAL)	0	0	0	0	0
0.4	EXHAUST NOZZLE (EXTERNAL)	0	4	0	0	0
0.5	EXHAUST NOZZLE EXIT (EXTERNAL)	0	4	0	0	2

Fig. 2.1 UETP Engine Referee Instrumentation

### 2.3 Test Conditions

#### 2.3.1 Altitude Testing

In an altitude facility it is possible to vary independently the three major parameters affecting engine performance - inlet total pressure, inlet total temperature and ram ratio.

When choosing the matrix of test conditions for the UETP, it was decided to vary each of these major parameters in turn while keeping the other two constant. In this way the effects of each on the engine performance could be examined.

The range of conditions selected was to a large extent determined by the capabilities of the participating facilities, but it was agreed that it was desirable to cover as wide a range as possible. Accordingly the following conditions were chosen:

TABLE 2-2 - UETP TEST CONDITIONS  
(Extract from Table III of Reference 1)

TEST CONDITION	INLET TOTAL PRESSURE		INLET TOTAL TEMPERATURE	RAM RATIO
	KPa	K		
1	82.7	253	1.00	
2	82.7	268	1.00	
3	82.7	288	1.00	
4	82.7	308	1.00	
5	82.7	288	1.06	
6	82.7	288	1.30	
7	51.7	288	1.30	
8	34.5	288	1.30	
9	20.7	288	1.30	
10*	82.7	288	1.70	
11	101.3	288	1.00	

\* Optional sea level static test condition for altitude facilities

It will be seen that conditions 1, 2, 3 and 4 examine the effect of inlet temperature; conditions 6, 7, 8 and 9 the effect of inlet pressure and conditions 3, 5, 6 and 10 the effect of ram ratio.

At each test condition data scans were taken at nine engine power settings approximately equally spaced between the engine power settings for "bleeds just closed" to Military power. The speeds used are given in Reference 1, they generally varied from 87 to 96% for NH and 85 to 100% for NL. The test sequence for the nine power settings was chosen to reduce the effect of hysteresis and thermal equilibrium effects; it is graphically represented in fig.2-2.

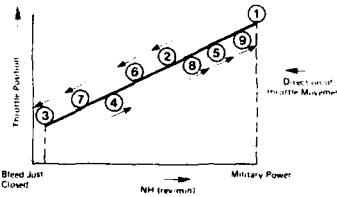


Fig. 2.2 Power Setting Sequence

When approaching each setting the throttle lever was moved slowly towards the throttle position where the required speed was expected to be achieved and the engine allowed to stabilise. The set speed had to be within  $\pm 25$  rpm of the desired. In going between two set speeds, the throttle direction was not allowed to change. In the event of a speed overshoot outside the tolerance band, the throttle setting was backed off approximately 100 rpm (appr one %) and the speed reset.

At each power setting two data scans were obtained. The intent was to obtain stabilised engine aerodynamic performance (ie. stabilised gas path). It was experimentally established that stabilised performance could be assessed after five minutes at set conditions for the initial data scan and after two minutes for the repeat data scan. Tests to confirm these values are described in Ref.12).

#### 2.3.2 Ground Level Testing

For ground level testing, two regions of engine operation were specified.

- Engine power settings from the 'bleeds just closed' speed to mil power (ie. same as for the altitude facilities).
- Engine power settings from the 'bleeds just open' speed to idle power.

As ground level test beds do not have environmental control, the engine power settings had to be established for the test temperature. For the high power region, values of NH were established for bleed valve closed and mil power. By dividing up the test range into 8 equal increments, 9 values of NH were obtained.

The sequence of power settings was the same as detailed in fig 2.2. Two data scans after engine stabilisation were taken at each test condition. For the low power region, the speed range between idle and bleed valve closure was also divided up into 9 equally spaced values of NH and the power settings sequenced in the same manner as for the high speed range.

#### 2.4 Data Scan Changes During Testing

At each Test Condition it was planned that a total of 18 data points would be obtained (ie two data scans at each of the nine power settings). The actual number of data points used at each test facility when analysing the test results is presented in Table 2-3. Variations from the plan were the results of differing facility practices, facility limitations or identified data faults.

TABLE 2-3 NUMBER OF DATA POINTS USED FOR ANALYSIS  
a) Engine S/N 607594

Test Condition	Planned Data Points	Actual Data Points					
		NASA(FE)	AEDC	NRCC	CEPr	RAE(P)	TUAF
1	18	18	17	-	18	9	-
2		18	18	-	18	9	-
3	-	16	-	16	8	-	-
4		18	16	-	16	18	-
5		18	18	-	15	9	-
6		18	18	-	17	9	-
7		18	19	-	18	9	-
8		20	18	-	18	9	-
9		18	18	-	18	17	-
10		19	16	-	18	9	-
11		-	18	18	18	-	-

b) Engine S/N 615037

Test Condition	Planned Data Points	Actual Data Points					
		NASA(FE)	AEDC	NPCC	CEPr	RAE(P)	TUAF
1	18	18	17	-	-	-	-
2		18	18	-	-	-	-
3		20	17	-	-	-	-
4		17	17	-	-	-	-
5		17	18	-	-	-	-
6		18	16	-	-	-	-
7		21	17	-	-	-	-
8		18	18	-	-	-	-
9		18	18	-	-	-	-
10		19	18	-	-	-	-
11		-	18	16	16	-	16

#### 2.5 Measurement Uncertainty

The GTP (Ref. 1) specified that each participant provide an estimate of steady-state measurement uncertainty for engine airflow, net thrust and specific fuel consumption at Test Condition 11 (Refer to Table 2-2) for ground-level facilities, and Test Conditions 3 and 9 (Table 2-2) for altitude facilities. It should be noted that all measurements considered in this report are steady-state. During the course of the UETP, the Uncertainty Sub-Group expanded these requirements to include Test Condition 6 (Table 2-2) for altitude facilities and uncertainty estimates for basic measurements (i.e., speeds, pressures, temperatures). Measurements uncertainties for each test condition were estimated at approximately the mid-thrust point.

### 3 UNCERTAINTY METHODOLOGY

#### 3.1 Introduction

The General Test Plan (ref.1) requires each participant to provide a pre-test estimate of measurement uncertainty using the methodology developed by Dr. R.B. Abernethy and J.W. Thompson (ref.2). In this Section of this report an overview of the Abernethy methodology as applied to the UETP is presented, including material from ref.2) and some of his later work (ref.13). In addition the practices in use by some of the participants are mentioned. Appendix III and IV list the nomenclature and terminology used in uncertainty work.

Pre-test estimates of uncertainty are usually based on contributions to the overall errors determined from previous test programs, which then are used in a combination which can be unique for the test under consideration. A part of the test data analysis, which can be done during or after the test, is to check whether the errors conform to the pre-test estimate and to calculate the post-test estimates of uncertainty at the target point values.

### 3.2 Error Types

Definition of the measurement process is a prerequisite to determining measurement uncertainty estimates. A Defined Measurement Process (DMP See Appendix IV, Glossary) consists of the procedure used to arrive at a desired test result identifying all measurements involved including calibration of all instrumentation and installed systems. In making the uncertainty analysis, all the elemental errors which affect the DMP must be identified.

In ref 2, elemental error sources are classified as either precision (random) errors or bias (fixed) errors. Using this criterion, any errors which vary in the DMP are classed as precision, while fixed errors are bias. This criterion then has the consequence, that errors may change class according to the DMP used to define the uncertainty estimates.

For the UETP, different DMP's were employed by each of the test facilities to make pre-test predictions, test assessment and post-test analysis. For instance, the RAE(P) DMP covers the uncertainty predictions and assessment of a single engine performance curve fitted (by least squares) to the test results for the nine engine power settings at a specified test condition. RAE(P)'s estimated Precision Index is then based on the predicted data scatter that will occur about a curve fit through the nine power settings. The predicted Precision Index is then verified by a post-test determination using a third order curve fit through the test data and observing the residual standard deviation about the curve fit. Using the RAE(P) DMP, differences between a collection of curves, representing different test conditions and day-to-day variations are classified as bias.

In contrast, the DMP used at AEDC for the UETP is based on the results of the overall measurement program for a given installation. Therefore estimates of the Precision Index at AEDC reflect the variation in the test results at the mid thrust point, at a specified test condition for a given measurement system and test installation and also includes the variations that would result from day to day tests.

The above error types remain after the measuring process has been carried out as well as man can do it; i.e. mistakes and malfunctions (like leakage) have been eliminated. This elimination can be done by careful control that the right calibrations have been used and comparing redundant instruments or measurements, which in general requires a post-test analysis. In the following Sections definitions of Precision Error, Bias Error and Uncertainty Interval are adapted from Ref.2 and 13.

#### 3.2.1 Precision (or Random) Error

Precision Error is seen in repeated measurements of a single value. Measurements do not and are not expected to agree exactly. There are always numerous small effects which cause disagreements. The variations between repeated measurements within one DMP can be quantified by the Precision Index or Sample Standard Deviation

$$S = \sqrt{\sum(x_i - \bar{x})^2 / (N-1)}$$

where  $\bar{x}$  is the average value of  $N$  individual measurements  $x_i$  in the sample. (See Appendix IV, Glossary).

#### 3.2.2 Bias (or Fixed) Error

The second error component is the systematic error, which is constant for repeated measurements and can only be determined by comparison with the true value of the quantity measured. This is normally impossible within a single DMP, but the tests can be arranged - possibly in different DMP's - to provide some bias information. Examples are:

- a) Interlab and Interfacility tests on measurement devices, test rigs, and full scale engines.
- b) Special comparisons of (lab) standards with the measuring instruments during the test, eg incorporating a standard in the scanning cycle.
- c) Employing redundant instruments or measuring techniques.

Large differences can usually be attributed to a mistake but this progressively gets more difficult as the size of the difference reduces. Hence one tends to be left with small unexplained differences, which constitute part of the bias limit. There can be common bias elements in the DMP's compared at any one facility, which may or may not be found by interfacility comparison.

#### 3.2.3 Combined Error

For comparison of measurement results a single number is desirable to express a reasonable error limit. This must be a relevant combination of bias and precision. The latter value is a statistic, which lends itself to the calculation of confidence limits, within which the actual value can be reasonably expected to lie in the absence of bias error. It is however impossible to define a single rigorous statistic for the total error, because bias is an upper limit, which has unknown characteristics, and is to some extent dependent on engineering judgment. A working solution is given in Section 3.5.

### 3.3 Error Evaluation

#### 3.3.1 Data Sequence

Basically a single measuring chain stretches from flow field via probe and connecting line to the transducer, and from there usually via an electric line - sometimes pre-amplified - to multiplexer, amplifier and signal conditioner to be recorded. Afterwards the signal is played back, an instrumental calibration applied, and a number of single measurements combined to determine a value representative for the flow field, usually by averaging in space and/or time. These Basic Measurements are then used to calculate the Engine Performance Parameters (EPP), which are in referred form and constitute the end product of the measurement, e.g. WAIRD = WA/0.5.

Each dependent EPP can be given as a function of (i.e. correlated against) an independent parameter which can be chosen at will (usually RPM or EPR). For comparison either within or between facilities it is necessary to determine each dependent parameter for one value of the independent parameter. This requires an interpolation procedure, as it is not possible to set the exact test condition and engine power.

### 3.3.2 Error Propagation

Each step in the above-mentioned data sequence contributes to the overall data error in its own specific way, which is treated below.

The first step is to assess the elemental errors, organized in four error categories (see 3.4.1) for both bias and precision, in a separate table for a single measurement of each basic physical parameter FS, WF, P2 etc., keeping bias limits  $B_i$  and precision indices  $S_i$  strictly apart. These are combined by Root-Sum-Square (RSS) addition to give the total  $B$  and  $S$  values for each single measurement. An important condition required to justify RSS combination is that each item must be independent.

Once the elemental errors have been estimated for each single measurement they can then be combined to obtain the  $B$  and  $S$  values of the average or the effective flow field value called a Basic Measurement. The resulting error estimate is further discussed in 3.4.2.

The next step is to propagate  $B$  and  $S$  separately for each basic measurement to the final performance parameter. This is done by multiplying the  $B$  and  $S$  values by the appropriate Influence Coefficient (IC). The overall effect on the performance result is found by RSS addition. (See chapter 3.4.3.).

$$\text{Thus } B(\text{perf. param.}) = \sqrt{(\sum_i (IC_i * B_i)^2)} \\ \text{and } S(\text{" " }) = \sqrt{(\sum_i (IC_i * S_i)^2)}$$

Only after the last step can a combined uncertainty be determined, as is indicated in Section 3.5.

Schematically the Error Propagation proceeds as follows; each step is detailed in the Sections 3.4.1 to 3.4

- 1) elemental errors in the determination of the basic physical parameters: pressure, temperature, force, length and time
- 2) errors in the determination of the Basic Measurements which define the effective values in the engine (sampling and averaging)
- 3) Influence Coefficients to determine the combined effect on the engine performance parameters
- 4) Curve Slope effect to determine the error in an engine performance parameter when read from a curve at a chosen value of the independent variable, which itself is not error-free. This has to be done with care, as both parameters may contain common sources of error and the error items are not then independent.
- 5) determination of the uncertainty by combining bias and precision values.

## 3.4 Error Sources

### 3.4.1 Elemental Error Sources

The Abernethy/Thompson method described in Ref.2 details the evaluation of the elemental errors.

Basically the elemental errors of a single measuring chain can be separated in four groups as follows:

- a) Calibration Hierarchy
- b) Data Acquisition
- c) Data Reduction
- d) Other Effects e.g. Non-Instrument Effects, Errors of Method, Sensor System Errors, Spatial Profile Sampling etc.

In conducting the elemental error audit for the UETP it was found that the error groups defined above were too general in scope for the purpose of conducting a detailed assessment of the facility measurement uncertainties. Instead it was necessary to define error subgroups for each of the test facility basic measurement systems. For instance, in defining force measurement elemental errors, the error group "Calibration Hierarchy" was subdivided into load cell laboratory calibration errors and test cell system in-place calibration errors. The error group "Other Effects" was subdivided into installation errors, environmental errors and probe errors. The UETP elemental error groups along with a definition of each error source are presented in Tables 3-1 through 3-6. The general definitions of the elemental error sources are given below.

- a) Calibration Hierarchy traces the possible instrument error back to the National Standard, usually in steps via a Working Standard, a Laboratory Standard and a Transfer Standard. In each step the original bias of the instrument is removed by the calibration and replaced by the (smaller) combination of systematic error of the reference instrument and the random error of the comparison.

The random error of the calibration process gives an uncertainty in the average of  $t95 * S/\sqrt{n}$ , which is fossilized into a systematic error. This approach permits determination of part of the bias error of the calibration hierarchy in a statistical manner, except for effects like long-term stability of the interim standards, which require a certain amount of engineering judgement to translate into measurement errors. When several calibrations are relevant the calibration process contributes both a systematic and a random error to the final test result. With enough (i.e. more than 30) points in the calibration the 95% confidence limit ( $t95$ ) of the resulting error due to scatter assumes the numerical value of twice the RMS value; with fewer points the Welch-Satterthwaite formula (see Ref.2) has to be used to calculate the combined  $t95$  value.

When successive calibrations differ more than  $\pm t95 * S/\sqrt{n}$  it is wise to analyse the history of a number of calibrations. If a systematic variation occurs with parameters like ambient temperature or instrument age this could be taken into account in the calibration, but usually the effect is random and therefore can only be assigned to precision error. One source of random error is caused by the instrument manufacturer already having compensated for the average temperature sensitivity in the design of the instrument. Variation of the outcome of this compensation network can introduce day-to-day errors; this can often be reduced by keeping the instrumentation system switched on day and night throughout the test.

b) Data Acquisition errors can be caused by slight variations in exciter voltage, outside influences on data transmission and on the transducer, signal conditioning and recording. The first three items cause non-repeatability. Another factor is sensor hysteresis; this usually depends on the measuring range and could be reduced if the sensor is only calibrated over the minimum range and if the measuring history is known. It could then be classified as bias. Usually this is not a practical proposition, anyway with modern instruments hysteresis is small.

The way the test is executed could introduce hysteresis or a bias through the engine, but that should be apparent in a systematic variation of the measuring points at different power settings relative to the curve fit. This effect will be discussed in Section 6.6.

Recording of the output of a single transducer is usually done in a matter of milliseconds or even less. To prevent aliasing errors, high-frequency components of the signal have to be eliminated by a low-pass filter. As this introduces some lag, a settling time has to be allowed in the case that a number of pressure probes is multiplexed on to a single transducer. Usually the tube transient - in the case of multiplexed pressure channels - can be made negligible by using a low-volume transducer which is close-coupled to the scanning valve. Of course overall faster sampling is possible if each channel is allocated to a separate transducer. If a low frequency variation is present, it is desirable to record a number of scans and average the results.

c) Data Reduction errors consist of resolution error and calibration curve fit errors and can usually be made negligible, compared with the other categories. An error of half the biggest error elsewhere only contributes 10% to the overall error when added RSS; therefore it is not effective to use extreme resolution in the computational hardware and software. Calibration curve fit errors can be minimized by choosing the appropriate functional relationship, qualified by visual and numerical inspection.

When a higher than second order curve fit is used it is important that the calibration points are spaced evenly, otherwise the densely populated part may introduce a calibration bias in the sparsely populated part.

d) Other Effects, Non-Instrument effects or Sensor System errors (including Errors of Method, Ref.14) are difficult to separate and as such are open to different interpretations. In general they are concerned with the interaction between the medium and the measuring chain. This is the case for design and fabrication of probes and hole patterns, which renders a measured pressure sensitive to flow angle.

Internal flow is nearly always non-uniform, both in space and in time, and not necessarily the same in different installations. This can give a bias error even when using the same referee instrumentation, both for pressure and temperature. A possible Error of Method is constituted by the assumption that static pressure is constant over the flow area of the parallel section of the inlet, where total pressure is measured.

The mechanics of the thrust stand can introduce bias and/or precision errors - notably in the thrust stand zero - which can not be determined exactly, not even in an end-to-end calibration as the conditions with a running engine are different from the calibration. The transducer zero can be checked mid-run by taking up the load separately, but the thrust stand zero can only be checked in quiescent conditions. Pre-test and post-test zero are different, and it is usually assumed - but without true justification - that the test zero lies in between.

Length and time can generally be measured very accurately, but when determining flow area the metal temperature must be known as well to compensate for growth. Engine speed and fuel flow depend on time measurement, but can be influenced by pulse shape and the fuel flow pulse rate by residual swirl in the fuel pipes after turning a corner, if turbine type meters are used. Fluid flow codes recommend 10-20 diameters of pipe straight section upstream and downstream of the flow meter, and preferably calibration in-situ, but discrepancies still exist. Determination of fuel properties (lower heating value and specific gravity) can introduce errors of 0,3 to 1% because of reproducibility and repeatability of evaluation methods (ref. 12 App VII).

### 3.4.2 Basic Measurement Error

Basic Measurements consist of the effective values of pressures and temperatures, rotor speeds, fuel flow and scale force i.e. the input parameters required for the engine performance calculations. The existence of time and spatially dependent pressure or temperature profiles across a duct makes it impractical to measure the exact mean value that determines engine performance, because that would require too many probes which would block the flow. Hopefully, a compromise can be achieved, that - while not being exactly thermodynamically correct - is sufficiently reproducible to allow engine performance to be determined with minimum variation. The uncertainty of effective pressure or temperature values obviously decreases with the number of probes. Although the precision component of the error decreases with  $1/n$ , this should not only be related to the - more or less known - transducer error, also the unknown pattern variation must be taken into account. More about these aspects is given in Section 4.1.

Failure of any probe in a multiple probe sensor system can alter the effective average value; this may specifically be noticed in the jetpipe, where profiles are pronounced and the chance of failure high. A four-rake system was used in the UETP, which was located behind the 8 spokes that fix the turbine bullet and rear bearing. Any failed probe value will be interpolated between the neighbouring probe values; extra rake arms were manufactured to replace arms with too many failed probes. The interpolation procedure used by each facility is documented in Ref 12 App. VI.

### 3.4.3 Influence Coefficients

The General Test Plan (Ref.1) gives the standard equations used to calculate engine performance parameters from the basic measurements. The influence of an error in any basic measurement on the outcome can be determined either by Taylor series expansion or numerically by perturbing the equation for a difference in that parameter, keeping all other parameters constant at their nominal value. The latter method is preferred when used with data reduction software because it accounts for implicit as well as explicit functional relationships. The resulting influence coefficient is usually expressed as a percentage variation of the calculated performance parameter (P) for a one percent deviation of a single input parameter (I).

$$\text{Influence Coefficient } IC = (\Delta P/P)/(\Delta I/I)$$

If the perturbation is small, non-linearity effects will be insignificant - but of course the value of the influence coefficient will vary over the operating range of the performance parameter and is therefore a function of engine power and test condition.

The bias and precision variation of the performance parameter can be determined by adding the product  $IC \cdot \Delta I/I$  Root-Sum-Square for all input parameters which appear in the equation; this must be done separately for bias- and precision errors to determine those values for the performance parameters. Examples for a typical test are given for the input parameters in Table 5-1. Since influence coefficients depend on several factors including the hardware installation and measurement configuration, direct comparison between facilities is not possible.

### 3.4.4 Curve Shift Effect

When comparing the value of an engine performance parameter (y), which is a dependent variable, - either within the facility or between facilities - it is necessary to read it from curves at a chosen value of an independent variable (z). The engine type has been selected to have only one independent variable at a fixed flight condition, but any variable in the engine can be chosen as this basis. Usually either  $NL/\sqrt{\theta_2}$ ;  $NH/\sqrt{\theta_2}$  or EPR are taken; different engine manufacturers have different preferences, also the selection is dependent on the engine type. Any uncertainty in the chosen independent variable translates into a discrepancy  $\Delta y$  in the performance curve (even though it has no effect on the individual y-values). The mechanism is illustrated in Fig. 3.1, in terms of bias limits.

Biases propagated directly to the Y-axis, shown as route P, are calculated by standard Abernethy methodology:

$$B_{y,\text{direct}} = \sqrt{\sum_i [B_{xi} \frac{\partial y}{\partial x}]^2}$$

where  $\frac{\partial y}{\partial x}$  are the Influence Coefficients. Similarly, biases propagated to the Z-axis, shown as route Q, are calculated as:

$$B_z = \sqrt{\sum_i [B_{xi} \frac{\partial z}{\partial x}]^2}$$

The  $B_z$  values do not affect the y-value of points on the graph, but they do affect the position of the fitted curve by shifting the points horizontally. Thus the y-value of the curve is given an extra bias, within the limits dependent on the slope ( $dy/dz$ ):

$$\begin{aligned} B_{y,\text{indirect}} &= B_z \cdot \frac{dy}{dz} \\ &= \sqrt{\sum_i [B_{xi} \frac{\partial z}{\partial x} \cdot \frac{dy}{dz}]^2} \end{aligned}$$

The total bias limits of the curve are therefore:

$$\text{total } B_y = \sqrt{B_{y,\text{direct}}^2 + B_{y,\text{indirect}}^2}$$

Strictly, a more refined theory should be used for any Basic Measurement that affects y and z simultaneously. In practice, however, the above theory is sufficiently accurate for the UETP.

As in a twin-shaft engine the percentage variation of NL is considerably larger than that of NH, the curve slope is less for parameters based on NL, and with that the resulting curve shift error is less. A drawback is that the relation between NL and engine performance parameters is only direct for Air Mass Flow therefore NL is not such a good basis for net thrust or SFC, at least not on a turbojet engine. EPR is a better correlating parameter for that case, but its measuring accuracy is not as good.

Because the RPM-based curve shift effect is large, the influence is often more than that of normal scatter or bias. If different performance parameters deviate in a pattern that is related to the different curve slopes, this points to a bias error in the basic parameter, that can be traced that way. This often is the case for temperature errors. In principle it is possible to set up a matrix of influence coefficients and solve it, using a Maximum Likelihood Solution approach. This method is extensively documented (ref. 15), but it is too complicated to set up for a single case and therefore it was not used in UETP.

### 3.5 Estimated Uncertainty.

It was mentioned before that a single rigorous statistic for the total error cannot be given, because bias is an upper limit, often based on judgment, which has some unknown characteristics. Usually the more or less arbitrary standard of bias plus a multiple of the precision index is used:

$$U = B + t_{95} * S$$

in which  $t_{95}$  is the 95th percentile point for the two-tailed Student's "t" distribution, defining the limits within which 95% of the points are expected to lie in the absence of bias error. If the predicted  $S$  is determined from a large number of points ( $n > 30$ ) the value  $t_{95} = 2.0$  can be taken; Monte Carlo simulations have shown that the coverage of  $U$  is about 99 percent (ref.16). This means that the comparable engine performance parameter results from all test conditions must be within a band of  $\pm U$ . If this is not the case either a data error exists or an important aspect of the uncertainty estimate has been overlooked. For the UETP the comparison was made at the target point, which was the mid point of the power range.

The target points for different test conditions cannot be measured at exactly the same value of the independent variable (eg RPM) therefore they must first be corrected to the target value of that independent parameter, using the linear slope determined from the results for the relevant test condition. A more accurate procedure is to determine the target point from a curve fit of the measurement results for that test condition.

### 3.6 Test Data Assessment

Where the pretest uncertainty analysis allows corrective action to be taken prior to the test to reduce uncertainties when they appear too large, the posttest assessment, which is based on the actual test data, is required to refine the final uncertainty intervals. It is also used to confirm the pretest estimates and/or to identify data validity problems. It can also be made to check for consistency if redundant instrumentation or calculation methods have been used in the data collection system.

Using this approach on-line, outliers can be flagged and the condition repeated while facility, engine and instrumentation are still running, thus saving time and resources. Comprehensive error analysis can of course not be performed on-line, but the test could be stopped if a drastic fault develops, resulting in a minimum of wasted effort. It is important to delete an outlier only after analysis and for good technical reasons; the analysis may show up otherwise hidden faults in the instrumentation or in the set-up of the experiment, or anomalies in the test article.

## 4 INSTRUMENTATION, DATA ACQUISITION AND CALIBRATION

### 4.1 Instrumentation

Reference instrumentation, consisting of inlet rakes and a modified tailpipe with rakes, developed by the first participant (NASA LeRC) is detailed in the GTP; the instrumentation system travelled with the engines, but each participant used its own transducers (except for the engine fuel flow) and recording system. Apart from the reference instrumentation each participant used its standard test cell instrumentation to determine engine performance, including separate fuel flow meters.

The main difference between altitude facilities and ground testbeds - apart from the air conditioning installation - is in the determination of net thrust. In the former case this includes a large inlet momentum term, which requires knowledge of the air mass flow. Usually this is measured separately with the facility instrumentation in a parallel section upstream of the engine. If a narrow cross-section is used flow velocity is high, with resultant high static depression and therefore good measuring accuracy. However, the possibility exists of degraded flow profiles in the diffuser leading to the compressor intake, which can influence the result, as is indicated in Ref.12. In one case (ALDC) air mass flow was determined with choked venturis, which give improved accuracy.

Detailed description of the relevant installations of the participants is given in App. V.

Determination of basic measurements entails averaging a certain parameter over the flow cross-section. This can be done by sampling a number of probes, each connected separately to its own transducer, by mechanically scanning or by manifolding, as is illustrated in fig.4-1. In most cases a combination of sequential scanning and multiplexing is used; the latter usually for the individual probes in a rake. Most facilities use mechanical scanning for pressures, where a number of pressure lines are connected in sequence to a single transducer. RAE(P) used electrical scanning at the time of the UETP testing, RAE(P) in one case used two transducers per tapping for the static pressure in the air meter, to further improve accuracy and estimate of instrument error. NASA's first entry used mechanical pressure scanning; for the repeat test the facility instrumentation has been changed to electrical scanning. All thermocouples are of course electrically scanned; all facilities use duplicated instruments for determination of scale force and facility fuel flow. Reference fuel property tests were done for all facilities at NRCC. (Ref. 12, App. VII).

In some cases the pressure scanning included a number of calibration points, that were also measured by a Working Standard. In this way an on-line calibration check can be affected. This is not possible with purely electrical scanning, but the system can be calibrated between tests; at NASA, the pressure systems are calibrated on command or automatically every 20 minutes, by switching all transducers over to a calibration manifold.

Individual transducers allow rapid scanning, allowing a number of scans to be made during one recording, but obviously require a large number of transducers. With electro-mechanical scanning minimum cycle time can be of the order of a few seconds for a short coupled, small transducer. In the order of one minute is required if line pressure stabilisation has to be allowed for, as is the case with large, high accuracy transducers which have a large internal volume. In this case it is more difficult to ascertain that engine and facility are stabilized. Manifolding to determine an average pressure with a single transducer must be done with restrictors between the different lines and the manifold; the probe heads sample pressures with flow through the holes. Both effects can result in bias errors relative to the case of scanning and mathematical averaging.

#### 4.2 Data Acquisition and Calibration

Differences in facility data acquisition and calibration methods can have a significant effect on measurement error; this is particularly true for pressure measurements. This Section presents the steady-state pressure measurement data acquisition and on-line calibration procedures used at each of the test facilities.

NASA used (in PSL-3) a multiple 24-port scanner valve system which included two separately measured calibration ports giving an on-line linear calibration. The scanner valve time was 4 secs; for the 24-ports one data point was obtained by averaging 5 cycles in a 20 sec period. Unsteadiness of engine and/or facility were signalled if the standard deviation of the cycle results exceeded a set tolerance.

AEDC used 12-port scanner valves with 2 check pressures and large volume high accuracy transducers. Settling time was 4 secs per port and data acquisition time of one second. During the data acquisition time a total of 50 samples was taken. Total cycle time for a data point was therefore one minute. The results were analyzed for outliers and engine/facility unsteadiness. The system is calibrated pre-test over the specified measuring range using eight pressure levels.

NRCC used 4 ranges of remotely installed capacitance type pressure transducers in a scanner valve arrangement. A scanning time of 5-10 secs per dwell with a sampling rate of 100 samples per second was used which resulted in a cycle time of about 6 mins. The pressure system was calibrated at the beginning and end of the test period.

CEPr used 24-port scanner valves with a cycle time of 6 secs, coupled to a 256 channel multiplexer. In each valve position 4 samples were taken. Pressure transducers were calibrated at 11 pressure levels and a second degree polynomial used to fit the data.

RAE(P) used individual transducers and in some cases 2 transducers per tap. The cycle was 5 secs, one data point consisted of 5 cycles. The results were analysed for outliers or excess scatter.

TUAF used manual registration, in many cases with taps manifolded to a single liquid-level manometer, or digital voltmeter in the case of thermocouples. The time required to record a data point was of the order of 5 mins.

### 5 UNCERTAINTY ESTIMATES

#### 5.1 Introduction

At the start of the UFTP bias and precision error estimates in airflow, net thrust and SFC were calculated and have been reported in the Facility Test Reports, (Ref. 5-11). An interim review showed large variations between facilities. To try and solve these an Error Audit form was put together by the North American facilities (Ref.3) which detailed the elemental errors in the measuring system for stand force, fuel flow, pressure, temperature, speed and area. The relevant error source diagrams are given as Table 3-1A/6A; with the error source description listed under B. All facilities have used this detailed Error Audit in their final Uncertainty Assessment (Ref. 5-11), except TUAF (Ref.10) which used simpler instrumentation and manual recording which is not amenable to assessment in such detail. Implementation at each facility followed local practice.

In most cases the range of test conditions was such that the variation of resulting basic measurement values and engine performance parameters was limited and not much difference was expected in the uncertainty level of each parameter over that range. The one exception is the intake pressure range in the altitude facilities, which varied by a factor of four, with attendant variation in fuel flow and scale force. Possible consequences are shown by reporting Uncertainty Estimates for both the high and the low altitude case.

Parameter values do not differ much between an altitude facility at low altitude and a ground test bed, but in this case instrumentation differences may play a role. The following section 5.2 compares the error estimates made by each facility for the basic measurements and section 5.3 the error estimates for the calculated performance parameters.

The Assessment Reports of the individual facilities (Ref. 5-11) often contain a great deal more data and can be referred to if more explanation is needed than can be given within the scope of the present report.

#### 5.2 Errors in Basic Measurements

Review of the elemental error audits from each test facility revealed a wide variation in the allocation of the bias and precision errors for each of the basic measurement systems. Figures 5-1 through 5-3 give the facility error audit results for scale force, fuel flow and pressure at Test Conditions 6 and 9. The results for Test Condition 3 are essentially a repeat of Test Condition 6 and therefore for the sake of clarity were not added to the figures. Also, included on the figures are the results for NRCC corrected to standard sea level Conditions (Test Condition 11). There is felt to be sufficient similarity between Test Conditions 3 and 11 for a direct comparison to be meaningful. The error audit results for CEPr's and TUAF's ground-level stand were not available for inclusion.

The variation in the elemental errors among the test facilities was attributed to the differences in the facility measurement systems and practices (App.V) and to the differences in definition of the elements of the measurement process. This flexibility in the definition of the elements, resulted in differences for the allocation of the bias and precision errors at the various facilities. For example, hysteresis errors were typically assessed by NRCC and RAE(P) to be bias and by AEDC and NASA to be precision. Another example is the classification of the error from repeated application of the calibration pressure standard to the pressure measurement system. RAE(P) classified this type of error as a bias, NASA as a precision and AEDC as part bias and part precision. This reflects the differences in calibration procedure and error assessment, which are indicated in Section 3 and 4.

Figure 5-4 summarizes the Root-Sum-Square of the elemental bias errors,  $B$ , and estimated uncertainty  $B+2S$ , for each of the basic measurements. Mainly as a result of the difference in Defined Measurement Process mentioned in 3.2 NASA and AEDC attributed a larger portion to precision error than did CEPr and RAE(P). Even with these differences however, there is an overall agreement among the facilities of better than one percent when combined errors (ie  $B+2S$ ) are considered.

The following overview is given of the error estimates that the different facilities have given for the basic measurements scale force, fuel flow, compressor inlet pressure and temperature, rotor speed, and area measurement.

#### 5.2.1 Scale Force

The estimated bias and precision of scale force at Test Conditions 6 agree within 0.5% between the different facilities; AEDC reports lower estimates at Test Condition 9 than the other facilities (Fig.5-1). NASA's largest bias limit in scale force is attributed to data reduction, followed by data acquisition and calibration. The largest bias at NRCC is environmental effects; for RAE(P) it is test cell system calibration, followed by instrument calibration and data reduction. At RAE(P) the difference between pre- and post test zero is the largest contribution to thrust cell bias, even after updating the reading for the average difference per test.

#### 5.2.2 Fuel Flow

NASA has the highest bias and precision estimate for fuel flow (Fig.5-2) mostly caused by data acquisition (precision) and data reduction (bias). The AEDC values are evenly spread over the contributory categories. AEDC and NRCC include an effect for the determination of calibration fluid properties, which the other facilities do not explicitly include, while RAE(P) accounts for it separately. RAE(P) uses displacement fuel flow meters and reports the lowest errors. However, an influence of reduced flow rate causes the bias to increase at Test Condition 9. All facilities agree in having little or no percentage increase in error at altitude due to use of multiple range flow meters whereas RAE(P) used a single range meter for both low and high altitude.

#### 5.2.3 Compressor Inlet Pressure

Pressure error is evaluated for the total value at the compressor inlet (Fig.5-3). The absolute pressure varies more than a factor of four over the simulated altitude range. From calibration hierarchy, NASA claims only a precision error, AEDC and RAE(P) only a bias error. Furthermore NASA and NRCC include a small probe effect, while AEDC, RAE(P) and CEPr have none. The largest NASA effect is hysteresis error in the transducers; the largest AEDC contribution is data acquisition. All of the participants have taken their number of transducers in account in determining the precision error. RAE(P) included a separate effect to account for bias error resulting from pattern variations.

#### 5.2.4 Compressor Inlet Temperature

The individual error sources of T2 are not presented, but Fig.5-4 shows the RSS totals as percentages. Most facilities agree in having a temperature bias limit at the compressor inlet with the absolute value in the order of 1 C (0.35%), the lowest estimate being 0.5 C (AEDC), the highest 1.2 C (NASA). CEPr claims a bias limit for the facility of 0.6 C, using resistance probes. Precision errors are 0.3-0.5 C, except for zero to 0.25 C at CEPr. RAE(P) claims no difference in measurement error between platinum resistance probes and thermocouples.

#### 5.2.5 Rotor Speed

AEDC (Ref.6) has a rather high bias error of 0.2% or 11 LPRPM, resulting from signal conditioning and frequency calibration, while NASA (Ref.5) claims 0.02% (0.8 RPM) from the same source. AEDC converts from frequency to analog and then to digital, while NASA counts time interval between pulses to give a direct digital output. Possibly the averaging system also has an influence, especially as RPM is the parameter that is apt to vary slightly in a periodical manner.

#### 5.2.6 Area Measurement

The measurements of nozzle area by four facilities (Ref.12) section 6.1.3 showed a maximum variation of  $\pm 0.13\%$  from the average, which is insignificant. Metal expansion makes a difference of 0.2%/100° C, but this has been taken into account.

#### Summary of 5.2.

In summary, the percentage range of the facilities estimated uncertainties for the UETP basic measurements are shown below for test condition 3,9 and 11

Altitude	Facilities	NL;NH	P2	T2	WF	FS
(TC3)	P2 = 82.7 kPa	$\pm 0.02$ to $0.5\%$	$\pm 0.1$ to $0.5\%$	$\pm 0.3$ to $0.6\%$	$\pm 0.2$ to $1.1\%$	$\pm 0.3$ to $0.7\%$
(TC9)	P2 = 20.7 kPa	$\pm 0.02$ to $0.5\%$	$\pm 0.3$ to $1.2\%$	$\pm 0.3$ to $0.4\%$	$\pm 0.5$ to $1.6\%$	$\pm 0.6$ to $3.0\%$

Ground Level Test Stands  $\pm 0.02$  to  $0.5\%$   $\pm 0.2$  to  $0.3\%$   $\pm 0.3$  to  $0.8\%$   $\pm 0.4$  to  $0.6\%$   $\pm 0.4$  to  $0.5\%$   
(TC11) P2 = 101.3 kPa.

### 5.3 Errors in Calculated Engine Performance Parameters

The results of the error propagation from the basic measurements to bias and precision estimates for engine performance parameters are presented in Tables 5-2 to 5-7. For comparison purposes in the present report and for inter-facility data review in ref 12, the details of the bias and precision estimates are shown in Figure 5-5 for referred airflow, thrust and SFC. Although the influence of the individual facility's DMP, error accounting and test equipment is visible, bias limits are within 0.5% at TC6, and 0.7% at TC9; the values at TC9 are significantly greater. At TC9, NASA quoted the highest value for net thrust. For Test Condition 9 CEP had to use back-up instrumentation so their results for this case are based on the values for Condition 8. The precision index values (Fig 5-5) for NASA and AEDC are about twice those of the other facilities for specific fuel consumption at Test Conditions 6 and 9. All facilities except AEDC show significant increase with altitude. The estimated precision index of the AEDC result is slightly more than the bias limit whereas the estimated precision for CEP, and RAE(P) is less than the bias limit estimates.

The bias and precision limits for the ground-level test bed at NRCC are comparable to those at altitude facilities for Test Condition 6 (Figure 5-5).

In addition to airflow, thrust and SFC, other engine performance parameters were used in the UETP. The percentage range of the facilities estimated uncertainties for the UETP calculated engine performance parameters, are shown below from Tables 5-2 through 5-7:

Altitude Facilities	NHRD	NLQNH	P7Q2	T7Q2	WAIRD	WFRD	FNRD	SFCRD
TC6 P2 = 82.7 kPa	0.2-0.5	0.02-0.7	0.1-0.7	0.3-0.6	0.6-0.8	0.4-1.3	0.5-1.2	0.6-1.7
TC9 P2 = 20.7 kPa	0.2-0.5	0.02-0.7	0.5-1.1	0.3-0.6	0.8-2.6	0.4-1.7	1.6-3.2	2.1-3.5
Ground Level Test Stands								
TC11 Pa = 101.3 kPa	0.4-0.7	0.1-0.8	0.2-0.3	0.5-0.9	0.3-0.7	0.4-1.1	0.5-0.6	0.9-1.2

## 6 DISCUSSION

Discussion of the different practices in instrumentation and error evaluation within the facilities will of necessity be limited to primary factors which affect the uncertainties. Further details can be gathered from the facility Uncertainty Assessment reports (Ref.5-11). The comparison between facilities is contained in Ref.12.

### 6.1 Validation within the Facility

A schematic of the data flow up to determination of the desired engine performance parameter is given in fig.6-1. The first column lists the four elemental error sources which influence the uncertainty in the basic physical parameters given in the second column.

The third column gives the basic measurements obtained by averaging over the flow area and/or over the data collection period. If more than one scan is used, deviations from known patterns can be checked for broken or leaking probes. Variation between scans is often monitored; it can indicate insufficient stabilisation of engine or facility, or other trouble.

From the basic measurements the engine performance parameters are calculated; the data flow is indicated in fig.6-1. As the number of power settings within one test condition accumulates some of these performance parameters (y) can be curve fitted on-line against an independent variable(z), such as RPM/V<sub>0</sub> or EPR. If outliers are detected, power settings can be repeated while engine, facility and instrumentation are still running, which reduces measurement errors. To prevent small differences in setting up of the test condition playing a role in this scatter, the performance parameters first have to be reduced to referred conditions as indicated.

In first instance, checks consist of making sure the proper data is used. If calibration points are included in the scan these can be used to check the transducer and data reduction during data acquisition, otherwise the quiescent conditions pre- and post test are used as a check, mainly for bias errors. In the last column of fig. 6-1 further checks are indicated making use of thermodynamic relations, nozzle coefficients and duplicated instrument systems. Some of these checks have been performed inter-DMP and inter facility, and are reported in Ref.12. The estimated uncertainties give a yardstick for judging whether an observed difference is scatter, bias or mistake.

### 6.2 Error Variation over Transducer Range

In reporting the pressure uncertainties, three types of error models were used; (1) constant absolute error model, (2) constant percent error model, and (3) linear error model.

NASA uncertainties were reported using the constant absolute error model. This is typically presented in instrument manufacturers' brochures where the instrument error is usually given at Full Scale Output (FSO) and assumed constant in absolute value over the whole range (see Fig.6-2). This approach results in a pessimistic estimate of uncertainty at the low end of the measurement range.

AEDC used the constant percent error model with the error specified at the 10 percent FSO. It was assumed that the percent error over the interval from 10 percent FSO to FSO was constant. From zero to 10 percent FSO a constant absolute value of error was assumed (see Fig.6-2). The use of the constant percent error model evaluated at 10 percent FSO results in a pessimistic estimate of uncertainty at the high end of the measurement range.

RAE(P) used the linear error model. This consisted of determining the error at both zero input and FSO and then assuming that the error values varied linearly between the zero input and FSO error values. In conjunction with a gauge pressure system, in which pressures are measured relative to barometric, this results in smaller errors at near atmospheric pressures.

Of the three models considered the linear error model gives the closest representation of the measurement error over the total measurement range. However, the linear error model somewhat overestimates the error at the low end of the measurement range.

### 6.3 Use of Multiple Measurements

Important parameters like scale force, fuel flow and some pressures are usually measured with multiple measurement systems which are as independent as possible. If the meters are of the same type, the standard deviation of the difference of the two meters will be  $\sqrt{2}$  times that of a single meter, which allows determination of the precision error of the average from the differences of two meters. Ref.2 Appendix C gives the theory, which is summarized in the following equations:

$$\begin{aligned} S(\Delta) &= S \text{ (difference of 2 meters)} \\ &= \sqrt{\left( \sum_{i=1}^N \frac{(\Delta_i - \bar{\Delta})^2}{N-1} \right)} \\ \text{but } S(\Delta) &= \sqrt{2} S \text{ (1 meter)} \\ \therefore S \text{ (average of 2 meters)} &= 1/\sqrt{2} S \text{ (1 meter)} = \frac{S(\Delta)}{2} \end{aligned}$$

In this equation  $\bar{\Delta}$  is the average difference of the measuring results of the two meters, after they have been calibrated. In the calibrating process this average is reduced to zero, but in practice often a finite value is found again, which is then a measure for part of the bias introduced through the testing environment.

### 6.4 Test Data Analysis

Local practices were used at each facility to analyse and verify the test data during acquisition and processing. The practices in use at RAE(P) are detailed in this section to show an example which is typical of that used by all facilities.

Test Data Analysis may be directed to a detail, like an instrument calibration check, or to calculation of the target point values of different parameters for one test condition from the curve fit through the nine measured points. At the same time the Random Error Limit of Curve Fit (RELCF) can be evaluated from the Residual Standard Deviation (RSD) of the points relative to the curve, taking into account the number of degrees of freedom, determined by the number of points and the degree of the curve fit. The model used by RAE(P) is described in Ref.17, it shows that the RELCF reduces in first approximation with the square root of the number of points, but modified by the uncertainty in the curve coefficients and the distance from the centroid of the data.

For a data spread of appr. 20% a parabolic fit usually gives good results, but in the case of the UETP the spread of appr. 40% necessitates a cubic fit in some cases. In the latter cases a parabolic fit may introduce a bias error, when the curve is read off-centre. This is not relevant for UETP as Target Points were practically in the centre of the data. A cubic fit always gives a better approximation for interpolation, but the calculating time is longer and the RELCF may come out slightly higher, because of Student's "t" factor, which depends on the degrees of freedom, which number one less in the cubic case. Extrapolation is dangerous with a cubic curve, but that has not been used in the UETP. In general the lowest order curve fit should be used that reasonably fits the data. If visual inspection shows the remnant not to be random, a higher order curve fit is warranted.

It has been mentioned before that test data analysis by curve fit can only directly evaluate one aspect of data precision; no bias information can be obtained this way. Often the results for different test conditions differ more than  $\pm$  RELCF. This difference is a further aspect of data precision as defined by AEDC; according to the RAE(P) definition of the measurement process it is called bias. In section 6.6 and 6.7 some examples are given of reasons for data scatter about the curve fit for different test conditions. Comparison with other DMP's may still yield more bias errors, though.

RELCF values for RAE(P) data for Test Conditions 1 through 10 are shown in Fig.6-3. The average RELCF values are 0.13 percent for WARD, 0.25 percent for FNRD, and 0.15 percent for SFCRD. These values are consistent with the RAE(P) pretest predictions for precision error which are indicated in the figure and show an increase with altitude (test conditions 6 to 9) while the scatter for the other test conditions should be of the same magnitude. The high altitude case (TC9) shows a relatively low RELCF, but this was based on all 18 points (first and second scan together) while the other values at RAE(P) are based on the second scan only.

It is shown that the FN RD values are consistent with RAE(P) prediction for the altitude cases, if RELCF is based on 9 points.

Test Condition 5 shows a larger-than-expected RELCF; in this case the nine power settings were separated over two days, which introduced more differences. A useful tool for analysing such a discrepancy is to plot the results for the nine power settings on an enhanced scale, which was done in this case by plotting the difference relative to the straight line connecting the end points (fig.6-4). In this case the increased RELCF results from some difference between the day-to-day results at the lower power settings.

For the case of Test Condition 1 the large RELCF in net thrust FNRD vs NHRD is probably caused by some difficulty in T2 measurement at 258 K, which affects the value of NHRD. The RSD for this case is twice that for TC 2), while for FNRD vs P5Q2 the RSD is of the same order for the two test conditions, indicating that the scatter is not in FNRD. This illustrates the importance of choosing the comparison parameter; the effect of a slight error in NHRD is enhanced by the curve shift effect, which is of the order of 7 for this case (i.e. 7% change in FNRD for one % change in NHRD).

#### 6.5 The Relationship between Standard Error of Estimate (SEE) and Estimated Precision Index(s)

Precision Indices(S) for all of the engine performance parameters were estimated by each facility for test conditions 3,6 and 9 (Table 5-2 through 5-7). In the course of fitting the test data with curves of degree 2 by least squares as shown in Fig 9 of Ref 12, the residual standard deviations (RSD) were calculated. RSD is identical to the Standard Error of Estimate (SEE). The relationship between RSD and S at each facility depends on the particular version of the defined measurement process (DMP) adopted by the facility. This dependency exists because certain of the elemental errors will appear as either a bias error or a precision error depending on the specific DMP (Section 3.2). In the case of RAE(P), the DMP was taken to be a single engine performance curve, for example SFCRD versus FNRD, obtained during one test run. On this basis, the values of RSD are expected to agree with the values of S because the distribution of data points about one curve is assumed to be a complete manifestation of precision errors. For the RAE(P) DMP certain errors in data obtained during multiple test runs are included as bias errors. Other facilities adopted a different DMP in which certain errors which appear in data obtained during multiple test runs are included as precision errors. For the latter definitions, the values of S are expected to be larger than the RSD values from the single curve obtained during a single test run. The vast majority of the data presented in Fig. 9 of Ref 12 was obtained during a single test run at each facility.

Predicted values of S are compared in Fig. 6-5 with observed values of RSD from the curve fit of: SFCRD v FNRD, FNRD v P7Q2, WFRD v NHRD, WAIRD v NLRD for test conditions 3(82.7/1.0/288), 6(82.7/1.3/288) and 9(20.7/1.3/288) at NASA, AEDC, CEPr and RAE(P).

In the case of RAE(P), the values of S and RSD are in approximate agreement as expected from the DMP for SFCRD and FNRD, but for WFRD and WAIRD the values of S are consistently much lower than the RSD's. Hence, the S predictions were probably under-estimated for the latter two performance parameters.

In the case of AEDC the values of S are higher than RSD for SFCRD, FNRD, WFRD, and WAIRD as expected from the DMP. However, the S values and RSD values for WAIRD are closer together than for the other 3 parameters indicating that the precision error contribution estimate for WAIRD for multiple test runs is smaller than for the other 3 parameters.

In the case of CEPr there is general agreement between S and RSD for 5 of the 6 values of SFCRD and FNRD. (SFCRD at Test Condition 9 is the exception). This relationship between S and RSD is essentially the same as for RAE(P). For WFRD, the RSD values are very high, which suggests unexpected measurement scatter. For WAIRD, the values of S are much lower than RSD's which suggest that these S values were under-estimated.

#### 6.6 Engine Power Handling

As described in section 2.3, the UETP General Test Plan was designed to minimize the effects of non-steady state engine behaviour eg thermal equilibrium and hysteresis. Most facilities took their first data scan five minutes after reaching a power setting; then the second scan was taken within two minutes. Deviations from this procedure could introduce errors unaccounted for in the estimates of Section 5.3.

The data from several test facilities were examined to determine if there was a difference resulting from hysteresis in the data taken with increasing throttle angle and decreasing throttle angle (see Fig. 2.2.). Although the data are not included in this report, it was concluded that the effects of throttle hysteresis, if any, were negligible.

Special tests were performed at NASA and at RAE(P) to establish and verify the 5 minute and 2 minute stabilization intervals specified in the General Test Plan. The adequacy of these intervals was confirmed (see Section 12.4, Ref. 12). Additional analysis of the thermal equilibrium effects was performed as a part of this measurement uncertainty evaluation by examination of the differences between the first and second data scan (Fig. 6-6). Figure 6-6 A shows negligible difference between the first and second data points at AEDC.

CEPr used a 2-3 minute stabilization time before taking two back to back data points. Scatter between the first and second points is significantly increased (Fig 6-6B) relative to, for instance, AEDC (Fig 6-6A). Thus, the curve fit of the complete set of CEPr data could be expected to introduce both precision errors (due to random scatter) and bias errors (due to systematic thermal effects). These errors amount to 0.5 percent in the comparison of FNRD versus P5Q2, in addition to that shown in Table 5-4 and section 5.3. Other biases, particularly in engine speed, are expected to be present but have not been calculated.

#### 6.7 The Relationship between Measured Inter-facility Spreads and Estimated Uncertainties.

A display of the data spreads for the individual test conditions for FNRD, WAIRD and SFCRD is shown in Figure 18-1 of Reference 12. The results have been re-arranged in Figure 6.7 to show the effects of increasing inlet temperature, decreasing inlet pressure and increasing ram ratio. In addition to the data spreads an estimate of the total uncertainty interval, based on median uncertainty values from Table 5-7 to 5-5, is shown, including the relevant curve shift effects, as discussed in Section 3.4.4. This is calculated as follows, taking the graph of FNRD vs P7Q2 at Test Condition 3 as an example:

$$\begin{aligned} \text{Median UFNRD} &= 0.65\% \\ \text{Median UP7Q2} &= 0.51\% \end{aligned}$$

$$\text{Slope } \frac{d\text{FNRD}}{d\text{P7Q2}} = 1.9$$

$$\text{Estimated total uncertainty} = \sqrt{0.65^2 + (1.9 \times 0.51)^2} = 1.17\%$$

NOTE : This information assumes that the error sources in FNRD and P7Q2 are independent. There is a small effect of the error in P2 which is common to both FNRD and P7Q2 and which would reduce the value of 1.17 % by (0.1-0.2%).

This effect of common error has been neglected in this example. Similarly, there is a small effect (less than 0.1 percent) due to error in T2 which is common to both WAIRD and NLRD and a small effect of the error in FNRD which is common to both SFCRD and FNRD which also would reduce these uncertainty intervals by (0.1-0.5%). All errors have been treated as independent and the small effects of common errors in both the dependent and independent variables have been neglected in these examples.

$$\text{Total uncertainty interval} = 2 \times 1.17 = 2.3\% \text{ (based on median values)}$$

A somewhat more pessimistic estimate of the uncertainty interval can be obtained making use of the larger error estimates of some facilities. It can be argued that one facility's results may be as much as the maximum estimated error displaced from the (unknown) true value. (This is not necessarily the facility that made the high error estimate). However it should not be possible that another facility's result are an equal amount in error in the opposite direction; the maximum error in that direction can be assumed to be the next highest estimate. Therefore the logical maximum spread (uncertainty interval) is the sum of the highest two estimates, with each contribution calculated in a way similar to that shown above.

The complete results are presented in Table 6-1.

The magnitudes of these estimated total uncertainty intervals are plotted in Figure 6.7 for Test Conditions 3, 6 and 9 with dashed lines indicating the expected variation over the other Test Conditions. These lines are fairly constant over most Test Conditions - the exception being Test Conditions 6, 7, 8 and 9 where all the lines increase as engine inlet pressure decreases. The measured spreads remain fairly constant in nearly every case - the exception being FNRD with CEPPr omitted where the spreads increase as pressure falls. It was noted in Reference 12 that the large differences between the spreads in FNRD with and without CEPPr data were attributed to problems with the measurement of P7. It can also be noted that the spreads in this case with the CEPPr data omitted are considerably less than the estimated uncertainty interval, which indicates that given good P7 measurement - the estimated errors may be excessive. Also it should be noted that the interfacility spreads of SFCRD vs FNRD do not increase as inlet pressure decreases from test condition 6 to 9 as was estimated. The reasons why the interfacility spreads are surprisingly small at the difficult test conditions 8 and 9 could be due to self-cancelling effects of common errors, but this was not established during the analysis of the UETP results.

In judging the compatibility of the measured spreads with the estimated uncertainty intervals, it should be remembered that the latter represent LIMITS within which the observed data spreads should lie with 99.7 confidence. It is reassuring to find that these estimated uncertainty intervals are reasonably compatible with the observed spreads. This inspires confidence for future application of the uncertainty methodology.

## 7 CONCLUSIONS

In the AGARD-UETP, a single methodology for determining the bias limits, precision indices, and overall uncertainties of the basic measurements and calculated engine performance parameters was adopted and implemented at each facility. This approach provided a common basis for comparison of the quality of measurements made at the participating test facilities. As a result of this work major advances in the assessment and understanding of data quality were made by the AGARD turbine engine test community.

The key conclusions from the UETP measurement uncertainty assessment are:

- 1) Error analysis for propulsion test facilities proved to be a highly specialised subject and required that each facility complete a rigorous elemental error audit for each of the facility basic measurement systems.
- 2) Estimated errors must be assigned as precision or bias according to criteria which make up the Defined Measurement Process. Different Defined Measurement Processes were used by each facility; as a result, elemental errors were classed as bias in one facility and as precision in another.
- 3) Although a common uncertainty methodology was used to make the measurement uncertainty estimates, flexibility in the definition of the Defined Measurement Process and allocation of the bias and precision errors dependent on the data acquisition and calibration system of each facility resulted in considerable variation in these error components. However, there is overall agreement among the facilities when combined errors (i.e. measurement uncertainty) are considered.
- 4) The uncertainty estimates for the basic measurements - scale force, fuel flow, inlet pressure, inlet temperature and rotor speed - varied from 0.3 to 0.7 percent, 0.2 to 1.1 percent, 0.1 to 0.5 percent, 0.3 to 0.6 percent and 0.02 to 0.5 percent respectively, with little difference between the ground-level test beds and the altitude cells at near sea level inlet pressure. Some facilities assumed that the percentage uncertainty remained constant as the engine inlet pressure was reduced, whereas others assumed the absolute value of the uncertainty to remain constant. The latter assumption resulted in uncertainty values for scale force of 0.3 to 3.0 %.
- 5) For the altitude facilities the ranges of uncertainty estimates for the major engine performance parameters, net thrust, specific fuel consumption and airflow were  $\pm 0.4$  to  $1.2$ ,  $\pm 0.6$  to  $1.7$  and  $\pm 0.4$  to  $0.8$  percent respectively at high inlet pressure (82.7 kPa). At low inlet pressure 20.7 kPa both the values and spreads were considerably higher, ranging to just over  $\pm 3.0$  percent for net thrust and specific fuel consumption. For the ground-level test beds both the values and the spreads were generally smaller than those for the altitude facilities.
- 6) The overall uncertainty of a parameter obtained from an engine performance curve is made up of the uncertainty in both the dependent and independent parameters. The effects of both contributions were of similar magnitude.
- 7) Two measurement systems were especially notable for demonstrated low measurement uncertainty within their category; the positive displacement fuel flow meters at RAE(P) and the sonic air flow meter at AEDC.
- 8) A comprehensive post-test analysis is required to confirm predictions and detect mistakes. In particular, evaluation of the residual standard deviations (RSD) from the curves fitted to the data is recommended. Depending on the Defined Measurement Process, all or part of the observed RSD would be directly comparable to the estimated precision indices. Significant deviations would indicate that an improper estimate had been made in the prediction.
- 9) Three error models were used in estimating uncertainty of pressure transducers:
  - a. Constant absolute error
  - b. Constant percentage error
  - c. Linear absolute error
 Type (a) (noted at Full Scale Output (FSO)) is that favoured by instrument manufacturers and this was applied by three facilities. It gives large percentage estimates at low pressure. One facility specified Type (B) with the constant percentage uncertainty declared at 0.1 FSO. One facility, which had a gauge pressure system, used a linear model (Type (c)). This gave a large percentage uncertainty at low absolute pressure, but negligible percentage uncertainty at high absolute pressure.
- 10) The residual standard deviations calculated from the observed scatter about the curve fits to the engine performance parameters were in reasonable agreement with the predicted precision indices for all Test Conditions.

## REFERENCES

1. AGARD-PEP/WG15  
(Propulsion and Energetics Panel) Uniform Engine Testing Program (UETP), General Test Plan  
Revised Edition June 1983
2. R.B. Abernethy,  
J.W. Thompson HANDBOOK Uncertainty in Gas Turbine Measurements  
AEDC-TR-73-5 Febr. 1973
3. Arnold Eng. Development Center  
Sverdrup Technology Inc.  
S. Wehofers; W.O. Roals AGARD UETP Inter Facility Measurement Uncertainty Error Audit  
April 1985
4. AGARD-PEP/WG15  
J.P.K. Vleghert Meeting of the Sub-Group on Uncertainty Assessment  
AGARD-SR 65 Att3 July 1985
5. Nat. Aero/Space Admin.  
Lewis Research Center, Cleveland  
M. Abdelwahab; T.J. Biesiadny; D. Silver Measurement Uncertainty for the UETP, conducted at NASA/Lewis,  
NASA TM 88943 May 1987
6. Arnold Eng. Development Center  
Sverdrup Technology Inc.  
W.O. Roals; W.A. Turrentine; S. Wehofers AEDC Measurement Uncertainty Results for the AGARD UETP  
AEDC-ER-87-03 Oct. 1987
7. Nat. Research Council of Canada (Ottawa) Interfacility Uncertainty Error Audit 1451-44-41  
J.W. Bird Apr. 1985
8. Centre d'Essais des Propulseurs (Saclay) Essais Croises de Moteur J57 UETP;  
P. Maire Incertitude sur les mesures CEP 594, juin 1986
9. Royal Aircr. Establishment Farnborough  
(formerly NGTE)  
J.C. Ascough Prediction Synthesis of Error Limits for J57 UETP tests  
Tech Memo PI069 Sept. 1985
10. Turkish Air Force/Middle East  
Technical University F. Algün; A. Ucer Turkish Test Report  
UETP Apr. 1985
11. Naval Air Propulsion Center  
M.K. Fall Sea level Static Performance of a J57-P-19 W engine  
NAPC-PE-178 May 1988
12. AGARD-PEP/WG15  
P.F. Ashwood The Uniform Engine Test Programme  
AGARD Advisory Report No. 248, 1989
13. United Technologies/Pratt & Whitney  
R.B. Abernethy Fluid Flow Measurement Uncertainty  
IOSC ISO TC30 SC9 Draft Dec. 1985
14. Royal Aircr. Establishment Farnborough  
J.C. Ascough Preliminary Post Test Analysis of Bias Errors in UETP  
RAE Tech Memo PI068 Sept. 1985
15. SAE-E32 ECM Symposium  
L.A. Urban Developments in Turbine Engine Diagnostics  
SAE-F32 October 1985
16. R.B. Abernethy; B. Ringhiser History and Statistical Development of the new Measurement  
Uncertainty Methodology, AIAA Paper 85-1403 July 1985
17. National Gas Turbine Establishment  
J.C. Ascough Test Code for Contract Performance Measurement  
NGTE M78020 Apr. 1978

Table 3-1A Force Measurement Error Source Diagram

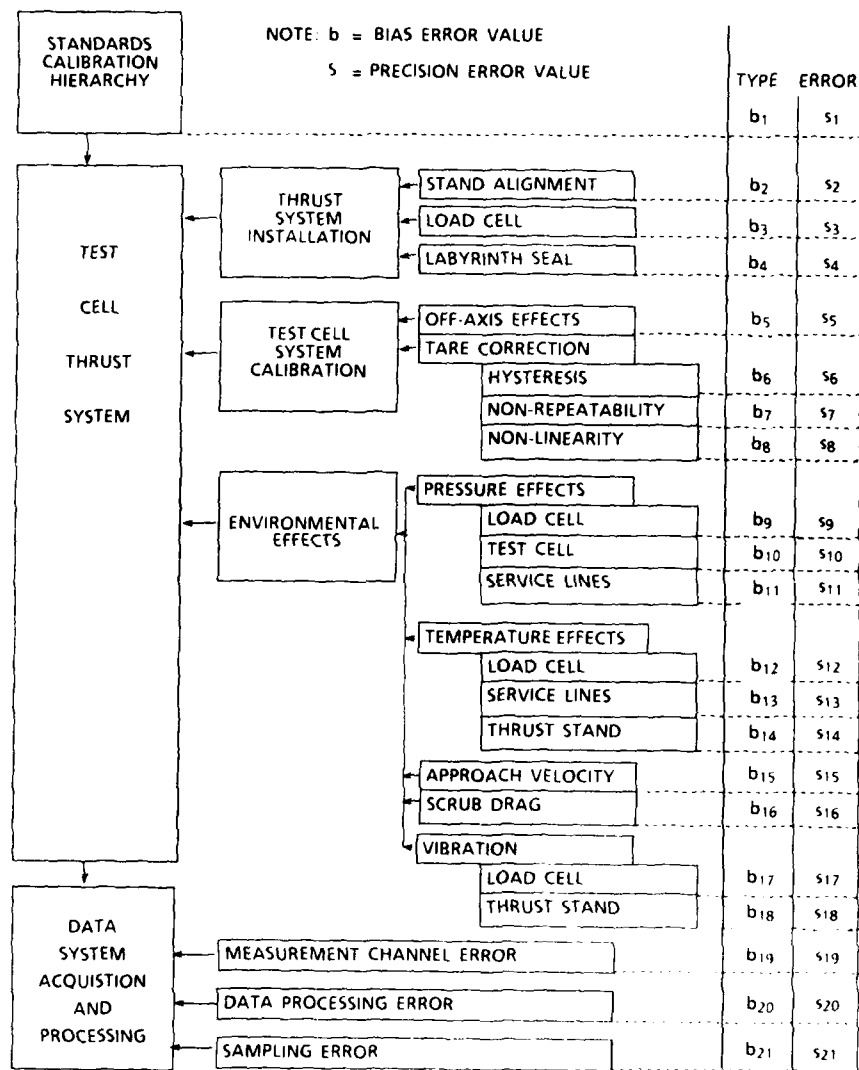
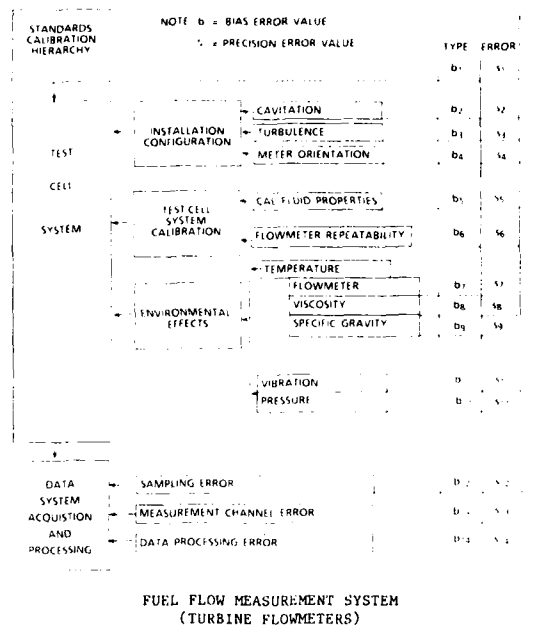


Table 3-1B Force Measurement System

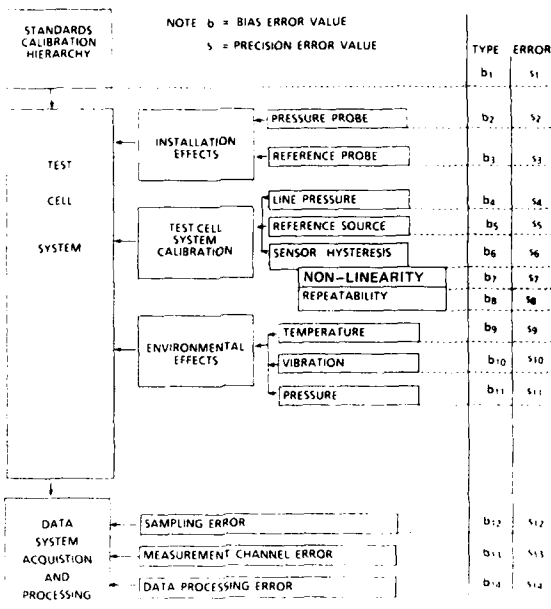
b	s	DESCRIPTION OF ERROR SOURCE
b <sub>1</sub>	s <sub>1</sub>	Error from standard lab calibration of load cells, including traceability to national standards.
b <sub>2</sub>	s <sub>2</sub>	Error due to misalignment between the engine force vector and the force vector measured by the data load cell train.
b <sub>3</sub>	s <sub>3</sub>	Error due to shift in load cell calibration caused by attachment of adaptors and flexures.
b <sub>4</sub>	s <sub>4</sub>	Error due to pressurization of the labyrinth seal.
b <sub>5</sub>	s <sub>5</sub>	Error caused by the measurement of the forces on an axis different from the engine centerline.
b <sub>6</sub>	s <sub>6</sub>	Error due to the system hysteresis.
b <sub>7</sub>	s <sub>7</sub>	Error due to the system non-repeatability, as determined by repeated calibration both pre and post test.
b <sub>8</sub>	s <sub>8</sub>	Error due to the system non-linearity.
b <sub>9</sub>	s <sub>9</sub>	Error due to the effect of changes in cell pressure on the load cell.
b <sub>10</sub>	s <sub>10</sub>	Error due to the effect of changes in cell pressure on the test cell wall which is the thrust system ground.
b <sub>11</sub>	s <sub>11</sub>	Error due to the effect of changes in line pressure on the tare forces exerted on the thrust measurement system by service lines, etc.. routed to the engine.
b <sub>12</sub>	s <sub>12</sub>	Error due to the effect of a change in temperature on the load cell.
b <sub>13</sub>	s <sub>13</sub>	Error due to the effect of changes in temperature on the tare forces exerted on the thrust measurement system by lines routed to the engine.
b <sub>14</sub>	s <sub>14</sub>	Error due to thermal growth of the thrust stand.
b <sub>15</sub>	s <sub>15</sub>	Error in force measurement as a result of inlet air ram effects on sea level test stands (this error is also present for altitude test cells but will be taken into account in the elemental error propagation activities).
b <sub>16</sub>	s <sub>16</sub>	Error in the force measurement as a result of secondary airflow external drag effects on engine surface and service lines.
b <sub>17</sub>	s <sub>17</sub>	Error due to the effect of vibration on the load cell.
b <sub>18</sub>	s <sub>18</sub>	Error due to the effect of vibration on the thrust stand.
b <sub>19</sub>	s <sub>19</sub>	Error from signal conditioning, shunt calibration, and digital system.
b <sub>20</sub>	s <sub>20</sub>	Error from curve fit of calibration data.
b <sub>21</sub>	s <sub>21</sub>	Error associated with the ability to determine a representative value over a specified time interval for data variations due to plant or engine instability.

Table 3-2 A/B Fuel Flow Measurement Error Source Diagram/System



b	s	DESCRIPTION OF ERROR SOURCE
b <sub>1</sub>	s <sub>1</sub>	Error from standard lab calibration of flowmeter, including traceability to national standards.
b <sub>2</sub>	s <sub>2</sub>	Error due to the effect of cavitation caused by insufficient static pressure within the flowmeter. (vortex, Beltrami)
b <sub>3</sub>	s <sub>3</sub>	Error due to the effect of turbulent flow caused by sharp bends, etc. upstream of the flowmeters. and downstream
b <sub>4</sub>	s <sub>4</sub>	Error due to the effect of orientation differentencies from calibration to application.
b <sub>5</sub>	s <sub>5</sub>	Error from determination of calibration fluid specific gravity, viscosity, and matching these to the characteristics of the test fluid to be used.
b <sub>6</sub>	s <sub>6</sub>	Error due to the flowmeter non-repeatability from repeat flowmeter calibration, including difference between pre and post test calibrations.
b <sub>7</sub>	s <sub>7</sub>	Error from the effect of ambient temperature changes on the flowmeter.
b <sub>8</sub>	s <sub>8</sub>	Error in the determination of test fluid viscosity.
b <sub>9</sub>	s <sub>9</sub>	Error in the determination of test fluid specific gravity.
b <sub>10</sub>	s <sub>10</sub>	Error from the effect of vibration on the flowmeter.
b <sub>11</sub>	s <sub>11</sub>	Error from the effect of ambient pressure changes on the flowmeter.
b <sub>12</sub>	s <sub>12</sub>	Error associated with the ability to determine a representative value over a specified time interval for data variations due to fuel pressure or engine instability.
b <sub>13</sub>	s <sub>13</sub>	Error from signal conditioning, calibration, oscillator, and digital system.
b <sub>14</sub>	s <sub>14</sub>	Error from curve fits of calibration data and fluid property correction

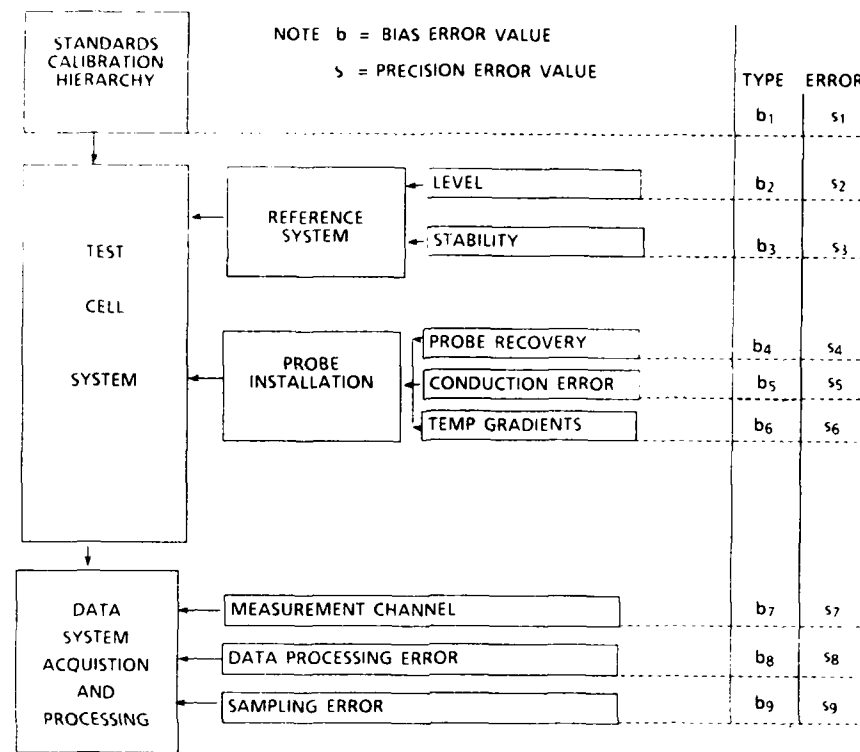
Table 3-3 A/B Pressure Measurement Error Source Diagram/System



## PRESSURE MEASUREMENT SYSTEM

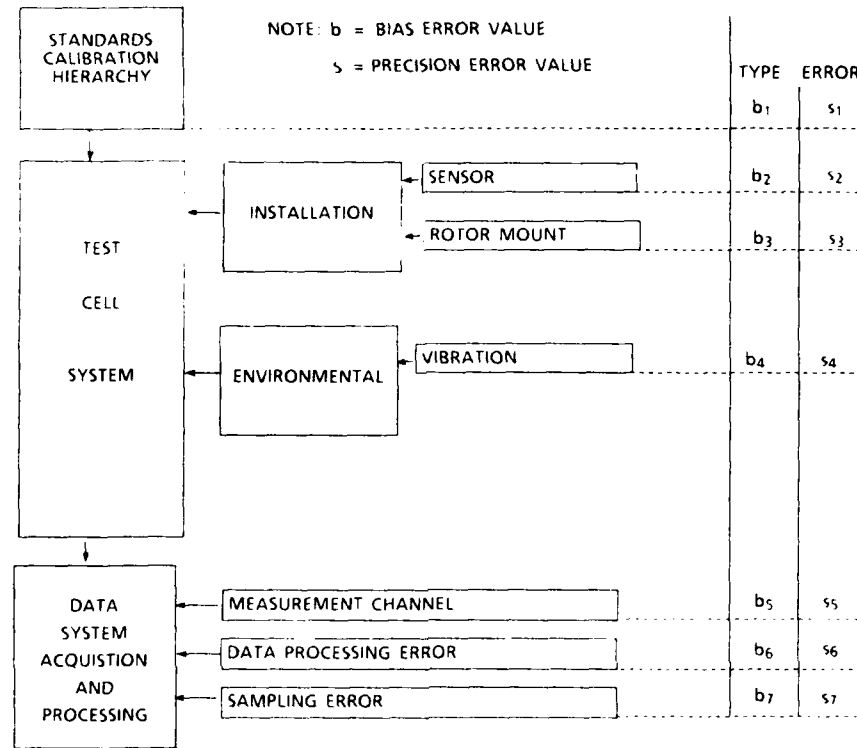
b	s	DESCRIPTION OF ERROR SOURCE
b <sub>1</sub>	s <sub>1</sub>	Error from the standards lab calibration of the in place pressure generator or the sensor calibration, including traceability to national standards.
b <sub>2</sub>	s <sub>2</sub>	Error from the design/fabrication of the static or total pressure probe.
b <sub>3</sub>	s <sub>3</sub>	Error from the design/fabrication of the reference pressure probe for delta pressure measurements.
b <sub>4</sub>	s <sub>4</sub>	Error due to changes in transducer calibration with line pressure for delta pressure sensors.
b <sub>5</sub>	s <sub>5</sub>	Error from the determination of reference pressure.
b <sub>6</sub>	s <sub>6</sub>	Error due to sensor hysteresis.
b <sub>7</sub>	s <sub>7</sub>	Error due to sensor non-linearity.
b <sub>8</sub>	s <sub>8</sub>	Error due to sensor non-repeatability.
b <sub>9</sub>	s <sub>9</sub>	Error due to the effect of changes in temperature on the pressure sensor.
b <sub>10</sub>	s <sub>10</sub>	Error due to the effect of vibration on the pressure sensor.
b <sub>11</sub>	s <sub>11</sub>	Error due to the effect of changes in line pressure on delta pressure sensors.
b <sub>12</sub>	s <sub>12</sub>	Error associated with the ability to determine a representative value over a specified time interval for the data variations due to plant or engine instability.
b <sub>13</sub>	s <sub>13</sub>	Error from signal conditioning, electrical calibration, and digital system.
b <sub>14</sub>	s <sub>14</sub>	Error from curve fit of calibration data.

Table 3-4 A/B Temperature Measurement Error Source Diagram/System

TEMPERATURE MEASUREMENT SYSTEM  
(THERMOCOUPLE TYPE)

b	s	DESCRIPTION OF ERROR SOURCE
b <sub>1</sub>	s <sub>1</sub>	Error due to manufacturer specification of wire or standard lab calibration, whichever is used.
b <sub>2</sub>	s <sub>2</sub>	Error due to reference temperature level.
b <sub>3</sub>	s <sub>3</sub>	Error due to reference temperature stability.
b <sub>4</sub>	s <sub>4</sub>	Error due to probe design caused by radiation, friction, etc., when measuring gas temperatures.
b <sub>5</sub>	s <sub>5</sub>	Error due to heat conduction.
b <sub>6</sub>	s <sub>6</sub>	Error due to temperature gradients along nonhomogeneous thermocouple wire.
b <sub>7</sub>	s <sub>7</sub>	Error from signal conditioning, millivolt calibration source and digital system.
b <sub>8</sub>	s <sub>8</sub>	Error from curve fit of thermocouple tables furnished by national standards laboratory.
b <sub>9</sub>	s <sub>9</sub>	Error associated with the ability to determine a representative value over a specified time interval for the data variations due to plant or engine instability.

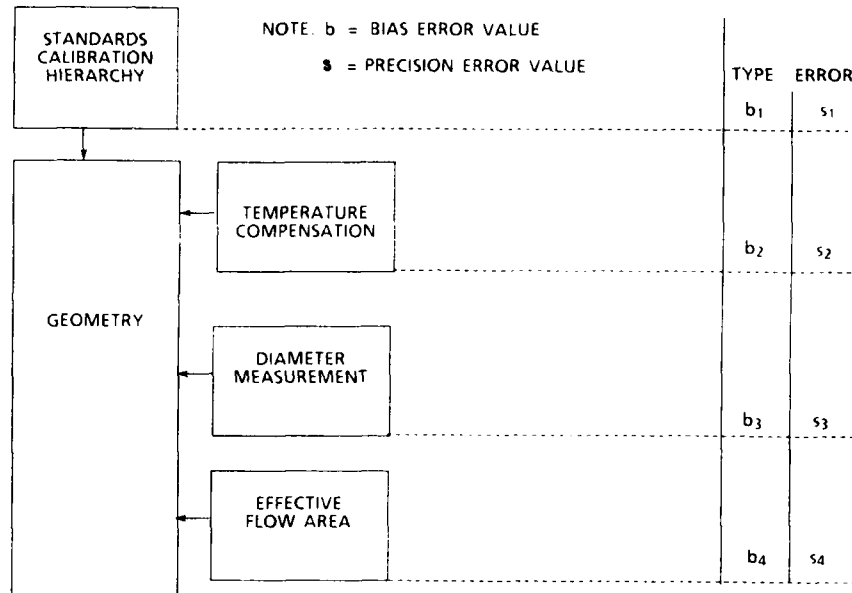
Table 3-5 A/B Rotor Speed Measurement Error Source Diagram/System



## ROTOR SPEED MEASUREMENT SYSTEM

b	s	DESCRIPTION OF ERROR SOURCE
b <sub>1</sub>	s <sub>1</sub>	Standards Lab calibration of frequency calibration source, including traceability to national standards.
b <sub>2</sub>	s <sub>2</sub>	Error from sensor design (gear tooth shape, etc.).
b <sub>3</sub>	s <sub>3</sub>	Error from rotor mount (gear ratio).
b <sub>4</sub>	s <sub>4</sub>	Error due to the effect of vibrations on the speed sensor.
b <sub>5</sub>	s <sub>5</sub>	Error from signal conditioning, calibration oscillator, and digital system.
b <sub>6</sub>	s <sub>6</sub>	Error from calibration curve fit.
b <sub>7</sub>	s <sub>7</sub>	Error associated with the ability to determine a representative value over a specified time interval for the data variations due to engine instability.

Table 3-6 A/B Area Measurement Measurement Error Source Diagram/System



## AREA MEASUREMENT

b	s	DESCRIPTION OF ERROR SOURCE
b <sub>1</sub>	s <sub>1</sub>	Error from the standards laboratory calibration of the precision instrument used to make the physical measurements.
b <sub>2</sub>	s <sub>2</sub>	Error due to differences in temperature from area measurement and testing, including effect of temperature error.
b <sub>3</sub>	s <sub>3</sub>	Error in area measurement as a result of defining the geometry cross section.
b <sub>4</sub>	s <sub>4</sub>	Error in determining the effective flow area (i.e., nozzle discharge coefficient).

TABLE 5-4A ERROR PROPAGATION AT CONDITION 9, TARGET POINT (20.7 P2/1.3 RR/288 T2/8750 NRD)

Basic measurements (input parameters)	Bias limits	Precis index	Influence coeffs $\theta_{ik}$ [%]			Bias limits of results $\pm B_{ik} = B_i \cdot \theta_{ik}$ [%]				Precis index of results $S_{ik} = S_i = \theta_{ik}$ [%]				
	$B_i$	$S_i$	$B_i$	$S_i$	$B_i$	$S_i$	$B_i$	$S_i$	$B_i$	$S_i$	$B_i$	$S_i$	$B_i$	
$x_1$ (units)	(%)	(%)	SPORD	PNRD	WAIRD	WFRD	SPORD	PNRD	WAIRD	WFRD	SPORD	PNRD	WAIRD	WFRD
* PSA 19.50 kPa	0.38	0.021	0.11	-0.11	0.51	0	0.04	0.04	0.19	0	0.002	0.002	0.010	0
PA 2.311 kPa	0.71	0.130	0.11	-0.11	0.50	0	0.08	0.08	0.36	0	0.014	0.014	0.065	0
TA 288.2 K	0.35	0.024	-0.11	0.11	-0.49	0	0.04	0.04	0.17	0	0.003	0.003	0.012	0
T2 287.8 K	0.35	0.038	-0.39	-0.11	0.50	-0.50	0.14	0.04	0.17	0.17	0.015	0.004	0.019	0.019
PS1 20.27 kPa	0.44	0.030	-3.51	-3.64	0	0	0.81	0.84	0	0	0.104	0.108	0	0
PC 15.94 kPa	0.58	0.044	2.19	-2.15	0	0	0.30	0.30	0	0	0.096	0.094	0	0
LOAD 2550 N	1.61	0.470	-0.55	0.55	0	0	0.89	0.89	0	0	0.259	0.259	0	0
QF 193.2 mL/s	0.24	0.078	1.00	0	0	1.0	0.24	0	0	0.24	0.078	0	0	0.078
D15 0.8023 kg/l	0.12	0	"	0	0	1.0	0.12	0	0	0.12	0	0	0	0
NCV 43187 J/g	0.18	0	"	0	0	1.0	0.18	0	0	0.18	0	0	0	0
TF 288.9 K	0.35	0	-0.25	0	0	-0.25	0.09	0	0	0.19	0	0	0	0
CDA 0.981 -	-0.72	0	0.23	-0.23	1.00	0	0.17	0.17	0.72	0	0	0	0	0
BARO 98.65 kPa	0.13	0	0.06	-4.64	-2.15	-4.70	0.01	0.60	0.28	0.61	0	0	0	0
CCP -80 kPa,g	0.04	0	0.05	-3.71	-1.72	-3.76	0.00	0.15	0.07	0.15	0	0	0	0
P2 20.71 kPa	0.33	0.014	-0.78	-0.22	-1.00	-1.00	0.26	0.09	0.33	0.33	0.011	0.003	0.014	0.014

RSS TOTALS  $\pm B_k$  and  $S_k$  (%) 1.44 1.54 0.97 0.81 0.306 0.296 0.071 0.081

TABLE 5-4B ERROR PROPAGATION AT CONDITION 6, TARGET POINT (82.7 P2/1.3 RR/288 T2/8875 NRD)

* PSA 75.95 kPa	0.06	0.005	0.10	-0.10	0.51	0	0.00	0.00	0.03	0	0.001	0.001	0.003	0
PA 11.30 kPa	0.27	0.027	0.10	-0.10	0.50	0	0.03	0.03	0.14	0	0.003	0.003	0.013	0
TA 287.7 K	0.35	0.024	-0.09	0.09	-0.49	0	0.03	0.03	0.17	0	0.002	0.002	0.012	0
T2 287.8 K	0.35	0.038	-0.40	-0.10	0.50	-0.50	0.14	0.03	0.17	0.17	0.015	0.004	0.019	0.019
PS1 80.35 kPa	0.67	0.007	-3.23	-3.34	0	0	0.13	0.13	0	0	0.024	0.025	0	0
PC 63.35 kPa	0.17	0.011	2.03	-1.99	0	0	0.08	0.08	0	0	0.022	0.022	0	0
LOAD 12220 N	0.33	0.098	-0.62	0.62	0	0	0.20	0.20	0	0	0.061	0.061	0	0
QF 718.9 mL/s	0.13	0.021	1.00	0	0	1.0	0.13	0	0	0.13	0.021	0	0	0.021
D15 0.8023 kg/l	0.12	0	"	0	0	1.0	0.12	0	0	0.12	0	0	0	0
NCV 43187 J/g	0.18	0	"	0	0	1.0	0.18	0	0	0.18	0	0	0	0
TF 287.8 K	0.35	0	-0.25	0	0	-0.25	0.09	0	0	0.09	0	0	0	0
CDA 0.985 -	-0.72	0	0.20	-0.20	1.00	0	0.14	0.14	0.72	0	0	0	0	0
BARO 98.66 kPa	0.13	0	0.05	-1.24	-0.54	-1.29	0.01	0.16	0.07	0.17	0	0	0	0
CCP -20 kPa,g	0.04	0	0.01	-0.25	-0.11	-0.26	0.00	0.01	0.00	0.01	0	0	0	0
P2 82.47 kPa	0.14	0.004	-0.80	-0.20	-1.00	-1.00	0.11	0.03	0.14	0.14	0.003	0.001	0.004	0.004

RSS TOTALS  $\pm B_k$  and  $S_k$  (%) 0.44 0.34 0.79 0.39 0.074 0.070 0.026 0.029

\* Note : Facility-Peculiar Nomenclature - Defined in Ref. 9

Table 5-2 NASA Calculated Performance Parameter Uncertainty Estimates

PARAMETER	TEST CONDITION			ERROR, BIAS(B),%	PERCENT PREC.(S),%	OF READING UNCERT.(U),%
	NO.	P2kPa	T2,K			
NLQNH	3	82.7	288	1.00	0.02	0
	6	82.7	288	1.30	"	"
	9	20.7	288	1.30	"	"
NHRD	3	82.7	288	1.00	0.21	0.02
	6	82.7	288	1.30	"	"
	9	20.7	288	1.30	"	"
T7Q2	3	82.7	288	1.00	0.51	0.03
	6	82.7	288	1.30	"	"
	9	20.7	288	1.30	0.49	"
P7Q2	3	82.7	288	1.00	0.08	0.02
	6	82.7	288	1.30	"	"
	9	20.7	288	1.30	0.33	0.06
NLRD	3	82.7	288	1.00	0.21	0.02
	6	82.7	288	1.30	"	"
	9	20.7	288	1.30	"	"
WA1RD	3	82.7		1.00	0.48	0.13
	6	82.7	288	1.30	0.49	0.12
	9	20.7	288	1.30	1.47	0.55
FNRD	3	82.7	288	1.00	0.37	0.17
	6	82.7	288	1.30	0.45	0.20
	9	20.7	288	1.30	1.63	0.78
WF RD	3	82.7	288	1.00	0.67	0.30
	6	82.7	288	1.30	0.67	0.29
	9	20.7	288	1.30	0.71	0.50
SFCRD	3	82.7	288	1.00	0.75	0.34
	6	82.7	288	1.30	0.77	0.35
	9	20.7	288	1.30	1.69	0.91
						3.51

Table 5-3 AEDC Calculated Performance Parameter Uncertainty Estimates

PARAMETER	TEST CONDITION				BIAS (B), %	PERCENT	OF READING
	NO.	P2, kPa	T2, K	RAM RATIO			
NLQNH	3	82.7	288	1.00	0.28	0.21	0.70
	6	82.7	288	1.30	"	"	"
	9	20.7	288	1.30	"	"	"
	11	101.3	288	1.00	"	"	"
NHRD	3	82.7	288	1.00	0.22	0.16	0.54
	6	82.7	288	1.30	"	"	"
	9	20.7	288	1.30	"	"	"
	11	101.3	288	1.00	"	"	"
T7Q2	3	82.7	288	1.00	0.31	0.13	0.57
	6	82.7	288	1.30	"	"	"
	9	20.7	288	1.30	"	"	"
	11	101.3	288	1.00	"	"	"
P7Q2	3	82.7	288	1.00	0.28	0.21	0.70
	6	82.7	288	1.30	"	"	"
	9	20.7	288	1.30	"	"	"
	11	101.3	288	1.00	"	"	"
NLRD	3	82.7	288	1.00	0.22	0.16	0.54
	6	82.7	288	1.30	"	"	"
	9	20.7	288	1.30	"	"	"
	11	101.3	288	1.00	"	"	"
WA1RD	3	82.7	288	1.00	0.28	0.23	0.75
	6	82.7	288	1.30	"	"	"
	9	20.7	288	1.30	"	"	"
	11	101.3	288	1.00	"	"	"
FNRD	3	82.7	288	1.00	0.48	0.35	1.18
	6	82.7	288	1.30	0.51	0.36	1.24
	9	20.7	288	1.30	0.80	0.38	1.55
	11	101.3	288	1.00	0.47	0.35	1.17
WFRD	3	82.7	288	1.00	0.49	0.38	1.25
	6	82.7	288	1.30	"	"	"
	9	20.7	288	1.30	"	"	"
	11	101.3	288	1.00	"	"	"
SFCRD	3	82.7	288	1.00	0.68	0.53	1.73
	6	82.7	288	1.30	0.74	0.55	1.84
	9	20.7	288	1.30	0.96	0.56	2.08
	11	101.3	288	1.00	0.68	0.52	1.73

Table 5-4 CEPR Calculated Performance Parameter Uncertainty Estimates

PARAMETER	TEST CONDITION			ERROR, BIAS (B), %	PERCENT PREC.(S), %	OF READING UNCERT.(U), %
	NO.	P2,kPa	T2, K			
NLQNH	3	82.7	288	1.00	0.08	0.00
	6	82.7	288	1.30	"	"
	9*	20.7	288	1.30	"	"
	11	101.3	288	1.00	"	"
NHRD	3	82.7	288	1.00		
	6	82.7	288	1.30		
	9*	20.7	288	1.30		
	11	101.3	288	1.00		
T7Q2	3	82.7	288	1.00		
	6	82.7	288	1.30		
	9*	20.7	288	1.30		
	11	101.3	288	1.00		
P7Q2	3	82.7	288	1.00		
	6	82.7	288	1.30		
	9*	20.7	288	1.30		
	11	101.3	288	1.00		
NLRD	3	82.7	288	1.00		
	6	82.7	288	1.30		
	9*	20.7	288	1.30		
	11	101.3	288	1.00		
WA1RD	3	82.7	288	1.00	0.35	0.03
	6	82.7	288	1.30	0.47	0.05
	9*	20.7	288	1.30	0.84	0.08
	11	101.3	288	1.00	0.24	0.03
FNRD	3	82.7	288	1.00	0.37	0.11
	6	82.7	288	1.30	0.68	0.19
	9*	20.7	288	1.30	1.30	0.37
	11	101.3	288	1.00	0.35	0.11
WFRD	3	82.7	288	1.00	0.21	0.11
	6	82.7	288	1.30	"	"
	9*	20.7	288	1.30	"	"
	11	101.3	288	1.00	"	"
SFCRD	3	82.7	288	1.00	0.43	0.15
	6	82.7	288	1.30	0.72	0.22
	9*	20.7	288	1.30	1.34	0.39
	11	101.3	288	1.00	0.43	0.15

\*CONDITION 9 ERROR VALUES WERE NOT AVAILABLE, CONDITION 8 (34.5/288/1.30)  
VALUES SHOWN FOR REFERENCE ONLY.

Table 5-5 RAE(P) Calculated Performance Parameter Uncertainty Estimates

PARAMETER	TEST CONDITION				ERROR,	PERCENT	OF READING
	NO.	P2,kPa	T2, K	RAM RATIO			
NLQNH	3	82.7	288	1.00	0.03	0.03	0.09
	6	82.7	288	1.30	"	"	"
	9	20.7	288	1.30	"	"	"
NHRD	3	82.7	288	1.00	0.11	0.02	0.16
	6	82.7	288	1.30	"	"	"
	9	20.7	288	1.30	"	"	"
T7Q2	3	82.7	288	1.00	0.21	0.03	0.27
	6	82.7	288	1.30	"	"	"
	9	20.7	288	1.30	"	"	"
P7Q2	3	82.7	288	1.00	0.38	0.06	0.51
	6	82.7	288	1.30	"	"	"
	9	20.7	288	1.30	0.57	0.24	1.05
NLRD	3	82.7	288	1.00	0.11	0.03	0.17
	6	82.7	288	1.30	"	"	"
	9	20.7	288	1.30	"	"	"
WA1RD	3	82.7	288	1.00	0.79	0.03	0.84
	6	82.7	288	1.30	"	0.03	0.84
	9	20.7	288	1.30	0.97	0.07	1.11
FNRD	3	82.7	288	1.00	0.33	0.05	0.44
	6	82.7	288	1.30	0.34	0.07	0.48
	9	20.7	288	1.30	1.54	0.30	2.13
WFRD	3	82.7	288	1.00	0.38	0.03	0.44
	6	82.7	288	1.30	0.39	"	0.45
	9	20.7	288	1.30	0.81	0.08	0.97
SFCRD	3	82.7	288	1.00	0.48	0.06	0.61
	6	82.7	288	1.30	0.44	0.07	0.59
	9	20.7	288	1.30	1.44	0.31	2.05

Table 5-6 NRCC Calculated Performance Parameter Uncertainty Estimates

PARAMETER	TEST CONDITION				ERROR, PERCENT OF READING		
	NO.	P2,kPa	T2,K	RAM RATIO	BIAS (B), %	PREC.(S) %	UNCERT.(U), %
NLQNH	11	AMBIENT	AMBIENT	1.00	0.09	0.00	0.09
NHR	11	AMBIENT	AMBIENT	1.00	0.22	0.09	0.40
T7Q2	11	AMBIENT	AMBIENT	1.00	0.53	0.19	0.91
P7Q2	11	AMBIENT	AMBIENT	1.00	0.13	0.06	0.25
NLR	11	AMBIENT	AMBIENT	1.00	0.22	0.09	0.40
WA1R	11	AMBIENT	AMBIENT	1.00	0.60	0.04	0.68
FNR	11	AMBIENT	AMBIENT	1.00	0.43	0.10	0.63
WFR	11	AMBIENT	AMBIENT	1.00	0.45	0.13	0.71
SFCR	11	AMBIENT	AMBIENT	1.00	0.60	0.14	0.88

Table 5-7 TUAF Calculated Performance Parameter Uncertainty Estimates

PARAMETER	TEST CONDITION				ERROR, PERCENT OF READING		
	NO.	P2,kPa	T2,K	RAM RATIO	BIAS (B),%	PREC. (S),%	UNCERT.(U),%
NLQNH	11	AMBIENT	AMBIENT	1.00	NA	NA	0.81
NHR	11	AMBIENT	AMBIENT	1.00			0.61
T7Q2	11	AMBIENT	AMBIENT	1.00			0.45
P7Q2	11	AMBIENT	AMBIENT	1.00			0.19
NLR	11	AMBIENT	AMBIENT	1.00			0.67
WA1R	11	AMBIENT	AMBIENT	1.00			0.31
FNR	11	AMBIENT	AMBIENT	1.00			0.52
WFR	11	AMBIENT	AMBIENT	1.00			1.12
SFCR	11	AMBIENT	AMBIENT	1.00			1.23

TABLE 6-1 ESTIMATED UNCERTAINTY INTERVAL CALCULATIONS

TC 3					TC 6					TC 9					
Uncertainty Estimates from Table 5-2 through 5.5 ( $U_y$ and $U_z$ )															
	NASA	AEDC	CEPr	RAE(P)	Median	NASA	AFDC	CEPr	RAE(P)	Median	NASA	AFDC	CEPr	RAE(P)	Median
FNRD	0.71	1.18	0.60	0.49	0.65	0.86	1.24	1.07	0.48	0.96	3.18	1.55	2.04	2.13	2.08
SFORD	1.44	1.73	0.74	0.61	1.09	1.48	1.84	1.16	0.59	1.32	3.51	2.08	2.13	2.05	2.10
WAIRD	0.74	0.75	0.41	0.84	0.75	0.73	0.75	0.57	0.84	0.74	2.56	0.75	1.00	1.11	1.05
P7Q2	0.11	0.70		0.51	0.51	0.11	0.70		0.51	0.51	0.45	0.70		1.05	0.70
NIRD	0.24	0.54		0.16	0.24	0.24	0.54		0.17	0.24	0.24	0.54		0.17	0.24

$$\text{Uncertainty Interval} = 2 \sqrt{U_y^2 + \left( \frac{dy}{dz} \cdot U_z \right)^2}$$

y v. z	Slope $\frac{dy}{dz}$	Uncert Int %		Slope $\frac{dy}{dz}$	Uncert Int %		Slope $\frac{dy}{dz}$	Uncert Int %	
		Max	Med		Max	Med		Max	Med
FNRD v. P7Q2	1.9	2.8	2.3		1.8	2.8	2.6	2.3	6.5 5.4
SFORD v. FNRD	0	3.2	2.2		0.1	3.4	2.6	0.2	5.7 4.3
WAIRD v. NIRD	2.0	2.2	1.8		1.9	2.2	1.8	2.0	4.0 2.3

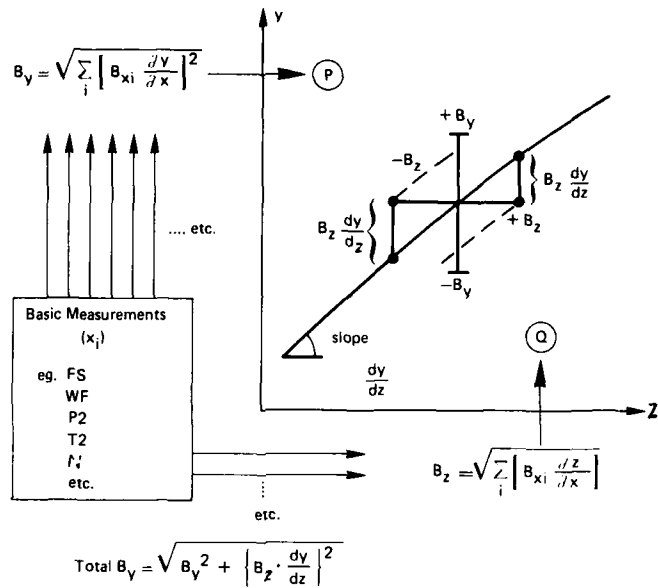


Fig. 3.1 Graphical propagation of bias errors

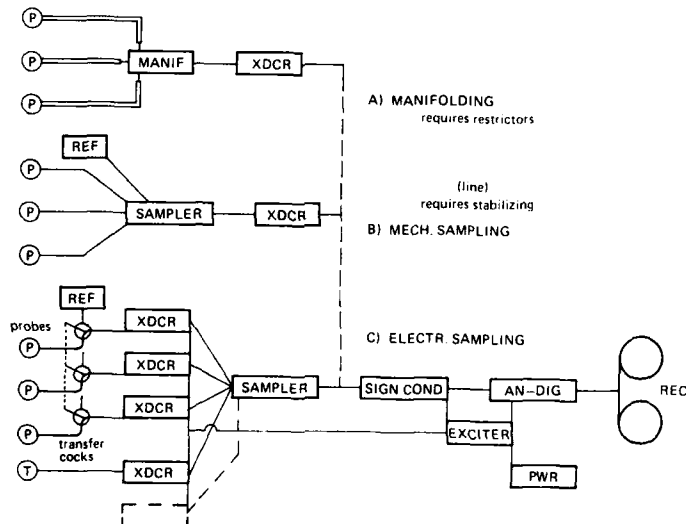


Fig. 4.1 Sampling systems

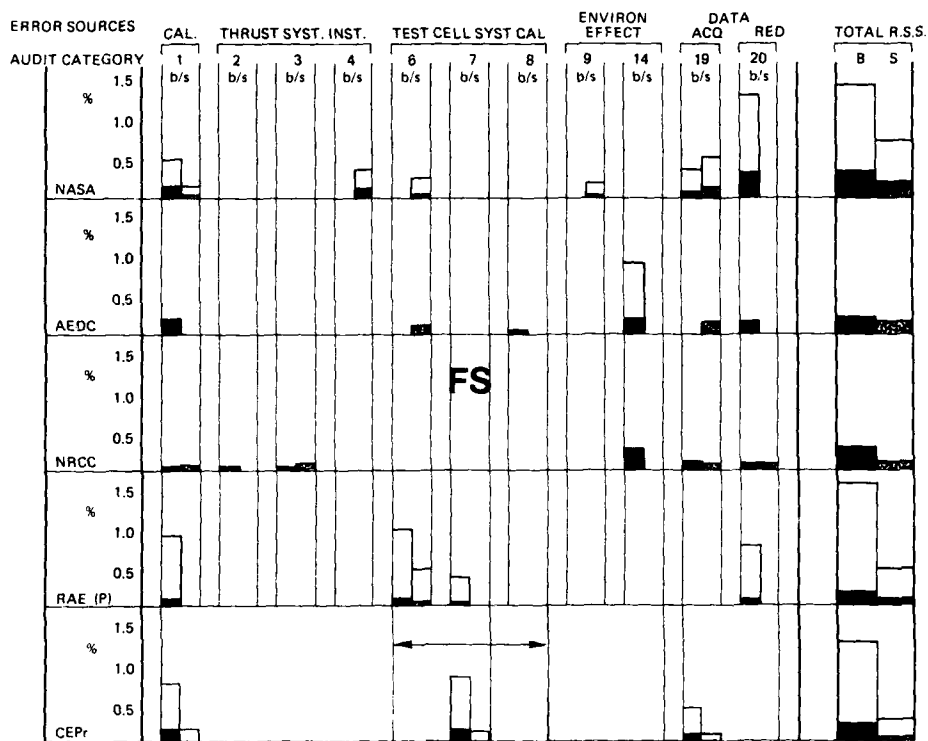


Fig. 5.1 Elemental Error Audit for the Basic Measurement of Scale Force  
percent of mid-thrust-level reading; low alt. TC6 (■), high alt. TC9 (□), NRCC TC44

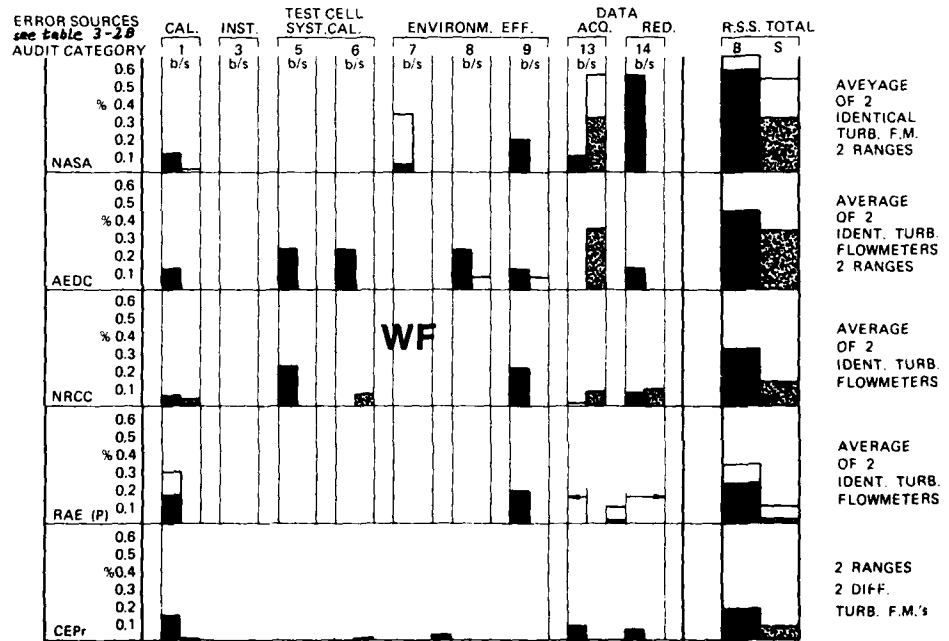


Fig. 5.2 Elemental Error Audit for the Basic Measurement of Fuel Flow  
percent of mid-thrust-level reading; low alt. TC6 (■), high alt. TC9 (□), NRCC TC44

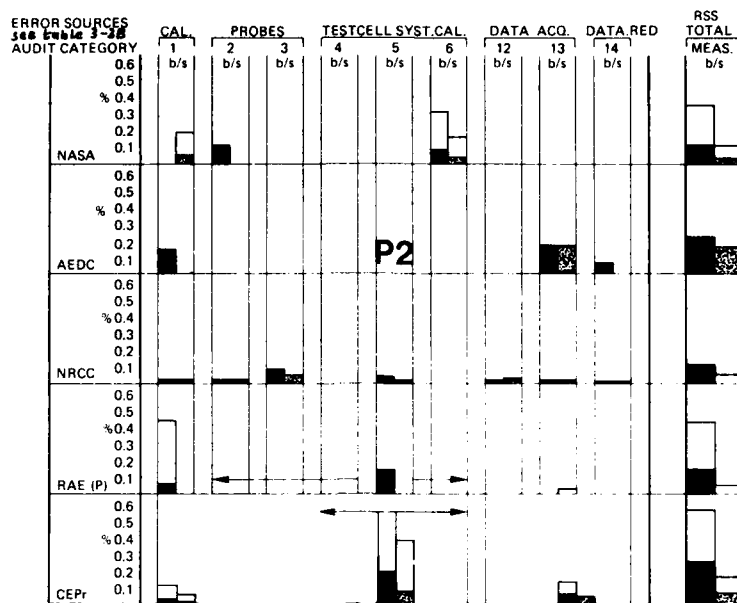


Fig. 5.3 Elemental Error Audit for the Basic Measurement of Intake Total Pressure  
percent of mid-thrust-level reading; low alt. TC6 (■), high alt. TC9 (□),  
at NRCC TC 11



Fig. 5.4 Estimated Errors for Basic Measurements

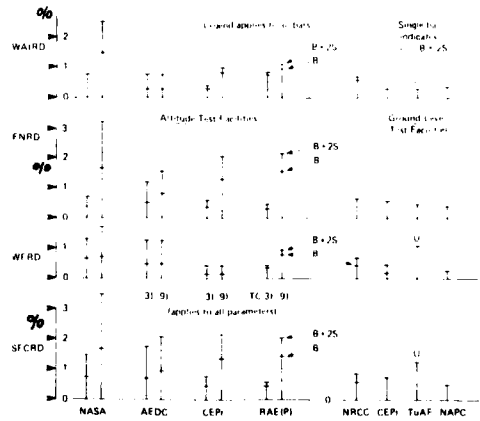
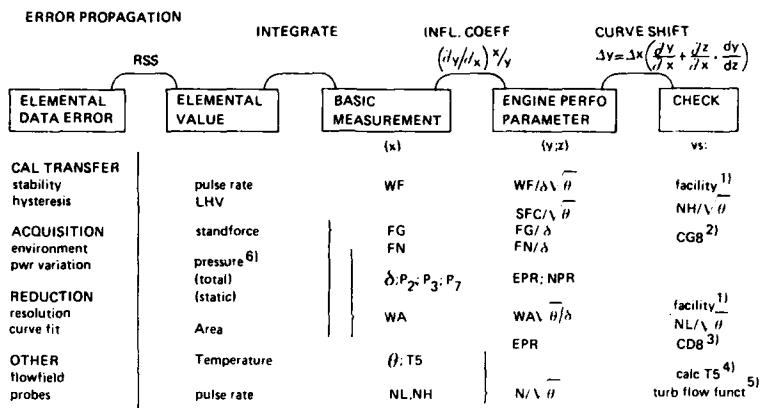


Fig. 5.5 Estimated Errors for Performance Parameters



- 1) Facility instrumentation separate from referee
- 2) Ratio of measured thrust vs calculation from NPR
- 3) Ratio of measured vs calculated airflow
- 4) T4,(T5) can be calculated from fuel/air ratio and compr discharge temp
- 5) WA  $\propto T_4 / P_3$ ; should be constant
- 6) Various stations, (see fig 2-1) defines impulse correction to stand force

Fig. 6.1 Schematic of Data Flow

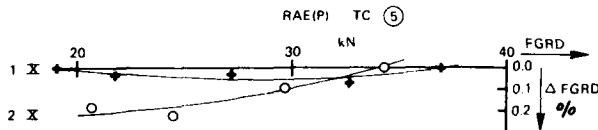


Fig. 6.4 DMP split over two days

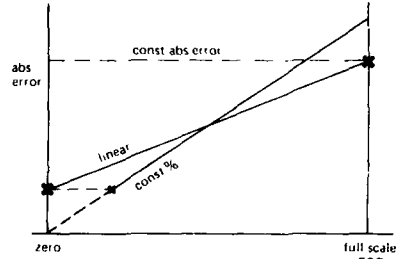


Fig. 6.2 Error Variation over Measuring Range

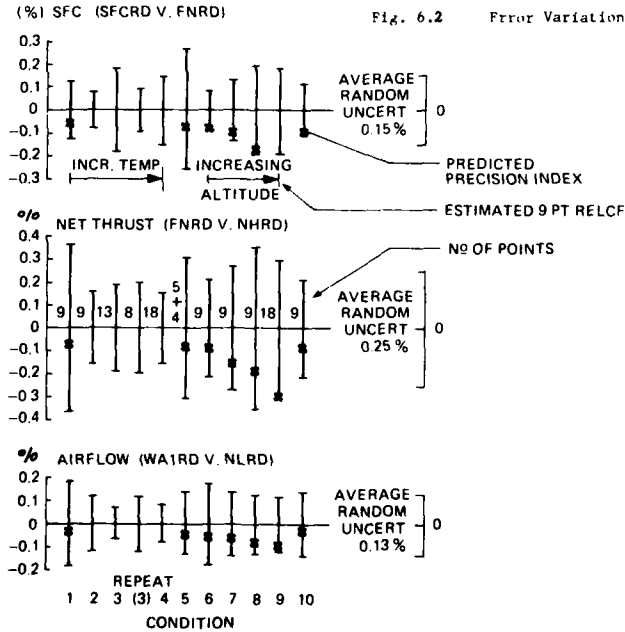


Fig. 6.3 Random Error Limit of Curve Fit at RAE(P) for each Test Condition

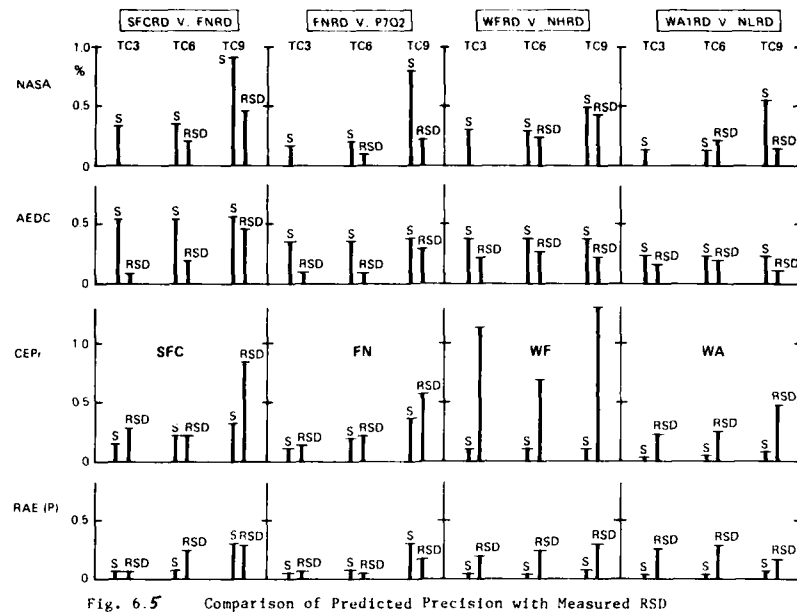


Fig. 6.5 Comparison of Predicted Precision with Measured RSD

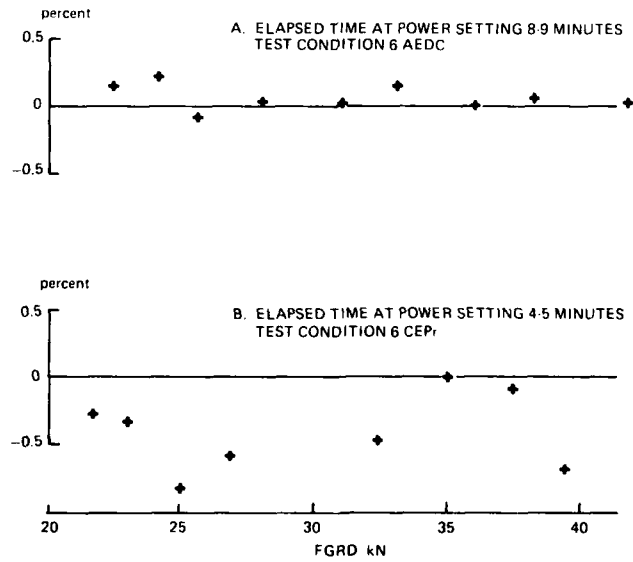


Fig. 6.6 Differences in Gross Thrust between First and Second Data Scans

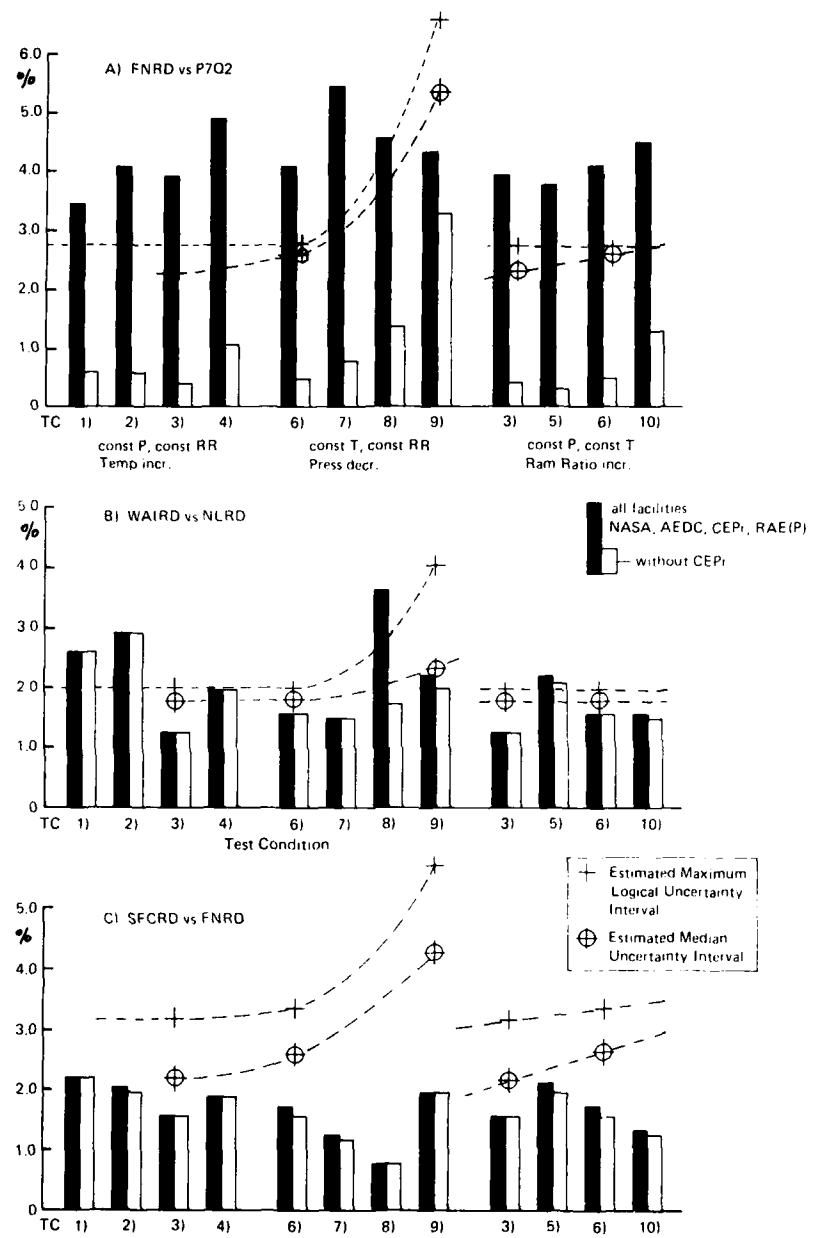


Fig. 6.7 Spreads in Net Thrust, Airflow and SFC Altitude Facilities

APPENDIX I  
Membership of Sub-Group on Uncertainty Assessment

M. Abdelwahab	NASA-Lewis Research Center Cleveland Ohio
T.J. Biesiadny	
J.H. Dicus	NASA-Lewis Air Force Systems Command Liaison
D. Silver	
J.G. Mitchell	USAF-Arnold Engineering Development Center, Arnold AFB, TN
W.O. Boals	Sverdrup Technology Inc., AEDC group,
J. Tate	Arnold AFB, TN
S. Wehofer	
D.M. Rudnitski	National Research Council of Canada, Ottawa
J.W. Bird	
P. Castellani	Centre d'Essais des Propulseurs, Saclay
F. Fagegaltier	Service Technique des Programmes Aéronautiques
M. Holmes	Royal Aircraft Establishment Farnborough
J.C. Ascough	
J.P.K. Vlieghert	Nat. Aero Space Laboratory NLR, Amsterdam

**APPENDIX II**  
**NAPC Measurement Uncertainty**

Information giving the Test Facility Description,  
the Primary Test Measurements and the Measurement Uncertainty was taken from Ref.12, App. VIII

**TEST FACILITY**

The NAPC outdoor test site is an open air ground-level test facility located at Lakehurst, NJ. The turntable test stand is set in the centre of an asphalt and concrete pad completely exposed to the open air in order to eliminate any of the test stand effects commonly encountered in enclosed test facilities. The turntable test stand consists of a rotating platform with a thrust bed supported by four short flexures that permit axial movement. Engine instrumentation, fuel and test stand services are provided from a boom over the centre of rotation of the turntable. A movable shelter is used to protect the test stand from the elements when the engine is not being tested.

**Installation Configuration**

Engine 615037 mounted in the UETP test frame was installed on the turntable thrust bed. Two NAPC manufactured adaptor spool pieces were used to connect the UETP engine inlet duct to an NAPC provided air-flow measuring station and bellmouth with a stone guard, all of which were mounted on the thrust bed.

**PRIMARY TEST MEASUREMENTS**

**Thrust Measuring System**

The thrust measurement system consisted simply of a strain-gauge type load cell mounted below the thrust bed along the centre line of the engine. A spring rate check to ensure the free movement of the thrust bed and calibration of the load cell were performed for three different turntable positions (30, 190, 180 deg) to ensure that there was no difference in the thrust measurement due to the turntable position.

**Airflow Metering System**

The Station 1.0 (facility) airflow measurement station consisted of a spool piece 1.027 m long, 0.931 m inside diameter containing a nine-fingered freestream total pressure rake and four wall static pressure taps. Station 1.0 air temperature was measured by two thermocouples mounted on the bellmouth stone guard.

**Fuel Flow Metering System**

The engine fuel flow was measured using two NAPC turbine fuel flow meters and the fuel temperature. The meters were calibrated in-house with test equipment traceable to the NBS.

**MEASUREMENT UNCERTAINTY**

The procedures for calculating measurement uncertainty were those laid out by Abernethy (Reference 2) and are described in a separate report. For the purpose of data comparison, the relevant values are listed below:

**NAPC CALCULATED PERFORMANCE PARAMETER UNCERTAINTY ESTIMATES**

Para- meter	Test Condition			Error, Percent of Reading			
	No	P <sub>2</sub> kPa	T <sub>2</sub> K	Ram Ratio	Bias percent	Prec S percent	Uncert U percent
NLQNH	11	AMBIENT	AMBIENT	1.00	0.01	0.01	0.02
NH1R	11	AMBIENT	AMBIENT	1.00	0.23	0.05	0.32
T7Q2	11	AMBIENT	AMBIENT	1.00	0.43	0.08	0.61
P7Q2	11	AMBIENT	AMBIENT	1.00	0.02	0.03	0.08
NLR	11	AMBIENT	AMBIENT	1.00	0.23	0.05	0.32
WATR	11	AMBIENT	AMBIENT	1.00	0.29	0.11	0.50
FNR	11	AMBIENT	AMBIENT	1.00	0.19	0.12	0.42
WFR	11	AMBIENT	AMBIENT	1.00	0.21	0.31	0.82
SFCR	11	AMBIENT	AMBIENT	1.00	0.28	0.33	0.93
PS7Q2	11	AMBIENT	AMBIENT	1.00	0.03	0.07	0.18

## APPENDIX III NOMENCLATURE

B	Bias Limit
BM	Basic Measurement
BPP	Basic Physical Parameter
CD8	Nozzle Flow Coefficient
CG8	Nozzle Thrust Coefficient
DMP	Defined Measurement Process
EPP	Engine Performance Parameter
EPR(=P7Q2)	Engine Pressure Ratio
EV	Elemental Value
FG	Gross Thrust
FN	Net Thrust
FNRD	Net Thrust Referred to Desired Conditions
GTP	General Test Plan
IC	Influence Coefficient
IP	Input Parameter
LHV	Lower Heating Value of Fuel
NH	High Pressure Compressor RPM
NHDR	High Pressure Compressor RPM Referred to Desired Condition
NL	Low Pressure Compressor RPM
NLRD	Low Pressure Compressor RPM Referred to Desired Condition
NPR	Nozzle Pressure Ratio
P	Total Pressure
RR	Ram Ratio
S (=PI)	Precision Index
SFCRD	Specific Fuel Consumption Referred to Desired Condition
T	Total Temperature
U	Uncertainty of Measurement
UETP	Uniform Engine Testing Programme
WA	Facility-Measured Air Flow
WAIRD	Facility-Measured Air Flow Referred to Desired Condition
WF	Fuel Flow
x	error source
y	primary
z	comparison parameter
t 95	multiplication factor to denote confidence limits
N	number of samples
$\delta$	pressure referred to standard conditions
$\theta$	temperature referred to standard conditions

## APPENDIX IV

## GLOSSARY

Accuracy - The closeness or agreement between a measured value and a standard or true value; uncertainty as used herein, is the maximum inaccuracy or error that may be expected (see measurement error).

Average Value - The arithmetic mean of N readings. The average value is calculated as:

$$\bar{x} = \text{average value} = \frac{\sum_{i=1}^N x_i}{N}$$

Bias (B) - The difference between the average of all possible measured values and the true value. The systematic error or fixed error which characterizes every member of a set of measurements (Fig. IV-1).

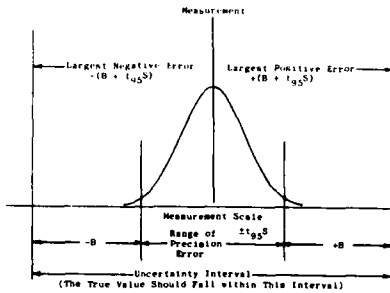


Fig. IV-1 Sampling Systems

Calibration - The process of comparing and correcting the response of an instrument to agree with a standard instrument over the measurement range.

Calibration Hierarchy - The chain of calibrations which link or trace a measuring instrument to the National Bureau of Standards.

Coverage - A property of confidence intervals with the connotation of including or containing within the interval with a specified relative frequency. Ninety-five-percent confidence intervals provide 95-percent coverage of the true value. That is, in repeated sampling when a 95-percent confidence interval is constructed for each sample, over the long run the intervals will contain the true value 95-percent of the time.

Cycle - A whole period of any multiplexer.

Data Point - Can be made up from a number of scans, resulting in an average in time and/or place (i.e. number of pick-ups).

Defined Measurement Process - DMP encompasses the overall procedure, including calibration, etc., to arrive at a desired test result using a specified installation or installations. This may be a single test point, a least squares curve fit of a number of test points, or a collection of such fits for different test conditions. Any error that propagates to the result as a fixed error is classified as bias, otherwise it is precision. What is bias for a single point or curve becomes precision overall, with a remnant test bias and - of course - the possibility of an installation bias.

Degrees of Freedom (df) - A sample of N values is said to have N degrees of freedom, and a statistic calculated from it is also said to have N degrees of freedom. But if k functions of the sample values are held constant, the number of degrees of freedom is reduced by k. For example, the statistic  $\sum_{i=1}^N (X_i - \bar{X})^2$ , where  $\bar{X}$  is the sample mean, is said to have  $N - 1$  degrees of freedom. The justification for this is that (a) the sample mean is regarded as fixed or (b) in normal variation the N quantities  $(X_i - \bar{X})$  are distributed independently of  $\bar{X}$  and hence may be regarded as  $N - 1$  independent variates or N variates connected by the linear relation  $\sum_{i=1}^N (X_i - \bar{X}) = 0$ .

Dwell - Time during which a transducer is connected to a pick-up; includes Settling (line or filter stabilisation) and reading.

Elemental Error - The bias and/or precision error associated with a single component or process in a chain of components or processes.

Fossilisation - random (live) errors in a single calibration run give rise to an uncertainty in the value of the calibration constants, which becomes a fixed "fossilized" bias when this calibration is applied to measurement results.

Laboratory Standard - An instrument which is calibrated periodically at the NBS. The laboratory standard may also be called an interlab standard.

Mathematical Model - A mathematical description of a system. It may be a formula, a computer program, or a statistical model.

Measurement Error - The collective term meaning the difference between the true value and the measured value. Includes both bias and precision error; see accuracy and uncertainty. Accuracy implies small measurement error and small uncertainty.

Multiple Measurement - More than a single concurrent measurement of the same parameter.

Multiplexer - A unit which connects a number of pick-ups sequentially to a transducer, or a number of transducers to a recorder.

NBS - National Bureau of Standards.

Parameter - An unknown quantity which may vary over a certain set of values. In statistics, it occurs in expressions defining frequency distributions (population parameters). Examples: the mean of a normal distribution, the expected value of a Poisson variable.

Precision Error - The random error observed in a set of repeated measurements. This error is the result of a large number of small effects, each of which is negligible alone.

Precision Index - The precision index is defined herein as the computed standard deviation of the measurements.

$$s = \sqrt{\frac{\sum_{i=1}^N (x_i - \bar{x})^2}{N-1}} \quad \text{usually, but sometimes } S = \sqrt{\frac{\sum_i s_i^2}{N}}$$

Random Error Limit of Curve Fit (RELCF) - The limits on both side of a fitted curve within which the true curve is expected to lie, with 95% probability; apart from a possible bias error of the DMP. It is calculated from observed random statistical data, including the Residual Standard Deviation.

Reading - A number of samples or an averaged value taken during a dwell.

Sample - A single value giving the momentary output of a transducer, possibly via a (low pass) filter.

Sample Size (N) - The number of sampling units which are to be included in the sample.

Scan - A period during which all pick-ups have been read at least once.

Standard Deviation ( $\sigma$ ) - The most widely used measure of dispersion of a frequency distribution. It is the precision index and is the square root of the variance.  $S$  is an estimate  $\sigma$  calculated from a sample of data.

Standard Error of Estimate (also known as Residual Standard Deviation (RSD)) - The measure of dispersion of the dependent variable (output) about the least-squares line in curve fitting or regression analysis. It is the precision index of the output for any fixed level of the independent variable input. The formula for calculating this is

$$SE = \sqrt{\frac{\sum_{i=1}^N (Y_{OBS} - Y_{CAL})^2}{N-K}}$$

for a curve for  $N$  data points in which  $K$  constants are estimated for the curve.

Standard Error of the Mean - An estimate of the scatter in a set of sample means based on a given sample of size  $N$ . The sample standard deviation ( $S$ ) is estimated as

$$S = \sqrt{\frac{\sum_{i=1}^N (x_i - \bar{x})^2}{(N-1)}}$$

Then the standard error of the mean is  $S/\sqrt{N}$ . In the limit, as  $N$  becomes large, the standard error of the mean converges to zero, while the standard deviation converges to a fixed non-zero value.

Statistic - A parameter value based on data.  $\bar{x}$  and  $S$  are statistics. The bias limit, a judgement, is not a statistic.

Statistical Confidence Interval - An interval estimate of a population parameter based on data. The confidence level establishes the coverage of the interval. That is, a 95-percent confidence interval would cover or include the true value of the parameter 95-percent of the time in repeated sampling.

Student's "t" Distribution (t) - The ratio of the difference between the population mean and the sample mean to a sample standard deviation (multiplied by a constant) in samples from a normal population. It is used to set confidence limits for the population mean.

Traceability - The ability to trace the calibration of a measuring device through a chain of calibrations to the National Bureau of Standards.

Transducer - A device for converting mechanical stimulation into an electrical signal. It is used to measure quantities like pressure, temperature, and force.

Transfer Standard - A laboratory instrument which is used to calibrate working standards and which is periodically calibrated against the laboratory standard.

True Value - The reference value defined by the National Bureau of Standards which is assumed to be the true value of any measured quantity.

Uncertainty (U) - The maximum error reasonably expected for the defined measurement process:  
 $U = \pm (B + t_{95}S)$ .

Variance ( $s^2$ ) - A measure of scatter or spread of a distribution. It is estimated by  
 $s^2 = \frac{\sum (X_i - \bar{X})^2}{N-1}$  from a sample of data. The variance is the square of the standard deviation.

Working Standard - An instrument which is calibrated in a laboratory against an interlab or transfer standard and is used as a standard in calibrating measuring instruments.

## APPENDIX V

## DESCRIPTIONS OF GROUND-LEVEL TEST BEDS AND ALTITUDE TEST CELLS

The descriptions given in this Appendix reflect the capability of each facility at the time of its participation in the UETP. Subsequent changes or improvements are not included.

## (A) GROUND-LEVEL TEST BEDS

## 1. NATIONAL RESEARCH COUNCIL CANADA - TEST CELL No 5

## 1.1 Description

## 1.1.1 Test Facility

The test cell used for the UETP is designated Cell No 5 and is one of three ground-level gas turbine test cells in the Engine Laboratory. This cell is capable of handling engines of up to 140 kg/s air inflow. Since environmental control is not available, the test condition is dictated by local ambient temperature and pressure. A sectional elevation and plan view of Cell No 5 are given in Figure A.

## 1.1.2 Installation Configuration

The UETP test engine was floor mounted and a facility bellmouth and airmeter were fitted. Engine efflux and entrained secondary air were ducted from the cell through a 2m diameter exhaust collector to a vertical silencer that discharged to the atmosphere. A 1m diameter insert in the collector tube allowed reduction of the induced secondary cell flow to 6 m/s or less.

## 1.2 Primary Test Measurements

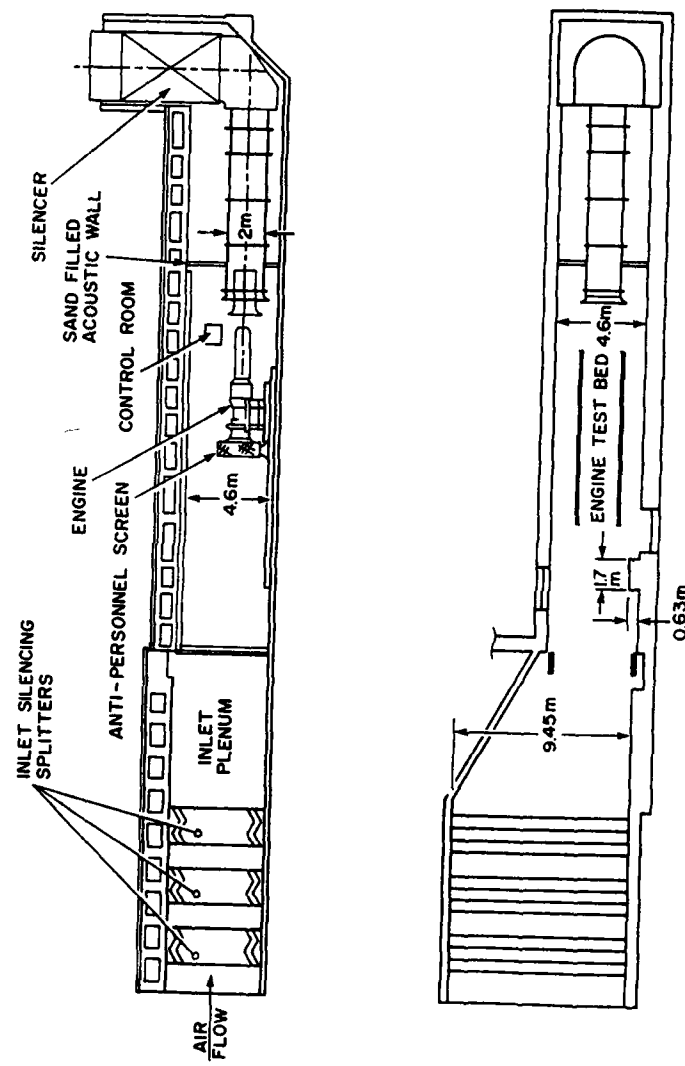
## 1.2.1 Thrust Measuring System

The test engine was mounted on a thrust bed which in turn was suspended through flexure plates to a mounting frame anchored to the floor. A series of strain gauge type load cells was available for placement between the thrust bed and mounting frame. The load cell used was calibrated in a deadweight tester, which is periodically checked against the Canadian Standards of Mass, NRCC. Friction and bending forces produced by the flexible plates were determined by a center-pull calibration.

The facility bellmouth airmeter assembly was attached ahead of the reference airmeter. A hard mounted, hemispherically shaped nosebullet was mounted on an extension of the reference airmeter centrebody. The bellmouth forces were transmitted to the engine stand, but decoupled from the engine and centred on the engine axis via a low stiffness inflatable seal.

The method of thrust accounting eliminated the need for a separate measurement of the bellmouth and nosebullet forces. However, static pressure data were obtained from a series of static taps in radial lines on the nose bullet and bellmouth.

FIG. A



NO. 5 TEST CELL - ENGINE LABORATORY - NRCC

### 1.2.2 Airflow Metering System

The compressor airflow was measured in an annular, straight measuring section, placed between the compressor inlet and bellmouth, by means of total pressure taps on the inner and outer walls.

### 1.2.3 Fuel Flow Metering System

Two NRCC turbine fuel flowmeters were installed in series at the engine/test cell interface. These flowmeters had been calibrated by the manufacturer using the ballistic flow method. Fuel temperature was measured in the supply line near the flowmeter exit with "Type T" (copper-constantan) thermocouples. Fuel mass flow was calculated using the measured fuel temperature, the indicated frequency from the turbine flowmeters, and the flowmeter calibration curve. Calibration data were used to prepare curves of meter output frequency per unit volume as a function of a corrected frequency. The corrected frequency is defined as the indicated frequency divided by actual fuel kinematic viscosity which is calculated from fuel sample properties and the measured fuel temperature.

## 1.3 Data Acquisition and Reduction

Raw engine data were acquired by a Data Acquisition System (DAS), comprising a minicomputer and a Compact System Controller (CSC). The low-level signals were filtered by 10 Hz filters and then amplified to +5 VDC full scale (nominal), before digitisation in the CSC. High level signals bypassed the amplifiers, but were filtered prior to digitisation. The digitisation was done with a 12 bit analogue-to-digital converter, giving a resolution of 0.024% of full scale.

Pressure signals were mechanically multiplexed using scanivalves and externally mounted capacitive type pressure transducers. Two calibration pressures were connected to each scanivalve to verify the calibration on each scan. Temperature signals were converted from thermocouple wire to copper using temperature reference plates; the plate temperature being measured with thermocouples referenced to an electronic ice-point.

Following a five minute engine stabilization period, two back to back data scans were made at each test point, each scan taking approximately 6 minutes. Steady-state engine performance data were obtained by sampling each parameter input signal at a constant rate of approximately 100 Hz over a short time period (ranging from 1 to 10 seconds depending on the parameters), and then averaging arithmetically to yield a single value. The raw data for each test point were reduced to engineering units using pre-stored calibrations and displayed on a video screen. A visual comparison of DAS acquired data to those displayed on the read-out instruments was made for verification before storage on a magnetic disk. Measured or calculated parameters could be cross plotted on an analogue X-Y recorder.

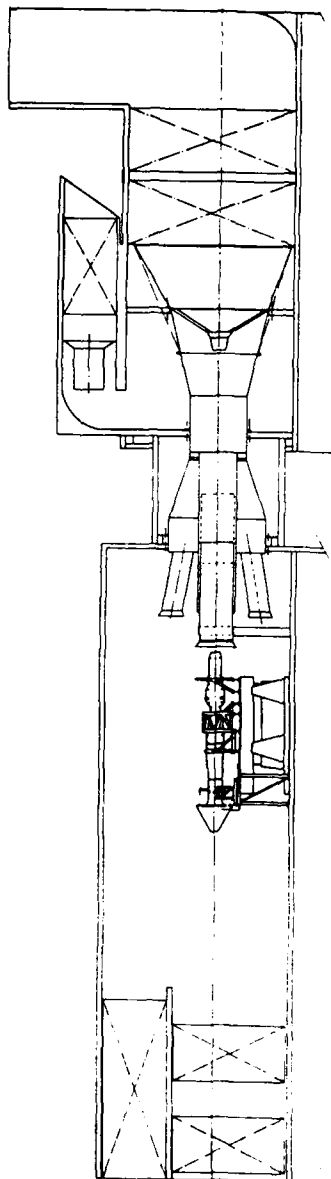
## 2. CENTRE D'ESSAIS DES PROPULSEURS TEST STAND TO

### 2.1 Description

#### 2.1.1 Test Facility

Engine test stand TO can provide engine tests at ground-level conditions. Airflow rates up to 1200 kg/s are available in this stand, the dimensions of which are: 10,2 x 10,85 x 26 m. A sectional elevation is given in Figure B.

FIG. B



TEST BED TO AT CER

## 2.2 Primary Test Measurements

### 2.2.1 Thrust Measuring System

The engine was mounted on a thrust measuring system supported by four thin blades. The thrust was measured by a load cell. The engine inlet duct was isolated from the bellmouth by a zero leakage seal.

### 2.2.2 Airflow Metering System

Airflow was metered by measuring the total and static pressures, total temperature and boundary layer profile downstream of the bellmouth. A cooled exhaust diffuser and a silencer ducted the exhaust gases to atmosphere.

### 2.2.3 Fuel Flow Metering System

Two fuel systems covered three ranges of fuel flow up to 7.5, 24 and 36 m<sup>3</sup>/h respectively. Fuel was metered with volumetric flowmeters calibrated by CEPr.

### 2.2.4 Pressure Measurements

The facility can provide either 144 pressure lines through a scanning valve system or 24 direct lines. Pressure lines and thermocouple wires were supported from a bearing located above the engine to minimise their influence on the thrust frame.

### 2.2.5 Temperature Measurements

264 thermocouple wires with multiplexed lines or 40 with direct lines can be used. They are routed to OC reference junctions. Also available are 10 lines for flow measurements, speed measurement and checking measurement (strain gauges ; 30, accelerometers:40).

## 2.3 Data Acquisition Processing System

Each time a data acquisition is ordered, the computer records all the data, executes a real time calculation program and provides the results on a line printer or non visual displays.

## 3. ESKISEHIR SUPPLY AND MAINTENANCE CENTER - TURKEY

### 3.1 Description

#### 3.1.1 Test Facility

Post-maintenance/overhaul Test Cell AF/M37-T6B is the major test cell utilised for health monitoring and acceptance testing of turbo-jet engines. It cannot provide any simulated flight environmental conditions.

The flow follows a U-Shaped path through the cell, sound-suppressors being fitted in the vertical air inlet and exhaust sections. The working section is 10 m high and 7 m wide. Every engine is tested with a bellmouth special to its model. There are no means for controlling the inlet air flow. This condition creates a natural depression within the test chamber.

#### 3.1.2 Installation Configuration

The UETP engine was mounted on a thrust frame which was linked to the ground through four flexure plates and which contained the two load-cells

for the thrust measurement system. The engine had no connections with the air inlet and exhaust discharge sections of the test cell. The inlet bellmouth was attached directly to the engine. The exhaust collector of the test cell could be moved aft or forward to achieve the required distance between the engine and the exhaust collector.

### 3.2 Primary Test Measurements

#### 3.2.1 Thrust Metering System

The thrust metering system was a scale force thrust stand flexure system mounted on the engine support cart as shown in Figure C. The dual bridge load cells were calibrated in situ by standards traceable to the National Bureau of Standards (NBS). The maximum system capacity is 156 kN.

#### 3.2.2 Airflow Metering System

Airflow is not normally measured in this cell. A rough indication can be obtained by measuring the depressions in the test chamber and at the engine inlet (bellmouth). For the UETP test, airflow was calculated using the Station 2 instrumentation.

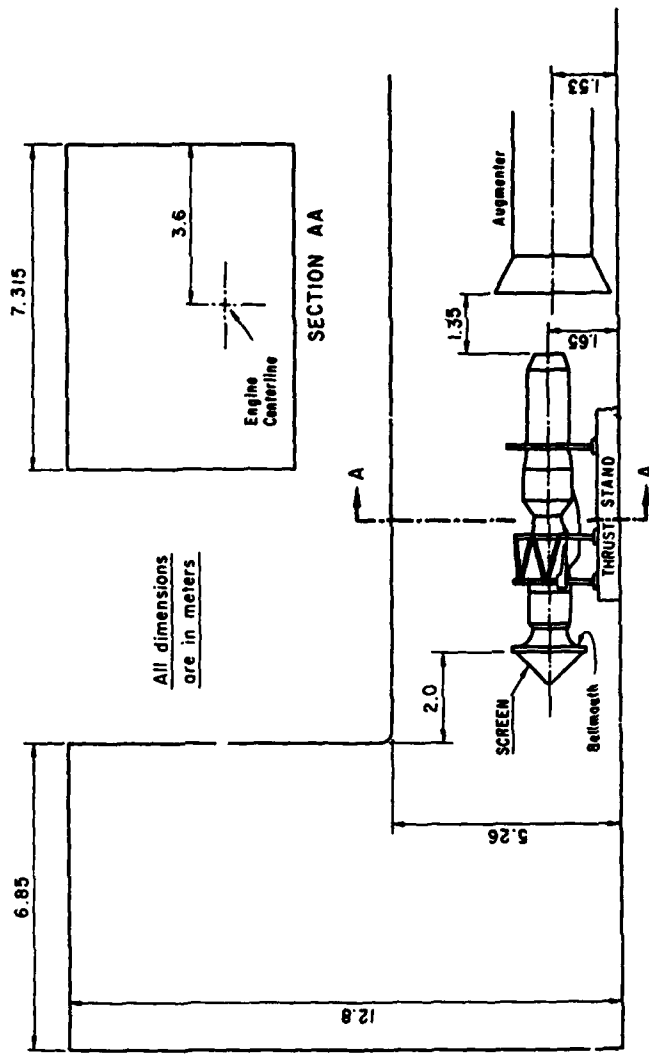
#### 3.2.3 Fuel Flow Metering System

Fuel is metered with turbine volumetric flowmeters. A high range and a low range metering system with two flowmeters in each range are provided to maintain the desired level of accuracy at all flow conditions. The meters are electronically calibrated and can compensate for changes in the specific gravity of the test fuel.

### 3.3 Data Acquisition/Processing System

There is no Digital Data Acquisition System. In normal use recording and calculations are performed manually with the use of some charts when applicable. Data are recorded and kept on standard log-sheets/charts. For the UETP the data were fed manually into a micro computer with an analysis program developed for this purpose.

FIG. C



TEST CELL AT SUPPLY AND MAINTENANCE CENTRE ESKISEHIR, TURKEY (TUSAf)

## (B) ALTITUDE TEST CELLS

## 5. NASA LEWIS RESEARCH CENTER TEST CELL PSL 3

## 5.1 Description

## 5.1.1 Test Facility

Propulsion System Laboratory-Test Cell 3 (PSL-3) has a working section diameter of 7.3 m and is one of two major test cells utilised for air breathing propulsion system testing at NASA Lewis Research Center. The PSL can provide simulated flight environmental conditions ranging from 1,500 m to 24,400 m and from 0 to 3.0 flight Mach numbers. Airflow rates up to 340 kg/sec are available for air-breathing propulsion system testing.

## 5.1.2 Installation Configuration

The NASA UETP utilised a typical direct-connect turbine-engine test configuration. The engine was mounted on a thrust stand, as shown in Figure D, which contained the thrust-measuring system. The engine inlet duct was isolated from the bellmouth and upstream ducting by a labyrinth seal. Airflow was conditioned to a uniform velocity profile upstream of the bellmouth inlet by flow straightening screens and grid assembly. The temperature and pressure levels could be either manually or automatically controlled at the engine inlet and exhaust to simulate the desired altitude and Mach number test conditions. A fixed geometry, water-cooled exhaust diffuser was used to collect the exhaust gases and direct them to the PSL exhaust system.

## 5.1.3 Environmental Control System

The temperature environment of the engine during testing as controlled by cooling air supplied from a torus manifold at the upstream end of the test cell. The flow was regulated to maintain the test cell temperature within specified limits. The environment pressure was controlled by valves in the facility exhaust ducting. The velocity over the nozzle external surface was controlled by sizing the engine exhaust diffuser to the range of engine operating conditions and to the plant exhauster capabilities.

## 5.2 Primary Test Measurements

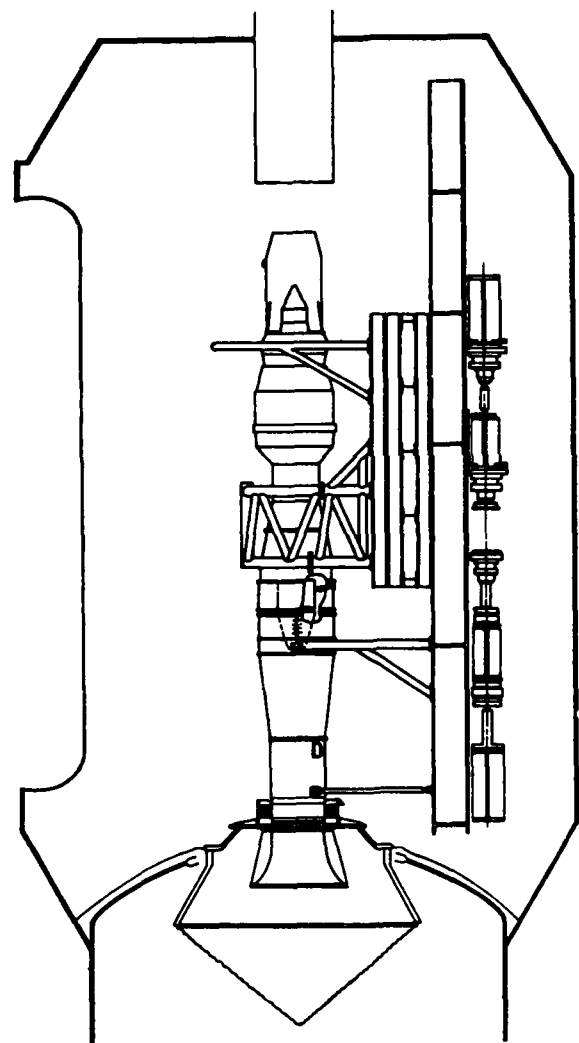
## 5.2.1 Thrust Metering System

The thrust metering system is a scale force thrust stand, flexure mounted to the test chamber supports as shown in Figure D, and free to move except as restrained by a dual load-cell system that allows the thrust stand to be preloaded and operated as a null position system, ie fixed position. The dual-bridge load cells are calibrated by standards traceable to the National Bureau of Standards (NBS)

## 5.2.2 Airflow Metering System

The NASA method of determining inlet total airflow is based on the integration of the flow per unit area calculated for each total pressure probe of a 4 rake array and the assumption that the static pressure is constant across the duct at the airflow station (approximately 1 duct diameter downstream of the labyrinth seal). This assumption was validated by a static pressure survey at representative test conditions. Based on boundary layer and a few total pressure and temperature in the free stream were measured.

Fig. D



J57 ENGINE INSTALLED IN NASA HIGH ALTITUDE TEST CELL PSL-3

### 5.2.3 Fuel Flow Metering System

Fuel was metered with turbine, volumetric flowmeters. A high and low range metering system with two flowmeters in each range was provided to maintain the desired level of accuracy for all flight conditions. The meters are 'in-water' calibrated in a laboratory traceable to the NBS.

### 5.3 Data Acquisition/Processing System

Pneumatic and electrical instrumentation, control, and service system lines were routed from the engine and thrust stand to the test cell wall in such a manner that the desired engine thrust measuring accuracy could be obtained. The pressure lines routed to transducers through a scanner valve system, and thermocouple wires for temperature measurement routed to 338K reference junctions. The electrical signals from pressure transducers, thermocouples, thrust measurement load cells, and turbine fuel flowmeters were conditioned for sampling by Propulsion Systems Laboratory Data Acquisition System (DAS).

The engine and facility conditions were monitored, real time, in the control room by sampling of all parameters and displaying of selected parameters using a test facility digital computer. At specified conditions, multiple samples of all parameters were recorded by the DAS for determination of engine performance. The multiple data samples were recorded by the test facility computer for averaging computation and display on a CRT of engineering units and performance parameters. The engineering unit data and performance data were tabulated on a facility line printer and also transmitted from the facility computer to one of the NASA Lewis large central computers for storage, further analysis and batch processing. Analysis of the stored data could also be performed on interactive graphics terminals to provide the plotted test results.

## 6. AEDC ALTITUDE TEST CELL T-2

### 6.1 Description

#### 6.1.1 Test Facility

Propulsion Development Test Cell T-2 is one of eight test cells at the AEDC used for air-breathing propulsion system testing. Test Cell T-2 can provide simulated flight environmental conditions from sea level to 24,000 m in altitude, flight Mach numbers from 0 to 3.0, and airflow rates up to 360 kg/s. The T-2 test chamber is 3.75m diameter. The layout of the cell is shown in Figure E.

#### 6.1.2 Installation Configuration

The UETP engines were tested in a "direct-connect" test configuration with each engine mounted on a support cart containing the thrust measuring system. The engine inlet duct was isolated from the bellmouth and upstream ducting by an automatic pressure balancing, "zero leakage", labyrinth seal. The engine bellmouth used for the UETP had an exit diameter 76mm less than the engine face diameter. A conical spool piece with a wall half angle of 2.8 deg was used to make the transition from the bellmouth exit to the engine inlet duct. Plant airflow was conditioned to a uniform velocity profile at the bellmouth inlet by a flow straightening screen and grid assembly. A fixed-geometry, water-cooled exhaust diffuser was used to collect and direct the exhaust gases to the ETF plant exhauster system.

## J57 ENGINE INSTALLED IN AEDC PROPULSION DEVELOPMENT TEST CELL T-2

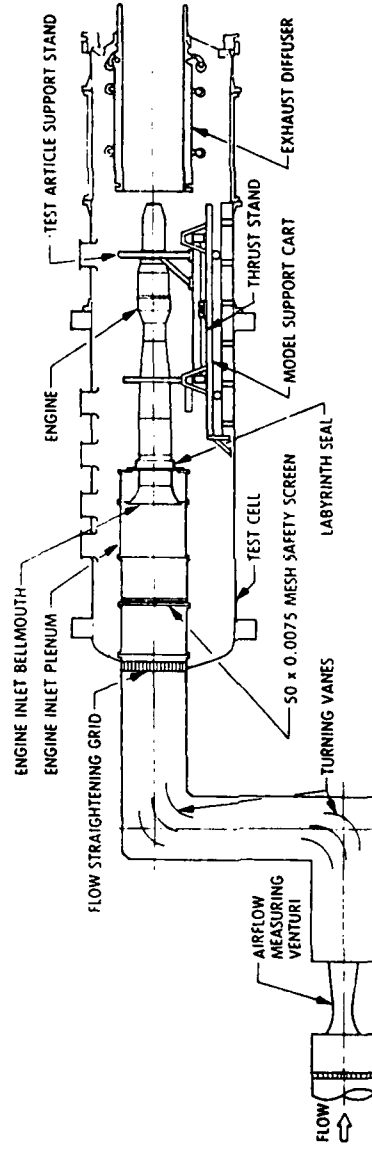


FIG. E

### 6.1.3 Test Cell Environmental Control Systems

The temperature and pressure levels at the engine inlet and exhaust were automatically controlled to simulate the desired altitude and Mach number test conditions. The test cell air temperature was controlled by cooling air supplied from a torus manifold at the upstream end of the test cell. The flow was regulated to maintain the test cell temperature within specified limits. The test cell pressure environment was controlled with the plant exhaust equipment.

## 6.2 Test Measurement Systems

### 6.2.1 Airflow

Engine airflow for the UETP was metered with a critical flow venturi located upstream of the inlet flow straightening plenum. The venturi was a standard AEDC EIF design as described in Reference 28. Test cell leak checks were conducted to insure no duct air leakage between the airflow measurement station and the engine inlet plane.

### 6.2.2 Thrust

Elastic flexures were used to mount the engine on the model support cart. Pneumatic and electrical instrumentation, control, and service system lines were routed perpendicularly from the engine and support cart through the test cell wall in a manner that minimized tare loads to the engine thrust measurement system. Tare loads to the engine thrust measuring system were determined by a centerline pull calibration. Dual-bridge load cells were located below the engine centerline. The load cell, load cell column, and thrust stand were water-cooled to prevent thermal stresses. A water-cooled panel was used to cover the aft portion of the thrust stand exposed to the thermal environment of the engine tailpipe.

### 6.2.3 Fuel Flow

The facility fuel-flow system was equipped with a high- and low-range flow leg with two axial-flow turbine flowmeters in each leg. This arrangement minimizes the measurement uncertainty by providing redundant measurements and by restricting the flow measurement to the linear portion of the meter frequency calibration curve. The four facility flowmeters were calibrated in the installed configuration with the test fuel (Jet A).

## 6.3 Data Acquisition/Processing System

Steady-state pressure lines were routed to transducers located in a multiplexing scanner valve system. All thermocouple wires were routed to a 338K reference junction system. The electrical signals from pressure transducers, thermocouples, thrust measurement load cells, and turbine fuel flowmeters were conditioned for sampling by a Digital Data Acquisition System (DDAS).

A central data computer used to record and process outputs from the steady-state, transient, and high-response instrumentation systems. The outputs of the steady-state instrumentation were fed into the DDAS system. One hundred ninety-two channels of data were recorded during each steady-state data point. The data were acquired in 12 equal time segments over one and one-half minutes with each segment scanned 50 times. The data were simultaneously recorded on magnetic tape and transmitted to the

digital computer for conversion to engineering units and calculation of performance parameters.

The output of selected transient instrumentation was transmitted to the DDAS which converts the signals to engineering units and calculated parameters. These parameters were displayed on a cathode-ray tube (CRT) in the control room at approximately 1-sec update intervals and graphically displayed on a CRT in the computer room for real-time data analysis. Transient data were also recorded on a continuous analogue recorder and magnetic tape in the frequency modulation (FM) mode.

The output of the high-response dynamic instrumentation was recorded on multiplexed magnetic tapes at 0.76 m/sec in the FM mode.

The engine and facility conditions were monitored, real time, in the control room by sampling selected parameters by the DDAS. At specified conditions, multiple samples of all parameters were recorded by the DDAS for determination of engine performance. The multiple data samples were recorded and transmitted to the central facility computer for averaging and computation of engineering units and performance parameters. The engineering unit data and performance data were tabulated on a line printer and transmitted by the facility computer to the central AEDC digital computer for storage. Analysis of the stored data was performed on interactive graphics terminals to provide the plotted test results.

## 7. CEPr ALTITUDE TEST CELL R6

### 7.1 Description

#### 7.1.1 Test Facility

Test cell R6 is 5.5m diameter and 30m long. It is separated into two parts to allow the setting of different upstream and downstream conditions for the engine under test.

Upstream limits are:  $P = 5$  to 700 kPa  
 $T = 243$  to 923K

Downstream limits are:  $P = 5$  to 200 kPa  
 $T = 253$  to 653K

Airflow rates up to 400 kg/s are available.

#### 7.1.2 Installation Configuration

The upstream part of the cell is provided with air by the air-conditioning plant.

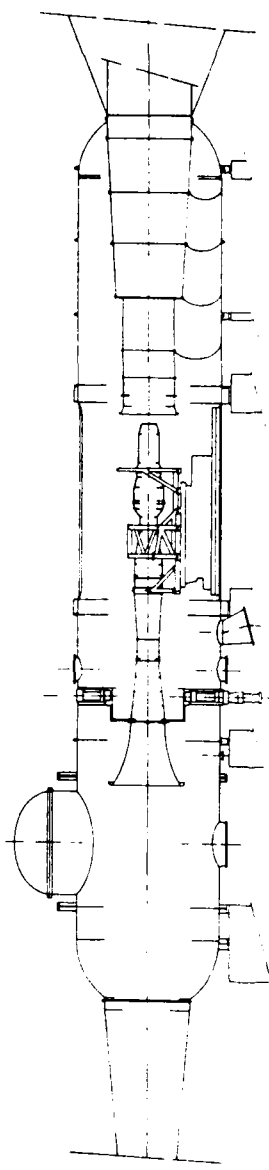
At the engine exhaust, a diffuser is connected to the air-conditioning plant which allows extraction and cooling of the exhaust gases.

The layout of the cell is shown in Figure F.

#### 7.1.3 Engine and Cell Cooling

A cooling loop for both engine and cell is provided to maintain the temperature to fixed limits.

FIG. F



ALTRUDE TEST CELL R6 AT CEP

## 7.2 Primary Test Measurements

### 7.2.1 Thrust Metering System

The engine was mounted on a thrust measuring system supported on four thin blades; the thrust was measured by a Baldwin load cell.

The engine inlet duct was separated from the bellmouth by a zero leakage seal. The load cell was calibrated by a calibrated actuator mounted on the thrust metering system. The net thrust was calculated by computer using the measured thrust with connections for the upstream and downstream engine conditions.

### 7.2.2 Airflow Metering System

Airflow was metered by measuring the total static pressures, total temperature and boundary layer profile downstream of the bellmouth.

### 7.2.3 Fuel Flow Metering System

High range (4.4 m<sup>3</sup>/h) and a low range (1.0 m<sup>3</sup>/h) fuel systems with volumetric flowmeters were used for the UETP.

### 7.2.4 Pressure Measurements

Test test facility can provide 288 pressure lines through a scanning-valve system. 84 direct lines are also available with individual transducers, allowing differential pressures, oil, fuel or any hydraulic system pressures to be measured.

### 7.2.5 Temperature Measurements

288 thermocouple wires, directly or with multiplexed lines are available. Each thermocouple has its reference junction (273K)

### 7.2.6 Other Measurements

Ten lines for flow or speed measurements and checking measures can also be used.

## 7.3 Data Acquisition System and Computer Installation

The data acquisition system includes the following:

- frequency meter lines: used for flow or rotation speed measurements.
- simple pressure lines: used for aerodynamic, differential or hydraulic pressure; they each have their own transducer and amplifier.
- scanned pressure lines: 24 pressure lines, one transducer and one amplifier for each scanning valve system.
- temperature measurements use multiplexers with 24 lines each.

There are two opto-electrical isolators before entering the computer. The command board is located in the facility and gives allowance to order the data acquisition, to choose a "real time calculation program" and provide various results.

Each time as data acquisition is ordered, the computer records the whole data and can execute a real time calculation program and provide the results of measurements and calculations on a line printer or on displays.

8. RAE PYESTOCK ALTITUDE CELL 3

8.1 Description

8.1.1 Test Facility

Cell 3 has a working section 6.1 m diameter and is one of five altitude test cells used to test air breathing propulsion systems over a wide range of simulated forward speed and altitude conditions. Air compressors and exhausters, of 300 MW total equivalent power, enable altitudes from sea level to 30,500 m and from 0 to 3.5 flight Mach number to be simulated, with airflow rates up to 636 kg/s.

8.1.2 Installation Configuration

The UETP engine was installed in Cell 3 in a similar configuration to that developed for military turbofan engines. It was pre-rigged and mounted on a pallet before installation in the cell (see Figure G). The pallet was then mounted on the thrust frame, which is supported on oil-borne bearings, and connected to the cell services and instrumentation lines. The engine inlet duct was isolated from the bellmouth in the plenum chamber and upstream ducting by a freely mounted slip joint with a controlled and calibrated leakage. Airflow was metered using a venturi type contracting section and conditioned to a uniform pressure profile using flow straightening gauzes (screens) supported by a coarse grid structure. The pressure at the inlet to and around the exhaust from the engine was automatically maintained to simulate the desired altitude and Mach number test conditions, with the correct inlet temperature attained by mixing separate hot and cold air upstream of the cell. A fixed geometry water cooled exhaust diffuser was used to collect the exhaust gases and direct them to the plant exhauster system.

8.1.3 Environmental Control System

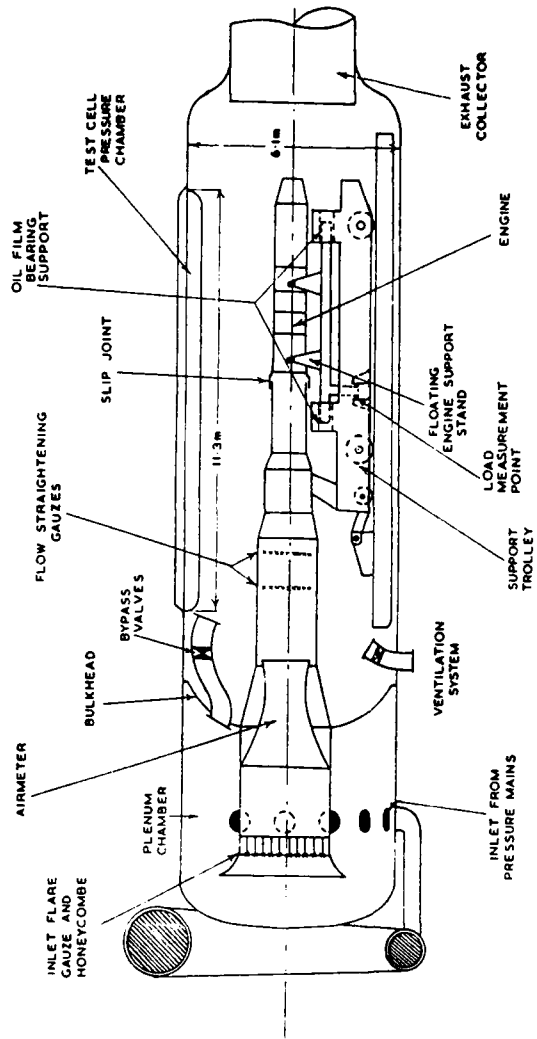
The temperature environment around the engine during testing was controlled by bleeding air from atmosphere via a cell ventilation valve. The flow was regulated to maintain the test cell temperature within specified limits. The environmental pressure around the engine was controlled by roughly sizing the engine exhaust diffuser to the range of engine operating conditions and to the plant exhauster capacity and finely trimming this by bleeding air in from atmosphere downstream of the diffuser through three automatic valves.

8.2 Primary Test Measurements

8.2.1 Thrust Metering System

The floating thrust frame was supported from oil-borne bearings on flexure plates. A direct measurement of frame reaction was made using Bofors shear force load cell. The system was calibrated in place before each test run using a compression and tension load cell with traceable calibration to the National Physical Laboratory (NPL) standards.

FIG.6



TYPICAL ENGINE INSTALLATION IN RAE (P) ALTITUDE CELL 3

#### 8.2.2 Airflow Metering System

The airflow was metered using a cubic profile subsonic venturi located upstream within the plenum chamber as part of the engine approach ducting. The venturi flow coefficient analytically accounts for a velocity profile at the throat due to the viscous boundary layer.

#### 8.2.3 Fuel Flow Metering System

Fuel was metered with two positive displacement flowmeters. The meters were calibrated using fuel in a laboratory test rig with traceable standards to NPL.

### 8.3 Data Acquisition/Processing System

Pneumatic and electrical instrumentation, control and service system lines were routed from the engine and support frame to the test cell wall in such a manner that the desired engine thrust measuring accuracy could be maintained. The pressure lines were routed to discrete transducers and the thermocouple leads routed through insulated flasks containing melting ice at 273K. The electrical signals from the pressure transducers, thermocouples, thrust measuring load cells, and fuel flow meters were conditioned for sampling by a Data Acquisition System (DAS).

The engine and test facility conditions were monitored in the control room. At specified conditions, multiple scans of all parameters were recorded by the DAS for determination of engine performance. The multiple data scans were recorded by a satellite computer and transmitted to the central facility computer for averaging and computation of cell conditions and engine performance parameters in engineering units. Some selected data were transmitted to the control room and displayed on numerical display units (NDU). The performance data were tabulated on a line printer and stored for later analysis. However, performance data could also be displayed on interactive graphics terminals during the course of testing to provide on-line monitoring of the quality of the data being gathered.

REPORT DOCUMENTATION PAGE											
1. Recipient's Reference	2. Originator's Reference	3. Further Reference	4. Security Classification of Document								
	AGARD-AG-307	ISBN 92-835-0508-5	UNCLASSIFIED								
5. Originator	Advisory Group for Aerospace Research and Development North Atlantic Treaty Organization 7 rue Ancelle, 92200 Neuilly sur Seine, France										
6. Title	MEASUREMENT UNCERTAINTY WITHIN THE UNIFORM ENGINE TEST PROGRAMME										
7. Presented at											
8. Author(s)/Editor(s)	J.P.K. Vleghert		9. Date								
10. Author's/Editor's Address		11. Pages									
See Flyleaf		74									
12. Distribution Statement	This document is distributed in accordance with AGARD policies and regulations, which are outlined on the Outside Back Covers of all AGARD publications.										
13. Keywords/Descriptors	<table> <tr> <td>Altitude testing</td> <td>Sea-level testing</td> </tr> <tr> <td>Engines</td> <td>Testing of engines</td> </tr> <tr> <td>Gas turbines</td> <td>Uncertainty</td> </tr> <tr> <td>Measurements</td> <td></td> </tr> </table>			Altitude testing	Sea-level testing	Engines	Testing of engines	Gas turbines	Uncertainty	Measurements	
Altitude testing	Sea-level testing										
Engines	Testing of engines										
Gas turbines	Uncertainty										
Measurements											
14. Abstract	<p>This AGARDograph is an outcome of the Propulsion and Energetics Panel Working Group 15 on 'Uniform Engine Testing Programme' (AGARD AR 248). During the performance of this Group it appeared that the results of some test runs were somewhat scattered, without an obvious explanation. The Group, therefore, formed a sub-Group with the task of carefully assessing the uncertainties of the measured data in order to find out whether the scattering was within the expected uncertainty or whether an explanation must be found. Since the results of the efforts of the sub-Group have some importance beyond the Working Group 15 tests, it was decided to report them in the form of an AGARDograph. In Chapter 5 the different uncertainties are estimated. The discussion on the uncertainties appears in Chapter 6 and in the following Chapter 7, ten conclusions are drawn from the efforts.</p> <p>This AGARDograph was prepared at the request of the Propulsion and Energetics Panel of AGARD.</p>										

<p>AGARDograph No.307 Advisory Group for Aerospace Research and Development, NATO MEASUREMENT UNCERTAINTY WITHIN THE UNIFORM ENGINE TEST PROGRAMME Edited by J.P.K. Vieghert Published May 1989 74 pages</p>	<p>AGARDograph No.307 Advisory Group for Aerospace Research and Development, NATO MEASUREMENT UNCERTAINTY WITHIN THE UNIFORM ENGINE TEST PROGRAMME Edited by J.P.K. Vieghert Published May 1989 74 pages</p>	<p>AGARDograph No.307 Advisory Group for Aerospace Research and Development, NATO MEASUREMENT UNCERTAINTY WITHIN THE UNIFORM ENGINE TEST PROGRAMME Edited by J.P.K. Vieghert Published May 1989 74 pages</p>	<p>P.1.0</p>	<p>P.1.0</p>
		<p>The AGARDograph is an outcome of the Propulsion and Energistics Panel Working Group 15 on 'Uniform Engine Testing Programme' (AGARD AR 2-48). During the performance of this Group it appeared that the results of some tests runs were somewhat scattered, without an obvious explanation. The Group, therefore, formed a sub-Group with the task of carefully assessing the</p>		
		<p>The AGARDograph is an outcome of the Propulsion and Energistics Panel Working Group 15 on 'Uniform Engine Testing Programme' (AGARD AR 2-48). During the performance of this Group it appeared that the results of some tests runs were somewhat scattered, without an obvious explanation. The Group, therefore, formed a sub-Group with the task of carefully assessing the</p>		
		<p>The AGARDograph is an outcome of the Propulsion and Energistics Panel Working Group 15 on 'Uniform Engine Testing Programme' (AGARD AR 2-48). During the performance of this Group it appeared that the results of some tests runs were somewhat scattered, without an obvious explanation. The Group, therefore, formed a sub-Group with the task of carefully assessing the</p>		<p>P.T.O</p>

<p>uncertainties of the measured data in order to find out whether the scattering was within the expected uncertainty or whether an explanation must be found. Since the results of the efforts of the sub-Group have some importance beyond the Working Group 15 tests, it was decided to report them in the form of an AGARDograph. In Chapter 5 the different uncertainties are estimated. The discussion on the uncertainties appears in Chapter 6, and in the following Chapter 7 ten conclusions are drawn from the efforts.</p> <p>This AGARDograph was prepared at the request of the Propulsion and Energetics Panel of AGARD.</p> <p>ISBN 92-835-0508-5</p>	<p>uncertainties of the measured data in order to find out whether the scattering was within the expected uncertainty or whether an explanation must be found. Since the results of the efforts of the sub-Group have some importance beyond the Working Group 15 tests, it was decided to report them in the form of an AGARDograph. In Chapter 5 the different uncertainties are estimated. The discussion on the uncertainties appears in Chapter 6, and in the following Chapter 7 ten conclusions are drawn from the efforts.</p> <p>This AGARDograph was prepared at the request of the Propulsion and Energetics Panel of AGARD.</p> <p>ISBN 92-835-0508-5</p>